Investigation of In-Service Pavement Performance

Ahmed Faheem

Arash Hosseini

Temple University

Hani Titi

University of Wisconsin-Milwaukee

WisDOT ID NO. 0092-18-05

June 2019

RESEARCH & LIBRARY UNIT

WISCONSIN HIGHWAY RESEARCH PROGRAM

WISCONSIN DOT

PUTTING RESEARCH TO WORK

TECHNICAL REPORT DOCUMENTATION PAGE

1. Report No. 0092-18-05	**2. Government Accession No.**	**3. Recipient's Catalog No.**
4. Title and Subtitle Investigation of In-Service Pavement Performance		**5. Report Date** June 2019
		6. Performing Organization Code
7. Author(s) Ahmed Faheem, Arash Hosseini, Hani Titi		**8. Performing Organization Report No.**
9. Performing Organization Name and Address Temple University 1801 N Broad St, Philadelphia, PA 19122		**10. Work Unit No.**
		11. Contract or Grant No. WHRP 0092-18-05
12. Sponsoring Agency Name and Address Wisconsin Department of Transportation Research & Library Unit 4822 Madison Yards Way Madison, WI 53705		**13. Type of Report and Period Covered** Final Report 30 June 2019
		14. Sponsoring Agency Code

15. Supplementary Notes

16. Abstract

This study is focused on understanding the in-service performance of Wisconsin pavements. The research focused on evaluating the performance of 12 pavement projects. These projects contain different test sections that vary in mix design or technology. The evaluation consisted of conducting an on-site distress survey and collection of field cores from the wheel path and between the wheel path. In addition, data regarding construction and construction quality parameters are collected and compiled from the contractors and DOT database. Analysis of the collected data included creating a geo-relational database, mechanical testing of the cores, rheological testing of the extracted binders, and sieve analysis of the recovered aggregate. Statistical analysis of the data resulted in the creation of regression models relating laboratory measurable material properties to specific field distresses. These models are intended to provide a basis for determining the appropriate limits for laboratory performance such that in-service performance is enhanced. The models are proposed as complementing tools for the development of a performance-engineered mix design procedure for the state of Wisconsin. In addition, deterioration modeling using artificial intelligence and machine deep learning was conducted using data for this project and previous WHRP project consisting of 42 roadway paving projects (about 250 miles) of Wisconsin network. The modeling is created for pavements thicker than 2 inches. This model is proposed to assist the DOT in its pavement management process. The resulting models showed a strong ability to predict field performance at any age during the pavements service life. It is highly recommended that Wisconsin DOT start adopting a geo-relational framework for its pavements' history. This will enhance the strength of the developed deterioration models and expand it to different classes of pavements. One major finding was the discrepancy between the DOT data of pavement in-service performance and that measured from the on-site distress surveying. Incorporation of new technologies for distress evaluation and re-evaluation of the segmentation of the network is highly recommended. In addition, increasing the frequency of surveying may prove beneficial in increasing the accuracy and resolution of the ranking schemes of the pavement network. This report provides information and guidance to evolve towards data-driven pavement life cycle management of its quality pre-construction and its deterioration post-construction.

17. Key Words In-Service Performance, Mix Quality, Construction Quality, Pavement Management, Pavement Life Cycle, Pavement Specifications, Mix Mechanical Testing, Binder testing, Deterioration Modeling In-Service Performance, Mix Quality, Construction Quality, Pavement Management, Pavement Life Cycle, Pavement Specifications, Mix Mechanical Testing, Binder testing, Deterioration Modeling	**18. Distribution Statement** No restrictions. This document is available through the National Technical Information Service. 5285 Port Royal Road Springfield, VA 22161

19. Security Classif. (of this report) Unclassified	**20. Security Classif. (of this page)** Unclassified	**21. No. of Pages** 120	**22. Price**

Form DOT F 1700.7 (8-72) Reproduction of completed page authorized

Disclaimer

This research was funded through the Wisconsin Highway Research Program by the Wisconsin Department of Transportation and the Federal Highway Administration under Project 0092-18-05. The contents of this report reflect the views of the authors who are responsible for the facts and accuracy of the data presented herein. The contents do not necessarily reflect the official views of the Wisconsin Department of Transportation or the Federal Highway Administration at the time of publication.

This document is disseminated under the sponsorship of the Department of Transportation in the interest of information exchange. The United States Government assumes no liability for its contents or use thereof. This report does not constitute a standard, specification or regulation.

The United States Government does not endorse products or manufacturers. Trade and manufacturers' names appear in this report only because they are considered essential to the object of the document.

Executive Summary:

This study focused on tracking the in-service performance of 30 pavement sections. The collected information covers pavement history from mix design to on-site distress surveys. Such information is used to

1. Model mix properties dependency of performance,
2. Model performance deterioration with time, as a function of construction and loading characteristics, and
3. Propose a framework for managing pavement life cycle information to utilize new computing technologies in upgrading the Wisconsin DOT pavement life cycle management.

The study started with evaluating the Wisconsin pavement network performance to highlight critical distresses commonly present. These distresses are alligator cracking, longitudinal cracking, transverse cracking, and rutting. the distribution of theses distresses among the selected pavements is comparable with that of the network. Furthermore, the test sections' history shows that these sections were built using 16 unique approved mix designs. The data and materials collected from these projects served to model the performance dependency on mix properties.

The report structure is divided such that it covers a review of previous studies on this topic, description of selected field projects and their general information. The collection process of the pavement life cycle history data and development of the relational geospatial database of this history are detailed in chapter 2. In order to compare the performance of the selected projects to the overall network performance, chapter 3 is structured to study the performance of the entire Wisconsin pavement database. The overall performance distribution and construction quality of the selected projects are then presented to show how comparable the selected projects are to the full network. Each project is discussed in more detail to illustrate the different types of distresses experienced and to evaluate where these distresses are caused by an obvious construction-related irregularity in terms of quality or consistency. Chapter 4 is designed to conduct a generalized analysis of the interaction between the different pavement characteristics and the noticed performance. This analysis is conducted on a one-to-one comparison between a given characteristic and given distress. In addition, this chapter clarifies other correlations such as the comparison between wheel-path and between-wheel-path material performance, and the correlation between the IDEAL and SCB testing at intermediate temperature

Chapter 5 focuses on the influence of mix design on in-service performance. The influence is quantified using multivariate regression modeling. This chapter is aimed to provide the foundation of building performance engineered mix design where the relationship between laboratory-measured properties and in-service performance is available. Chapter 6 focuses on the modeling of performance deterioration post-construction. This chapter details the machine learning tools used in building holistic models of predicting pavement deterioration as a function of full pavement history including structural design, production and construction quality, and traffic. The unique aspect of the modeling presented in chapter 6 is that it treats the network as individual segments rather than separate projects. Therefore, the resultant database is over 200 miles long, combining data from selected field pavements and additional data from another 30 pavements. Chapter 7 summarizes the findings and presents the conclusions of this study. This chapter also details recommendations regarding the implementation of a geospatially relational database in managing the Wisconsin pavement network.

Influence of Mix Properties on Performance

The multivariate analysis shows that the observed distresses can be correlated as follows:

A. Alligator cracking is correlated with:
    a) Age of mix,
    b) Intermediate true grade of the binder ($G^*.\sin\delta$),
    c) The cracking index measured using the IDEAL testing protocol.
B. Rutting is correlated with:
    a) Mix dust-to-binder ratio,
    b) Pavement structure,
    c) Mix dynamic modulus,
    d) Mix Densification.
C. Transverse cracking is correlated with:
    a) Winter climate,
    b) Binder low-temperature relaxation,
    c) Percent fines in the mix,
    d) Mixture low-temperature fracture energy.

These relations are critical in building performance engineered mix designs. It can be noted that these performance measures are dependent on measurable properties of the mix, or other external factors such as climate or structural design.

Performance deterioration modeling

The framework used to create the deterioration model is based on geo-relating all pavement life cycle data such that the change in performance with time can be connected to localized parameters. These parameters include material produced quality data, pavement placement, and compaction quality data, accumulated traffic loading during service, accumulation of climate loading in terms of temperature or forms of precipitation. This framework provides the essentials for developing a data-driven pavement life cycle management system. The data used in this study is expanded beyond the selected field sections. It covers over 200 miles of pavement sections belonging to the Wisconsin DOT network.

Given the complexity of the data and the database architecture, advanced computing techniques are employed in developing the deterioration models. Using Gene Expression program as one of the machine learning techniques employed in this study, the teaching process of the model resulted in developing dependency between the pavement overall quality and critical parameters such as:

1. As-built pavement thickness,
2. Production volumetrics,
3. Construction placed density,
4. Traffic,
5. Time in years.

While this model is showing promising accuracy as demonstrated by the validation process, it has the potential to continuously improve as long as new data is fed into the database. This requires the expansion of the geo-referencing of the pavement life cycle data to include the entire network. Rather than proposing a rigid model to be applied at all times and situations, this study presents the concept of life cycle pavement management. This requires treating the data pertaining to a given pavement section as a living organism. Therefore, the entire life cycle of data can be connected to a specific location and performance. If the network data is upgraded to this level, then developing adaptive models is a straight forward process. This is because the machine learning algorithms are available as end used applied tools rather than requiring programming. In addition, as new pavements are being constructed, the data pool continues to grow, which allows these models to become more precise. This can be achieved through the following steps:

1. Divide the network into segments for monitoring performance. The current segmentation is about one mile long. This is too long of a segment, especially because only 1/10 of this segment is monitored as a sample. It is suggested that the segmentation be about ½ a mile long at most.

2. Use new technology in distress surveying such as imaging techniques. This allows rapid surveys to be conducted more frequently, and on a greater area of the pavement at each segment. In addition, it provides the bases for geotagging the distresses to investigate location-based patterns.
3. Conduct non-destructive testing on pavement sections to obtain a baseline of mechanical stability and location.
4. Pavement structural plans should contain locations by the station and GPS coordinates. This is achievable at an easier level if the DOT adopts 3-D modeling in project documentation and plans.
5. Quality data collected during material production or during placement and compaction needs to be tagged with their GPS locations. Proper labeling of data needs to be a requirement as much as passing specification limits.
6. Maintenance activities must be recorded by location and time.
7. Data for all aspects of the pavement life cycle must be accessible and connected to allow for retrieval of complete pavement history.
8. Pavement machine learning deterioration models must be updated regularly as part of the management plan. The model update needs to be synchronized with distress survey efforts and maintenance activities.

Finally, the implementation of the aforementioned recommendations has the potential to be a resource for adopting performance-based specifications, either at the mix design level or the production and construction level. The data-driven trends should serve as a verification tool for developing new specifications limits in order to connect laboratory activities with in-service performance. The growth of the database within the network for all classes of pavements must be utilized at scheduled times as a means of self-validation of specification limits, construction practices, maintenance plans, and rehabilitation. They can serve for project scoping through evaluating the history of similar pavements with respect to location, traffic level, environmental condition, or structural design which can be easily retrieved to evaluate performance and apply improvements when needed.

Table of Contents

List of Figures

List of Tables

1. Introduction and Background

1.1 Introduction

Predicting pavement performance is always a point of interest for practitioners and researchers. Understanding the mechanism of pavement deterioration and being able to accurately predict it is necessary for better pavement design. Pavements are being designed to maintain a satisfactory level of performance within the targeted service life. However, there are many cases in which pavement deterioration rates do not follow the expected service life goals. Furthermore, given the evolution of specifications, construction methods, materials, testing methods, and in-service pavement monitoring over the last twenty years, it is logical to expect an extended service life and a more accurate deterioration rate prediction for our pavement infrastructure. Yet this is not the case.

Current performance prediction models are based on parameters such as climate, traffic, environment, material properties, etc. While all these factors play an important role in performance, the quality of construction and production are as important as the other factors. The designed properties of Hot Mix Asphalt (HMA) pavements, known as flexible pavements, are subjected to variation during production and construction stages. Therefore, the final product may not be the exact reflection of the design. In almost any highway project, these variations are common and are likely to occur from different sources, by various causes, at any stage. These variations often have considerable impacts on the long-term performance of a project (Kenley 2012). Asphalt mix design parameters such as mix volumetrics and asphalt content and construction factors like in-place density are examples of the pavement properties that could vary from the design to the as-constructed condition. Quality Management Programs (QMP) are trying to minimize and control these variations and keep them at the desired levels. However, these variations are often neglected in performance prediction methods.

Flexible pavement systems, as multiscale and multiphysics phenomena, require extending the analysis capacity to cover more than a single traditional discipline. Pavement systems experience multiple interacting mechanics work at different scales, which span over many science and engineering disciplines. From the chemistry of the constituent materials and their chemical reactions to the coupled mechanic and dynamic behavior of the different phases in the system, and

even other physical processes such as heat transfer, pore water movement, and concentration field; all have their own impact on the system. Therefore, it becomes essential to discrete the system into understandable pieces to enhance the accuracy of understanding their performance. Due to the advances in the field, simplification of this challenging problem and simulating the performance/deterioration through the single value indicators are no longer satisfactory.

Finally, most of the currently available prediction methods are based on deterministic approaches. Thus, their practicality is limited to cases in which all the needed inputs from the materials, environment, traffic, underlying layers, etc., are known and reliable. Given the uncertainty associated with the manufacturing and lifecycle of flexible pavements, such cases are often rare. Against this background, recent technological advancements have enhanced the researchers' capabilities of storing and analyzing historical pavement data. This not only allows quantifying the uncertainty with ranges of possible values and associated probabilities but also helps to extract trends that may not be found by conventional methods. Utilizing these advancements in pavement performance simulation would surely enhance the practicality and accuracy of developed models.

This research will investigate the in-service performance of selected pavements. Data collected regarding the pavements' life cycle from construction to in-service performance is used to establish a connection between mix design and performance, as well as model deterioration in performance with age. This is achieved by combining the state of the knowledge with a creative, experimental design for establishing statistical correlation and engineering cause and effect relationship between influential independent factors and in-service performance.

This study provides a path to examining the effectiveness of current quality control measures by implementing its data into deterioration modeling. The fundamental challenge in achieving the highest quality levels remain in the variable nature of the process of road building. If the optimum performance is expected from a given mix design, lots produced must match the design exactly. For example, if a target compaction level is expected to be optimum for a given mix, then this target needs to be achieved during production. However, this has never been the case in pavement construction, and will probably not be the case in the near future. It is understood that the current WisDOT specification targets (for mix production or compaction) will not be met every time and those mixes will fall within a range of variability to be affordable and realistically constructive. This study aims to accept this reality and incorporate it into the analysis process account for the

inherent variability in modeling pavement in-service performance. The modeling approach also provides an understanding of how the interaction of influential independent variabilities affects performance. How is the variability of performance affected by the variability of material production and pavement construction? Answers to these questions are crucial in evolving an effective performance based-data driven specification and quality programs.

For this study, 12 projects from the state of Wisconsin have been selected for the analysis. The pavement related information of these projects was extracted from the appropriate sources in the state of Wisconsin and other agencies. The data was processed appropriately to serve the purpose of the study. Data collection was finalized by the appropriate mechanical testing of project field cores. The detailed statistical analysis and the modeling were later built on this information.

With respect to the performance of pavements, this study describes a method in which four common flexible pavement distresses such as Rutting, Alligator, Longitudinal, and Transverse are being considered as the performance indicators. These distresses were selected after realizing their significant presence within the WisDOT highway network. By using an adaptive approach, these qualitative indicators converted to the quantitative values.

The following sections in this chapter will discuss the selected projects to identify asphalt parameters and performances. The current state of performance prediction of flexible pavements and the role of common QMP indicators on the performance will be discussed according to the literature. Also, different modeling approaches and the use of soft computing techniques will be shown.

The last chapter will provide a summary of the topics covered in this study. The conclusion of the analysis conducted, and comments regarding the implementation of the findings.

1.2 Studied Projects

This research involved evaluating the in-service performance of 12 highways in Wisconsin. They ranged in the years of construction from 2003 to 2015. All distress surveys were taken in 2018. Table 1-1 lists the selected projects and their information. The locations of the studied roadways are shown on the map in Figure 1-1.

Table 1-1 List of selected in-service highways investigated in this research

Project ID	Route No.	County	Construction Year	Type of Project	Surface Layer Thickness (in)*	Average PCI**
8530-14-71	STH 77	Ashland	2014	High Recycle Project	3.687	100.0
1491-08-71	USH 141	Marinette	2013	High Recycle Project	4.468	99.8
3070-00-72	STH 73	Dane	2014	High Recycle Project	4.178	94.11
1110-10-71	STH 26	Fond du Lac	2015	High Recycle Project	4.437	100.0
7010-01-61	STH 21	Juneau	2015	FHWA density demonstration	3.875	100.0
1620-03-70	STH 13	Wood	2016	Air-void regression	4.250	100.0
2240-13-60	STH 36	Waukesha	2015	High-recycle NCHRP	4.075	100.0
5939-00-61	STH 80	Iowa	2014	Thin overlay project	1.562	100.0
1595-09-60	USH 8	Oneida	2014	Thin overlay project	1.531	93.1
9040-05-70	STH 17	Oneida	2003	Perpetual Pavement	3.687	56.2
8600-02-71	STH 178	Chippewa	2003	Premature Failure	3.312	69.0
3180-10-70	STH 11	Racine	2003	Premature Failure	3.437	83.9

* Average measurements of the field core samples.
** PCI measured by the Wisconsin DOT

The information provided in Table 1-1 shows that most of the pavements are demonstrating an adequate level of PCI for the age. The lowest PCI value for 13 years old (at the time of the last survey) is STH 17 with PCI of 56.2. STH 178 and 11 are designated as premature failure pavements. The average PCI values for these pavements do not reflect such designation. In fact, STH 11 is showing a good level of PCI after 13 years of service. These observations will be further evaluated in the following chapters of the project.

The research plan focused on evaluating in-service performance as well as pavement history. Characterization of these pavements included:

- Collection of mix production data to track variation in production quality.
- Collection of pavement compaction data to track density at the time of construction.
- Collection of field cores to:
    - Validate pavement thicknesses.
    - Mechanically evaluate the cores.
    - Test the performance of extracted binders.
    - Evaluate aggregate gradation.
- Conduct a field distress survey for pavement sections.

Figure 1-1 Location of studied projects in Wisconsin

1.3 Field Coring and Performance Survey

In order to conduct the on-site investigation, a minimum of two sections was selected from each highway. Each testing section is 500 ft long. Some of the highways contained different experimental sections or different mix designs at the time of construction. Therefore, the sections were chosen in appropriate locations to cover these differences. All these sections were located at the 0.3 mile after the starting point of their associated SNs, except for STH 36. All these sections, except the ones for STH 36, are located at the same location where the DOT performance surveys are being conducted. However, in the case of STH 36, this was not possible due to the construction of different experimental sections in the short distances. For this project, there are five experimental sections within only two SNs. Therefore, the section locations do not overlap with the WisDOT surveys. Incorporating all sections in this study led to the creation of 30 test sections. These sections are detailed below.

Table 1-2 List of test sections investigated in this study

Section	Age	Thickness	Latitude	Longitude	SN	PCI
STH 21-A	2	3.88	44° 1'32.27"N	90°13'49.33"W	24130	100
STH 21-B	2	4.00	44° 1'30.45"N	90°10'22.58"W	24150	100
STH 21-C	2	3.75	44° 1'29.23"N	90° 7'34.50"W	24170	100
STH 17-A	13	3.63	45°37'46.37"N	89°22'54.39"W	20055	53
STH 17-B	13	3.75	45°38'15.41"N	89°22'42.22"W	20060	58
STH 178-A	15	2.63	45° 4'0.03"N	91°15'52.38"W	132140	82
STH 178-B	15	4.00	45° 5'32.25"N	91°13'56.06"W	132170	67
USH 141-A	3	4.13	45°18'49.75"N	87°59'28.12"W	122600	100
USH 141-B	3	4.81	45°21'22.15"N	87°57'17.82"W	122630	96
STH 13-A	2	4.38	44°41'20.51"N	90°12'7.88"W	13670	100
STH 13-B	2	4.13	44°41'45.52"N	90°12'42.75"W	13680	100
STH 36-A	1	4.13	42°51'21.42"N	88° 6'25.50"W	46880*	100
STH 36-B	1	4.63	42°51'27.72"N	88° 6'7.51"W	46880*	100
STH 36-C	1	4.75	42°51'38.32"N	88° 5'36.48"W	46880*	100
STH 36-D	1	3.63	42°52'25.57"N	88° 3'24.76"W	46890*	100
STH 36-E	1	3.25	42°53'5.18"N	88° 2'36.06"W	46890*	100
STH 73-A	4	4.22	42°53'18.10"N	89° 3'9.45"W	93470	97
STH 73-B	4	3.88	42°54'34.92"N	89° 3'21.11"W	93480	93
STH 73-C	4	4.88	42°59'48.83"N	89° 4'18.32"W	93540	85
STH 73-D	3	3.75	43° 0'54.84"N	89° 4'17.62"W	93550	98
STH 11-A	8	3.50	42°39'57.13"N	88°14'20.94"W	8330	89
STH 11-B	8	3.38	42°41'17.16"N	88°13'6.28"W	46750	99
STH 77-A	4	3.50	46° 9'16.17"N	90°50'43.75"W	97030	100
STH 77-B	4	3.69	46° 9'18.15"N	90°44'44.76"W	97070	100
STH 80-A	4	1.58	43° 8'12.94"N	90°21'32.01"W	98780	96
STH 80-B	4	1.58	43° 9'47.40"N	90°20'50.02"W	98800	100
USH 8-A	2	1.37	45°34'5.25"N	89°37'41.82"W	2890	100
USH 8-B	2	1.37	45°36'30.53"N	89°33'6.83"W	2930	97
STH 26-A	2	4.63	43°46'59.03"N	88°40'30.47"W	30600	100
STH 26-B	2	4.25	43°50'3.24"N	88°40'29.54"W	30630	100

*Some of the sections from project STH 36 are located within the same SN. This is the NCHRP project that has used multiple mix designs in a short distance next to each other.

For each of the sections shown in the table, a coring plan is devised to evaluate the mixture and binder properties within each of the samples. In addition, production, construction, and performance data were collected for the projects of which these sections belong. When available, all the data is geo-related such that the relationship between pavement history and performance can be investigated.

The coring plan is represented in the following diagram. The plan is designed such that evaluation of change in performance between wheel path (WP) and between wheel path (BWP) is conducted, enough cores for mechanical and binder testing is available, and overlapping distresses with binder and mixture properties is possible.

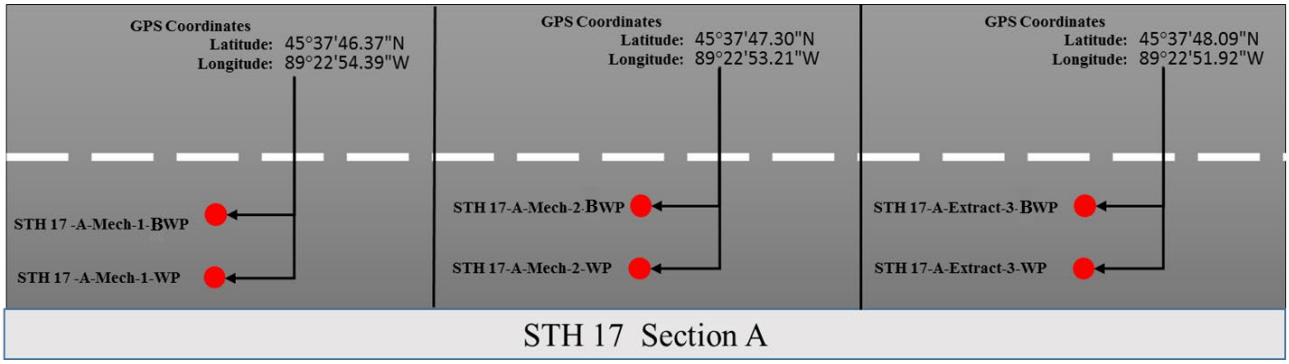

Figure 1-2 An example of the coring plan for STH 17, section A

The following flow chart shows how the cores were employed to characterize the mixes, binders, and aggregate.

1.4 Core Characterization Testing Plan

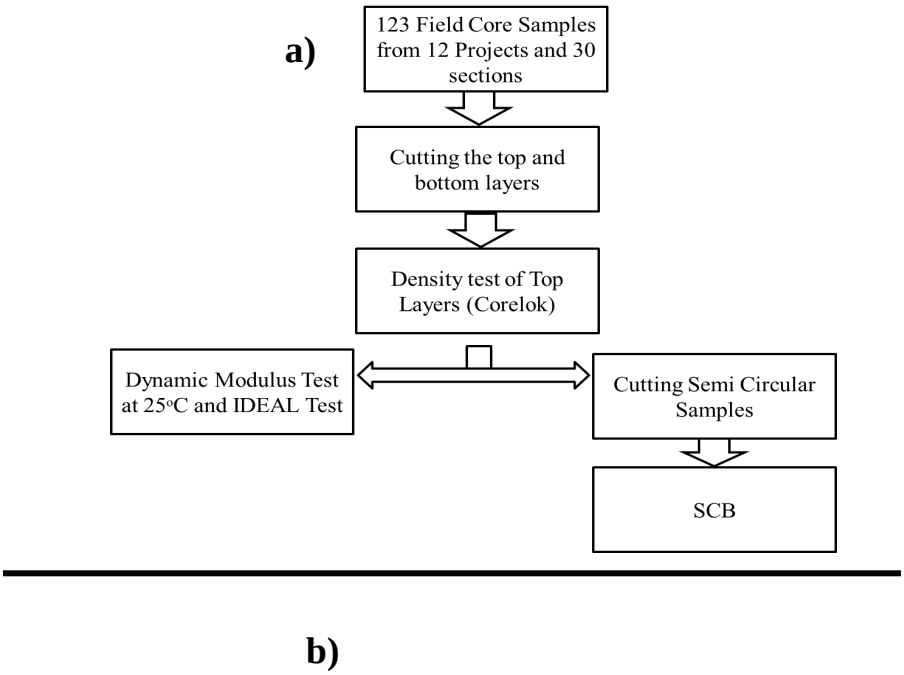

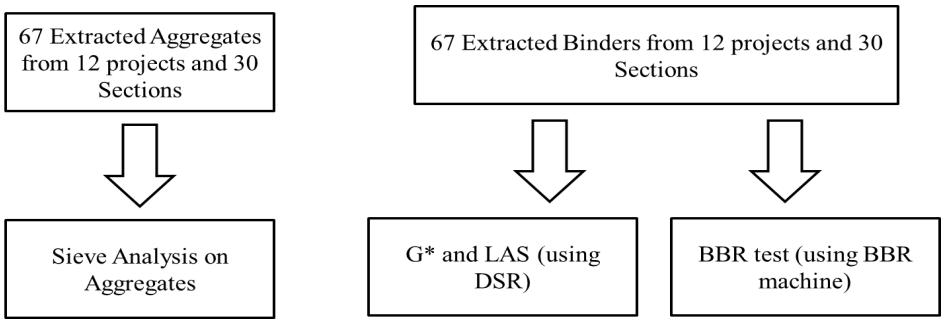

Figure 1-3 Flow chart for core testing a) mixture testing plan, b) binder and aggregate testing

The following tests were conducted on the field core samples.

1.4.1 Semi Circular Bending Test (SCB)

After verifying the air void content of the cores, the samples were cut to obtain two half-discs for the Semi-Circular Bend (SCB) test. The cutting process was made with the use of a circular diamond blade to obtain a disc of 50±1 mm in thickness. Each disc was cut in half and a notch was made in the middle of each SCB test specimen such that the depth of the cut was 15±1 mm and the width was 1.5±0.1 mm. Upon completion of the cutting process, the test specimens were placed in a water bath set at a temperature of 25^{o} C for 2-2.5 hours prior to testing. For low-temperature fracture testing the samples were conditioned at -18ºC for 3 hours.

The SCB test is a three (3) point bend test that is used to measure the ability of asphalt mixture samples to resist crack propagation. The test can be used to characterize crack propagation at both intermediate and low temperatures. For the purposes of this study, the test is conducted at both intermediate temperature and the low temperature. The low temperature used for this test was -18^{o} C, based on the low-temperature grading of the design binders in the mix, which extracted from the original mix design documents. The test procedures were in accordance to the AASHTO TP 124, “Standard Method of Test for Determining the Fracture Potential of Asphalt Mixtures Using the Flexibility Index Test (FIT)” for intermediate temperature testing, and AASHTO TP 105-13 “Determining the Fracture Energy of Asphalt Mixtures Using the Semicircular Bend Geometry (SCB)” for the low-temperature testing.

1.4.2 Indirect Tensile Asphalt Cracking Test (IDEAL)

Indirect tensile asphalt cracking test known as IDEAL is a practical cracking test that can be performed with regular indirect tensile strength test equipment. This test was conducted on samples taken from both WP and BWP locations from all 30 investigated sections. The test was

run at 25ºC on 60 mm width, 150 mm diameter disc-shaped samples. The samples are the same samples that were used for the IDT dynamic test. The procedure of this test is discussed in more detail in NCHRP Project 195 report (2019). An example of the test results on a sample from project STH 77 section B is presented in Figure 1-4.

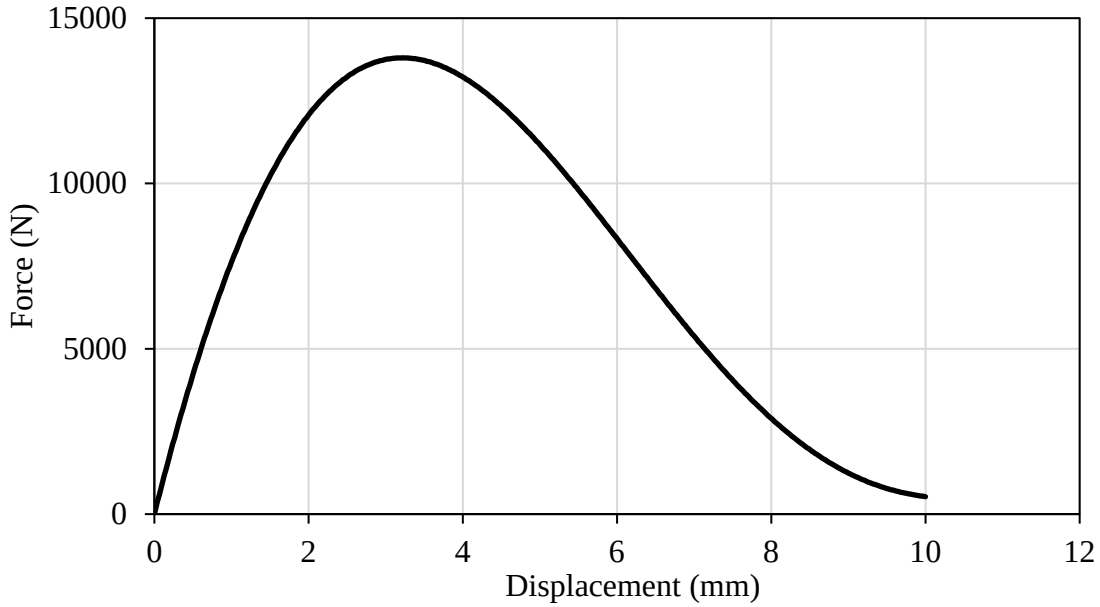

Figure 1-4 Example of IDEAL test results for STH 77, section B

The cracking test index for IDEAL is calculated according to Equation 1-1:

$$CT_{Index} = \frac{t}{62} \times \frac{G_f}{|m_{75}|} \times \left(\frac{l_{75}}{D}\right) \quad \text{(Equation 1-1)}$$

where fracture energy G_f is the work of fracture (the area of the load vs. vertical displacement curve) divided by the area of cracking face; parameter m_{75} and l_{75} are the slopes of the load-displacement curve, and the displacement at the post-peak point where the load is reduced to 75% the peak load, respectively. Parameters of t and D are the thickness and diameter of the sample respectively.

1.4.3 Indirect Tension Dynamic Test

The dynamic modulus of the core samples from 30 sections was measured using indirect tension (IDT) mode. This test was conducted on samples taken from both WP and BWP locations. For this study, 60 mm width disc-shaped samples with the diameter of 150 mm were cut and prepared from the surface pavement layer of the field cores. Using MTS® machine loading frame, dynamic load at frequencies of 0.1, 0.5, 1, 5, and 10 Hz was applied on the disc-shaped asphalt samples at room

temperature and in IDT mode. A video extensometer device was used to measure the gauge length extension between two vertical and two horizontal defined points at the center of the sample. The vertical and horizontal gauge lengths were marked at 50.8 mm prior to the test. Assuming the plane stress state, Hondros solution (Hondros 1959) for the IDT specimens subjected to a strip load was used to define the state of stress and strain in the sample. In this study, Kim *et al*.'s suggested method (2007) was used to analyze the measurements and find the complex modulus at each tested frequency.

1.4.4 Gmb Measurement (CoreLok©)

The Bulk Specific Gravity of the compacted sample, also known as Gmb, of the field core samples, was measured by using a Corelok vacuum sealing device. The test was conducted on samples that were cut and dried for IDT and IDEAL tests. This method is shown to determine the Gmb of compacted samples with greater accuracy than other methods, such as water displacement, parafilm, and dimensional analysis (Cooley *et al.* 2003).

1.4.5 Intermediate Continues Grading Temperature

In order to measure the rheological properties of the field core extracted binders, a dynamic shear rheometer (DSR) machine was used to test Intermediate Continuous Grading Temperature. This is the temperature at which the binder reached 5000 kPa for its G*sin δ. The DSR measures complex shear modulus (G*) and phase angle (δ) giving a complete analysis of the asphalt binder's rheological behavior. This test was conducted to characterize the viscous and elastic behavior of asphalt binders at intermediate temperatures. In DSR testing, the asphalt sample is sandwiched between a fixed plate and an oscillating plate which oscillates back and forth across the sample at 10 rad/sec (1.59 Hz) to create a shearing action. DSR tests were conducted on 8 mm plates. This test was conducted on both WP and BWP samples for the 16 available mix designs.

1.4.6 Bending Beam Rheometer and ΔT_c

For low-temperature grading, a bending beam rheometer (BBR) was used, in accordance with AASHTO T 313, to determine the asphalt binder stiffness and relaxation rates. In BBR testing, a load is applied to the center of a binder beam and stiffness is calculated based on measured deflection and standard beam properties. The m-value which is the slope of the stiffness curve at 60 seconds, is a measure of how the asphalt binder relaxes the load-induced stresses. BBR tests

were conducted to find the low failure temperatures of both relaxation and stiffness of the beam. The differences in these temperatures were calculated as the ΔTc parameter. This test was conducted on both WP and BWP samples for the 16 available mix designs.

1.4.7 Aggregates Gradation Parameters

Sieve analysis was performed on the extracted aggregates from the field cores. The percentage of the passing particles at each sieve number was used to fit the polynomial aggregate gradation curves. The fitting curve order was selected based on the least calculated error. The developed gradation curves were used to calculate the Coefficient of Curvature (Cc) and Uniformity Coefficient (Cu). These parameters are defined as;

$$C_u = \frac{D_{60}}{D_{10}} \quad \text{(Equation 1-2)}$$

$$C_c = \frac{{D_{30}}^2}{D_{60} \times D_{10}} \quad \text{(Equation 1-3)}$$

Where D_n is the particle size at which n% of the particles are finer.

2. Data Collection and Database Development

2.1 Developing a Holistic Database

In this study, the challenge was to reference and coordinate the different referencing systems to create a cohesive geo-reference system for the investigated pavement projects. Therefore, the research approach started with connecting the different data sources into geo-referenced locations and compiling them into a holistic relational database. Data pertaining to three stages of the pavement life; namely material production, construction, and in-service performance, are collected initially for compliance in the case of production/construction, and for maintenance/liability in case of performance. Therefore, the data housing, labeling, and level of details are not designed to be interconnected or meant for further analysis beyond these objectives. Example of such databases available in the WisDOT is shown below in Table 2-1.

Table 2-1 Databases available for the study

Source Database	Description
Pavement Inventory Files (PIF)	Descriptions and pavement distress data for each sequence number (SN) are provided in the PIF database, including International Roughness Index (IRI), Pavement Condition Index (PCI), rutting depth, and individual pavement distress measurements (Alligator, Transverse, and Longitudinal Cracking). This database also includes highway number, surface year, and segment termini description, a directional lane of measurement, date of measurement, region number, and county. Data from the PIF provide a direct measure of flexible pavement performance over a flexible base.
Construction Reports/Plans	Attributes of projects constructed in each year are detailed, including such fields as prime contractor, base type and/or preparation (DGBC, OGBC, milled, pulverized, rubblized, etc.), thickness asphalt layer placed, mixture design (SMA, Superpave ESAL series, etc.), lane-miles of paving, and project identification number. The paving year and highway number in this database merged with the SN in the Meta Manager and PIF databases to develop a holistic database.
Highway Quality Management System	This database developed by Atwood Systems contains important data for QMP material properties. This database cannot be electronically linked to the databases above and requires manual extraction. The research team obtained electronic mix designs and QMP quality control data charts and moving averages to supplement this database.

Different pavement related agencies or even different divisions within an agency often have data collection methods that are not necessarily compatible with the others. Therefore, it is common to see a variety of methods to reference a pavement section's location within the network of roadways. For example, in this study contractors are using a construction project numbering scheme of station numbering, while the DOT performance division use the highway sequence

number (SN) method for referencing the performance surveyed locations. The stations are length-dependent numbers which are based on the construction plans and length of the roadway. On the other hand, Sequence Numbers (SNs) are DOT defined segments of the highways that have referenced locations. These references are based on either landmarks or distances. NCHRP Synthesis 335 (2004) reported a survey in which 96% of highway agencies indicated using the milepost/logpoint method for referencing, while 15% additionally use landmarks in referencing. The milepost referencing method requires each roadway to be given a unique name and/or number, and a distance along the route from a given origin to define points along the route. The research team decided to use a linear referencing system, which consists of a set of procedures and a method for specifying a location as distance, or offset, along with a linear feature, from a point with a known location. Thus, this method includes three components; network of highways, location referencing method, and datum. The location reference method refers to how to identify a single location in the field. The primary domains of location referencing methods include administrative (e.g., county), linear, geodetic/geographic, and public lands survey. Common linear location referencing methods include route/milepost, link node, reference point/offset, and street address (Flintsch *et al.* 2004).

Based on the available information in the PIF database, the number of SNs for each project is first determined. Locations of start and end of SN are identified using the landmark references in the PIF. For some of the SNs, due to the unavailability of a detectable landmark, the length of consecutive SNs is used to determine the start and end location of each SN. Finally, the GPS location of each SN was determined and used to match the station locations in the plans. These steps were repeated for all the selected projects to form a database network-level positioning system that facilitates the connection of data points in the database. Based on the points above, data belonging to the selected projects are collected. All the construction and production data points are given stationing locations following the numbering in the plan's sheets. The data is then grouped by SNs. At this stage, the production, construction, and performance data can be connected. Data points for these three main components of the pavement history are then overlapped based on their geo-location. This allows for investigating localized variability in construction, the relation between production variability and construction variability, and the effect of variability and compliance on long-term performance. The following schematic (Figure 2-1) presents the process followed in creating the relational database.

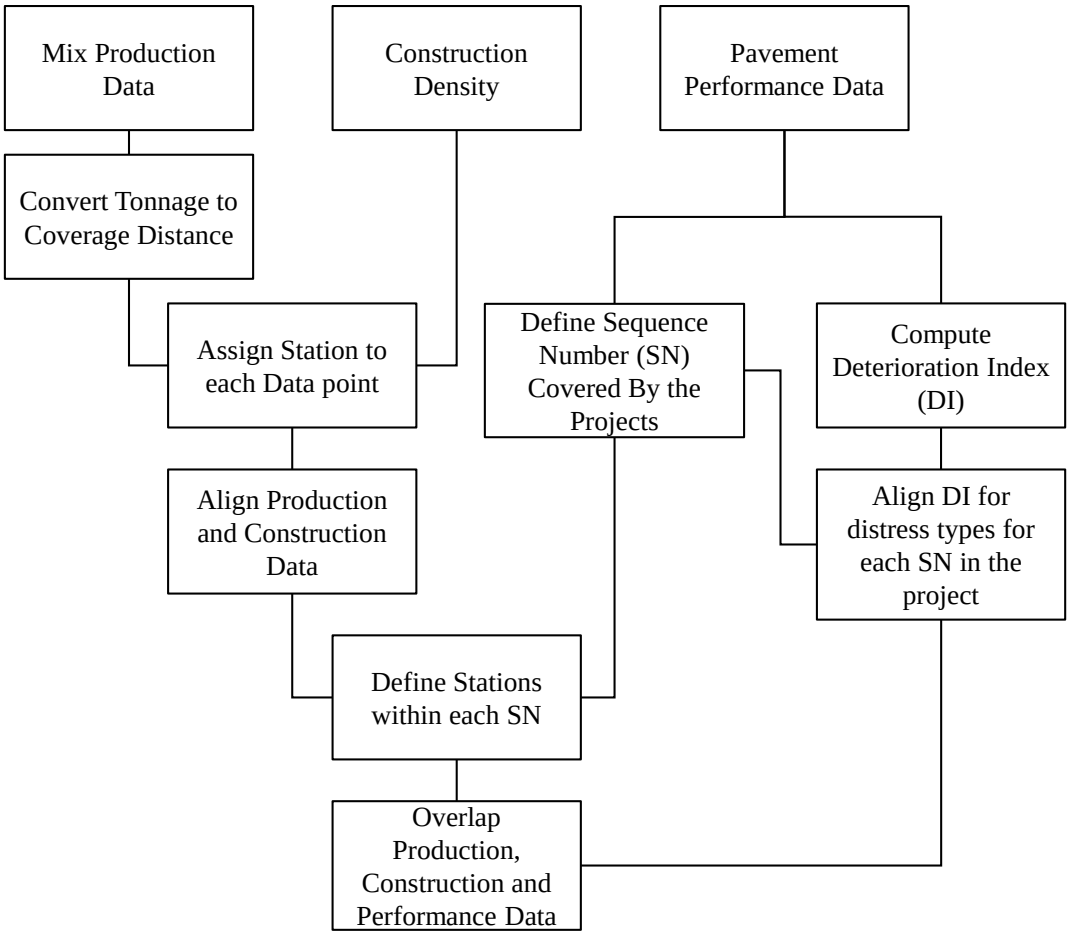

Figure 2-1 Process to connect data sources to obtain the relational database

This method of conversion selected due to its convenience as well as the increasing use of geo-referencing methods in the pavement industry. In fact, nowadays, the Geographic Information System (GIS) and Global Positioning System (GPS) technologies are propelling the use of coordinate-based referencing systems to identify points along routes. NCHRP Synthesis 335 (2004) stated the importance of using such systems for different pavement authorities nationwide. It identified that 35% of surveyed agencies using longitude and latitude, and 13% using state plane coordinate or related systems to reference the location of their performance measurements. Several works have been done in the field of pavement management that tried to improve the quality of decision making, analyzing, and reporting by the use of geographic information. (Lee *et al*. 1996, Harter 1998, Abkowitz *et al*. 1990, Osman and Yoshitsgugu 1994, Jalali *et al.* 2019). Geospatially referencing the data has a wide application in Airport Management (Parsons 2010), Transportation Management (Peng 2007), Environmental Resource Management (Zhang *et al*. 200), and Earthquake Management (Kim *et al*. 2017, Khademina *et al*. 2012). The key aspect of relating all

these systems is linking the separate databases by using their geographical location (Medina *et al*. 1999).

Figure 2-1 does not include activities such as the digitization of hard copies and some other details. The figure is intended to present the outline for creating a relational database assuming all data is digitally available in a format that allows manipulation using commercial database software. For this study, Microsoft Access software is used to execute and process the large data points and integrate the different databases into one relational database. The Access-based relational database is built on three individual core databases, namely, Production, Construction, and Performance. The design of database relationships is shown in Figure 2-2. The structure of the database is such that it allows for extracting queries related to a level of quality understudy, yet all information with respect to other components maintains their connection. For example, in order to investigate the effects of HMA density on the rutting of pavements within the database, an Access-based query was used with rutting as the search object. The query will then include all pavement sections with rutting as reported distress. In addition, it will pull the construction and production data of these sections. All the data retrieved is then presented in one table that includes the different fragments shown in Figure 2-2. Therefore, the extracted information is used for further analysis of the optimized investigation process, while the structure of the global relational database remains to be separate and independent. By using this feature, many queries regarding the effects of binder content, Va, VMA, In-Place Density on the individual distresses such as rutting, alligator, transverse and longitudinal cracking were extracted and analyzed, with results shown in the next chapters.

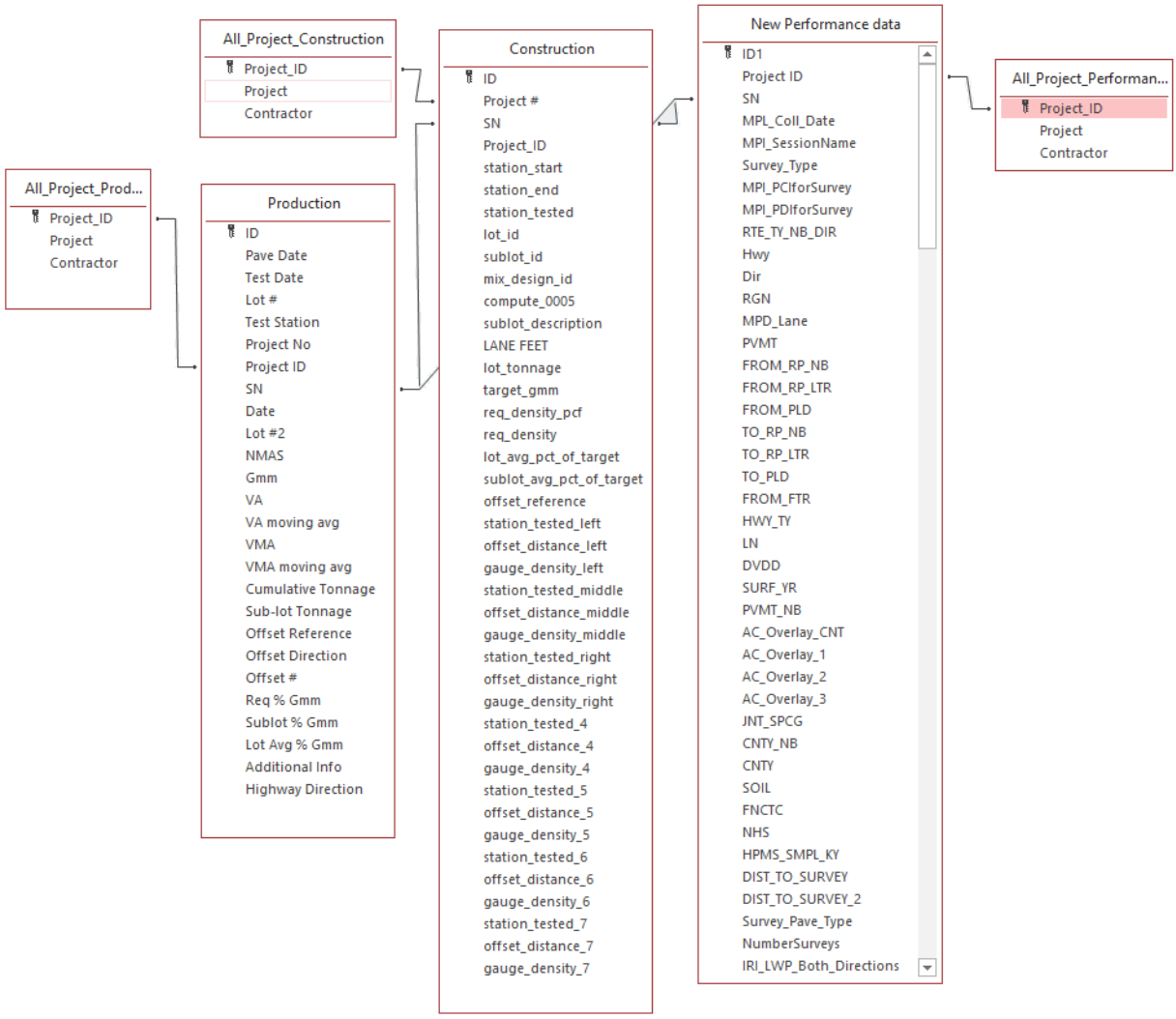

Figure 2-2 Database structure created using Microsoft Access®

2.2 Calculation of Deterioration Index (DI)

The pavement performance data is recorded by the DOT for different distresses. The distresses are surveyed every two years for a given SN. For flexible pavements, the distress survey is conducted to calculate the Pavement Condition Index (PCI) according to the ASTM D6433 (2016). However, for this study, individual distresses are more valuable for tracking the potential correlation of quality control indicators to pavement durability. Based on the PCI method, each distress is recorded in terms of severity level and extent. The recorded data obtained from the DOT underwent multiple steps in order to integrate it into the relational database for analysis. Therefore, four types of distresses are studied as representatives of the long-term performance of the pavement were selected to use for analysis. These types of distresses are as following:

1. **Rutting;** which can be the result of a permanent reduction in the HMA volume due to consolidation, traffic densification, or permanent movement with the constant volume due to the plastic deformation or shear (Morovatdar et al. 2019). It can also be a combination of them (Roque *et al*. 2004). This type of distress was selected to investigate the effects of construction and production parameters like density and asphalt content on it.
2. **Alligator Cracking;** also called Fatigue Cracking, happens due to the maximum tensile strain at the bottom of the asphaltic layer of a flexible pavement after repetitions of enough number of vehicular loads (Huang 2004).
3. **Longitudinal Cracking;** is an extension of top-down cracking that begins from the road surface and gradually extends to the depth of pavement, and it occurs along with the vehicle driving direction of the road. This type of crack is also a point of interest since it is widespread and has detrimental effects on the serviceability of the pavement.
4. **Transverse Cracking;** is happening roughly perpendicular to the pavement's centerline. Given that the majority of the studied projects do not include any overlays, most of the transverse cracks are correlated with the thermal shrinkage of the pavement. Although in a few overlay projects, reflection crackings are also recorded as transverse cracking data. The literature reports a high dependency of transverse cracking on the pavement production and construction parameters (Roberts *et al*. 1991)

According to Shahin (2005), there is a well-established procedure of essential steps in developing the Pavement Condition Index (PCI) value, which is a widely accepted parameter for describing the pavement distress state (ASTM D6433-09) (2017). However, this study focuses on the four types of distresses mentioned above. Based on the PCI method, the first step is to define each pavement distress types, the level of severity, and extent of distress. The next step is calculating the deduct value by using the deduct curves developed by Shahin (2005). The deduction value curves are shown in Figure 2-3, Figure 2-4 and Figure 2-5 for rutting, alligator cracking, and longitudinal/transverse cracking respectively.

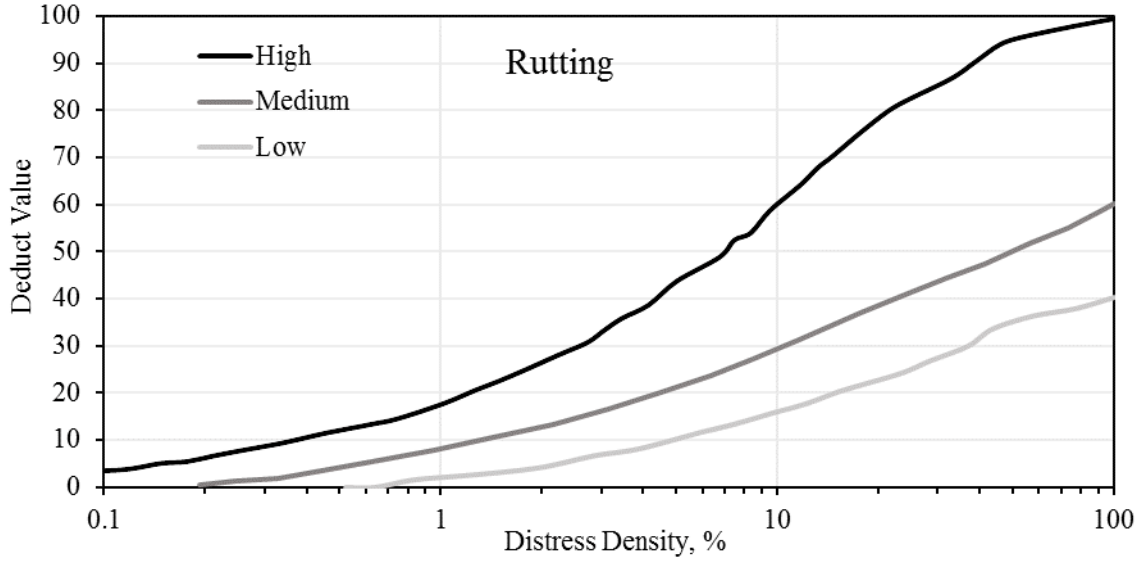

Figure 2-3 Deduct value curves for different severities of rutting (after Shahin 2005)

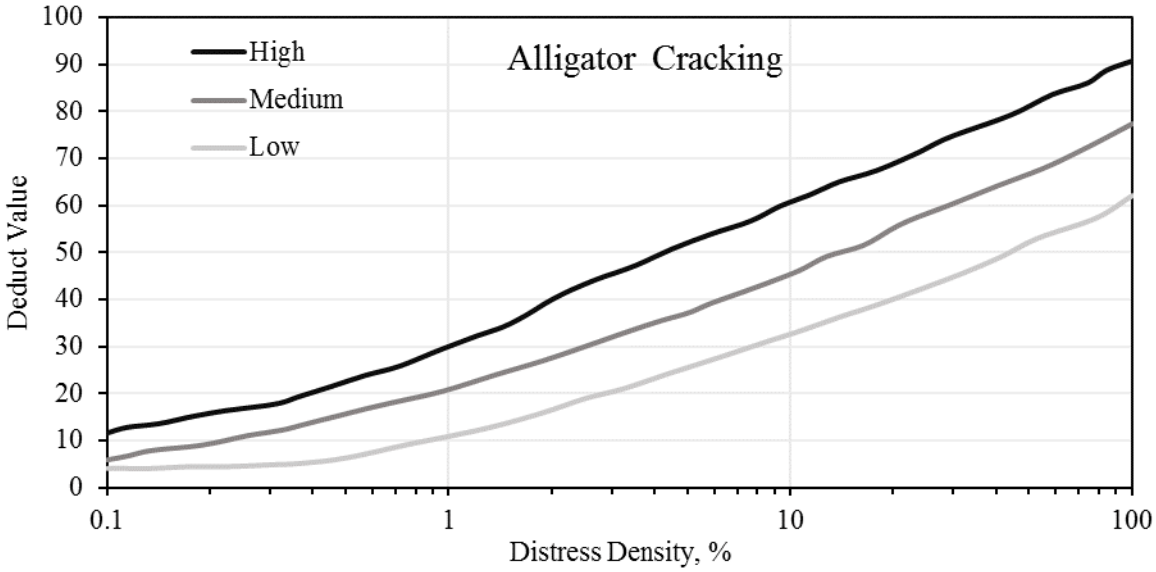

Figure 2-4 Deduct value curves for different severities of alligator cracking (after Shahin 2005)

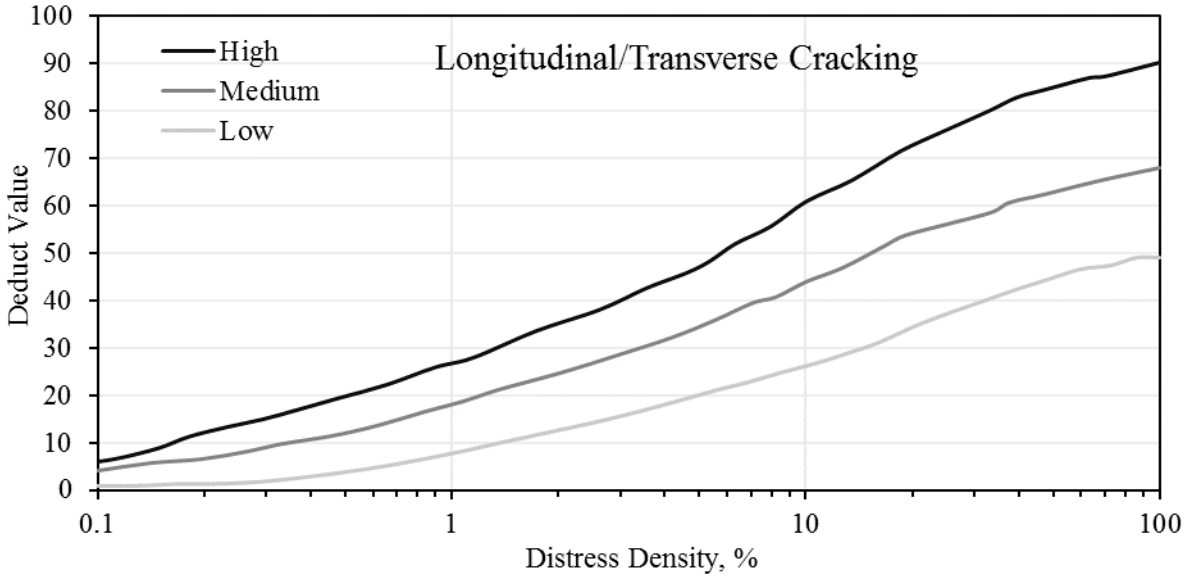

Figure 2-5 Deduct value curves for different severities of longitudinal/transverse cracking (after Shahin 2005)

In order to calculate the "Deterioration Index" values, the data related to the four selected distresses of rutting, alligator, longitudinal, and transverse cracking were identified and isolated from the state DOT performance survey in PIF database. This data contains information regarding the numbers, area, and severity of each distress. The density of different distresses at each severity level was independently calculated based on the length and area of the surveyed sections. Finally, the equations describing the curves shown above are used to convert the density at a given severity level into a deduct value and the total deduct values for all three levels of severities are added together representing a value for the overall deterioration in the pavement due to this given distress. This value is called Deterioration Index or DI, and each distress type is now receiving a single value reflecting its level of deterioration as a score out of 100. Therefore, the high DI represents a high deterioration of the pavement.

This process has been employed by one of the authors in a previous study (Bahia *et al*. 2013). This step is conducted to isolate the degree of deterioration per distress type rather than the generalized PCI. As a result, each SN possesses five distinct deterioration indices; one for each of the four distresses, and one represents the summation of all distresses deterioration indices. The DI values were calculated for all conducted performance surveys. By comparing the survey time and construction time of the pavement, the age of pavement at the time of the survey was determined. By matching the DI values versus the age of the SN for each performance survey, the deterioration

rate also can be easily calculated. During the process, it was noticed that in some cases, the pavement type for several SN was recorded differently than other data sources like the construction maps. Also, due to the contradiction of PIF information of construction year with the construction information, the reported construction years in the contractors' documents are used.

Separate field surveys were conducted by the research group in accordance with the Wisconsin Pavement Distress Survey Procedures to evaluate the pavement performance independently. Based on the results, DI values calculated with the same procedure. However, since the conducted survey reported distresses for every 25 ft and at three different locations of pavement including right wheel path, left wheel path and centerline, the calculated DI values have higher resolution compared to the WisDOT performed survey. This higher resolution enabled the identification of localized problems and construction-related problems. Based on the field surveys, it is observed that there is a high level of construction-related longitudinal cracks on the selected pavements. The research team decided to separate the construction-joint longitudinal cracks from the in-lane ones in order to better understand the sources of the performance problems. Therefore a separate DI value was calculated for the construction-joint longitudinal cracks.

It is important to note that DI is calculated based on the curves provided in ASTM D6433. The authors of this report did not validate the relationship between the distresses and their corresponding DI. This is beyond the scope of this project. The DI method provides a useful tool to quantify each distress independently for further analysis.

In addition to the field surveys, using the already identified GPS coordinates of the SNs ending and starting points, Google Earth satellite, and street photos were used to verify the extent of reported distresses in the field. The problem with this approach was the date of the available photo images in the Google database. Having clear and up-to-date photos of the selected projects was a challenge. However, field surveys and taken photos helped to overcome this issue.

2.3 Environmental Factors

The Environmental parameters were all extracted from the database of the National Oceanic and Atmospheric Administration (NOAA). The database provides information per county for each state. There are multiple weather stations within each county. In the state of Wisconsin, the relevant climate information of the nearby stations to each project was extracted, and they were ranked

based on their distance to the center of the project. The three nearest stations were used for further data interpolation and construction of an accurate climate database for each project. Names of the three nearest stations and their corresponding distance factor are presented in Table 2-2. The Haversine formula was used to calculate the distance between the coordinates of the project center and each station. These distance factors are calculated based on normalizing these distances to the farthest station in the county. Therefore, the lower the factor, the closer the station.

Table 2-2 Three nearest weather stations to each project and their distance factor.

Project	County	Station 1	Station 2	Station 3	Distance Factor 1	Distance Factor 2	Distance Factor 3
STH 77	Ashland	Ashland 0.5 WNW	Ashland 3 S	Madeline Island	0.505	0.550	0.295
USH 141	Marinette	Marinette	Peshtigo	Wausaukee	0.092	0.212	0.413
STH 73	Dane	Arboretum University Wis	McFarland 0.8 E	Stoughton	0.446	0.446	0.377
STH 26	Fond Du Lac	Fond Du Lac 2 SW	Fond Du Lac Co Airport	Fond Du Lac	0.268	0.278	0.294
STH 21	Juneau	Mauston 1 SE	Necedah 2 SE	Necedah 5 WNW	0.343	0.106	0.100
STH 13	Wood	Babcock 1 WNW	Marshfield Experimental Farm	Pittsville 0.1 NE	0.104	0.229	0.029
STH 36	Waukesha	Mukwonago 0.5 N	Big Bend 0.1 Wnw	Mukwonago 5.3 W	0.414	0.496	0.355
STH 80	Iowa	Dodgeville	Dodgeville Wisconsin	Mineral Point 7.3 Ene	0.860	0.746	0.915
USH 8	Oneida	Rhinelander Oneida Co Airport	Rhinelander	Rhinelander WJFW TV 12	0.306	0.265	0.280
STH 17	Oneida	North Pelican	Rhinelander 4 NE	Rhinelander WJFW TV 12	0.262	0.290	0.309
STH 178	Chippewa	Cornell 4.1 W	Jim Falls 3 NW	Holcombe	0.263	0.381	0.199
STH 11	Racine	Burlington	Rochester WWTP	Union Grove	0.279	0.342	0.314

Using these distance factors, a weight factor for the interpolation for each station was calculated. These weight factors are presented in Table 2-3. The data for each station were extracted for the years 2000 to 2019. Using the weight factors, the climatic information of each project is calculated. In the case of the absence of the data for a given station, the next closest station was substituted.

Table 2-3 Weight factors for the climate data interpolation for the three nearest stations

Project	County	Station 1	Station 2	Station 3	Weight Factor 1	Weight Factor 2	Weight Factor 3
STH 77	Ashland	Ashland 0.5 WNW	Ashland 3 S	Madeline Island	0.28	0.25	0.47
USH 141	Marinette	Marinette	Peshtigo	Wausaukee	0.60	0.26	0.13
STH 73	Dane	Arboretum University Wis	McFarland 0.8 E	Stoughton	0.31	0.31	0.37
STH 26	Fond du Lac	Fond Du Lac 2 SW	Fond Du Lac Co Airport	Fond Du Lac	0.35	0.34	0.32
STH 21	Juneau	Mauston 1 SE	Necedah 2 SE	Necedah 5 WNW	0.13	0.42	0.45
STH 13	Wood	Babcock 1 WNW	Marshfield Experimental Farm	Pittsville 0.1 NE	0.20	0.09	0.71
STH 36	Waukesha	Mukwonago 0.5 N	Big Bend 0.1 WNW	Mukwonago 5.3 W	0.33	0.28	0.39
STH 80	Iowa	Dodgeville	Dodgeville Wisconsin	Mineral Point 7.3 Ene	0.32	0.37	0.30
USH 8	Oneida	Rhinelander Oneida Co Airport	Rhinelander	Rhinelander WJFW TV 12	0.31	0.36	0.34
STH 17	Oneida	North Pelican	Rhinelander 4 NE	Rhinelander WJFW TV 12	0.36	0.33	0.31
STH 178	Chippewa	Cornell 4.1 W	Jim Falls 3 NW	Holcombe	0.33	0.23	0.44
STH 11	Racine	Burlington	Rochester WWTP	Union Grove	0.37	0.30	0.33

Among the all available climate parameters in the original database, the research team found the following ones more correlated with the scope of this study.

Precipitation related factors;

- Total annual snowfall, measured in millimeter (SNOW).
- Total annual precipitation, measured in millimeter (PRCP).
- The number of rainy days in a given year (DP01).

Temperature related factors;

- Cooling Degree Days; A cooling degree day is every degree that the mean temperature is above 18.3 C degrees during a day (CLDD). this factor considers the time and severity of heat at the same time. For example, if the temperature at day first is recorded at 20.3 C, and 21.3 C for the second day, the Cooling Degree Days would be 5.
- The total number of days above 32.2 C (DX90).
- The total number of days below -17.8 C (DT00).

2.4 Traffic Loading

An accurate account of traffic loading conditions substantially contributes to the proper evaluation of the in-service pavement performance (Morovatdar et al. 2020). In this research effort, the traffic data was collected from the WisTransPortal System. The traffic volume data at 72 Wisconsin

counties are being constantly collected at nearly 30,000 sites on streets and highways around the state. These measurements are available online and are categorized for each county and highway. For this study, the historical traffic reports and measurements of the 12 studied projects were extracted and reviewed. The average of the daily and annual passing traffic volume measured at the different sections of each of the 12 studied highways was calculated. This information was further used to calculate both the average daily traffic of each project as well as the total traffic over the course of pavement life.

3. Database Statistics

3.1 Statistics of WisDOT Highway Network

3.1.1 Four Studied Distresses

The percentage of sections showing signs of damage (non-zero DI) with respect to the age of pavement is presented in Figure 3-1. This data is obtained from the PIF database for 2017. The presented percentages are calculated out of the total segments within the DOT network. The distribution of these distresses shows that 66% of the WisDOT road network have transverse cracking issues after only 4 years from construction.

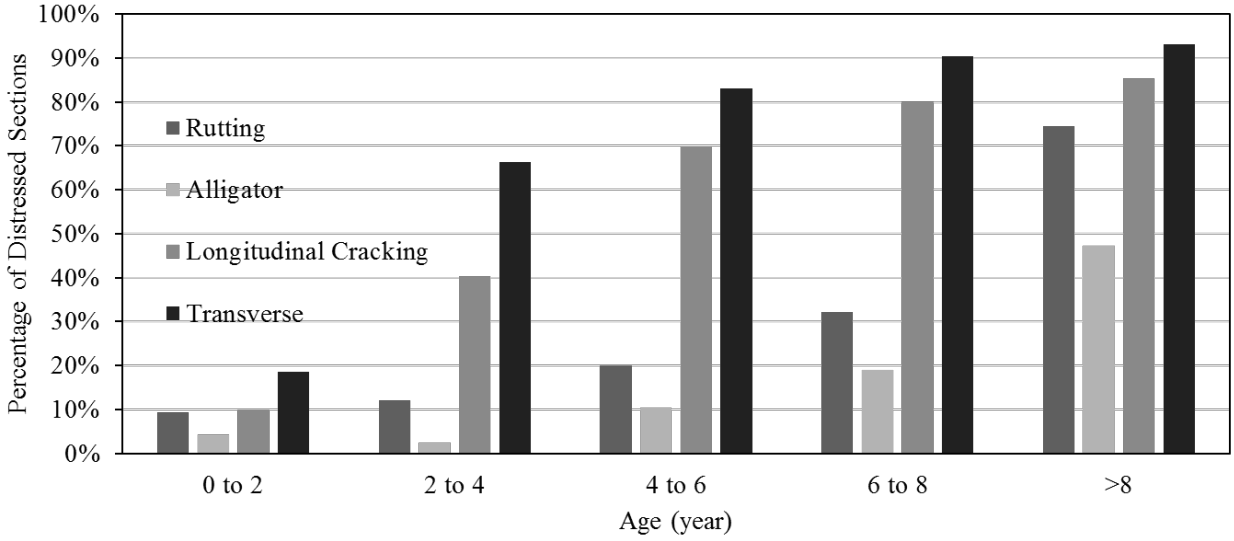

Figure 3-1 Percentage of distresses pavement sections at different ages in Wisconsin

With respect to the extent of damage, the average DI values of WisDOT segments showing distresses are provided in Figure 3-2. The data is distributed with respect to age. The distribution is showing that these sections continue to have a good rating up to 6 years of service. Between 6-8 years the rating can downgrade to fair. But for ages beyond 8 years, the poor condition starts to emerge.

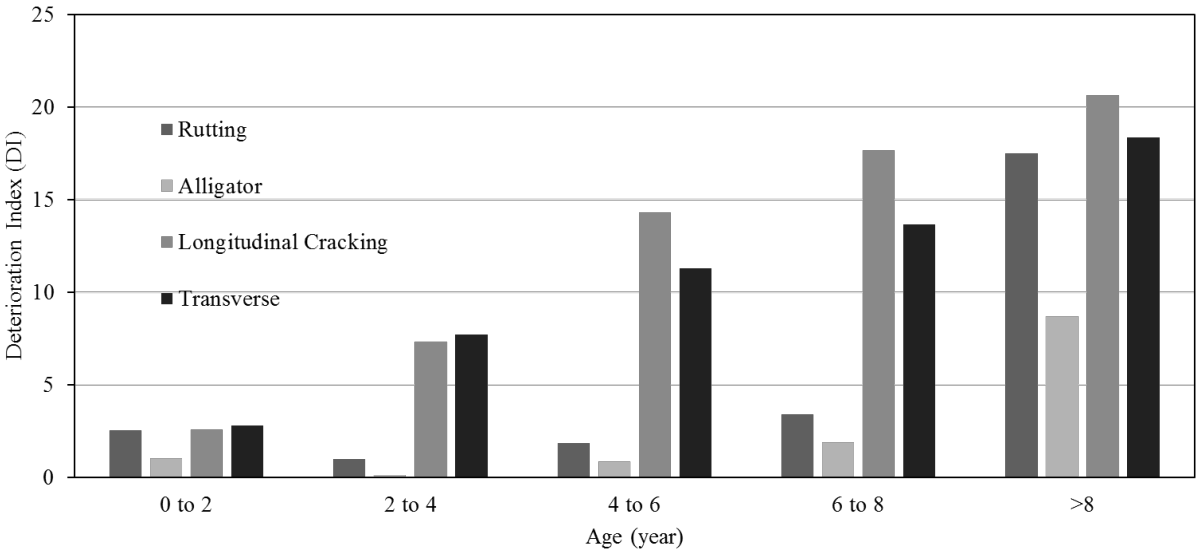

Figure 3-2 Average DI of four studied distresses at different ages in Wisconsin

3.1.2 Other Types of Flexible Pavement Distress in WisDOT Network

As the following tables show, the significance and presence of the other types of distresses are not comparable with the four above mentioned ones. The distribution shown below validates the decision to proceed with the four selected distresses as primary indicators of in-service performance. Figure 3-3 demonstrates a minimal number of sections exhibiting signs of the other distresses up to 8 years of service. After more than 8 years, only patching, block cracking and bleeding at a low level of severity are present in a noticeable portion of the network.

	Distress Type	Bleeding				
	Severity	L	M	H	Mixed	*Total Number of Sections*
Age of Pavement (year)	0 to 2	0.03%	0.00%	0.00%	0.03%	*7545*
	2 to 4	0.02%	0.00%	0.02%	0.04%	*4593*
	4 to 6	0.04%	0.00%	0.09%	0.13%	*4586*
	6 to 8	0.04%	0.00%	0.08%	0.12%	*4811*
	>8	0.10%	0.01%	0.77%	0.87%	*25671*

	Distress Type	Edge Cracking				
	Severity	L	M	H	Mixed	*Total Number of Sections*
Age of Pavement (year)	0 to 2	4.00%	0.87%	0.42%	4.24%	*7545*
	2 to 4	6.81%	0.24%	0.24%	6.92%	*4593*
	4 to 6	13.21%	0.92%	0.22%	13.41%	*4586*
	6 to 8	19.39%	0.87%	0.29%	19.58%	*4811*
	>8	36.24%	5.20%	2.97%	37.35%	*25671*

	Distress Type	PotHoles				
	Severity	L	M	H	Mixed	*Total Number of Sections*
Age of Pavement (year)	0 to 2	0.12%	0.01%	0.00%	0.12%	*7545*
	2 to 4	0.04%	0.00%	0.00%	0.04%	*4593*
	4 to 6	0.11%	0.00%	0.04%	0.15%	*4586*
	6 to 8	0.25%	0.06%	0.02%	0.31%	*4811*
	>8	0.34%	0.12%	0.04%	0.44%	*25671*

	Distress Type	Block Cracking				
	Severity	L	M	H	Mixed	*Total Number of Sections*
Age of Pavement (year)	0 to 2	1.64%	0.74%	0.69%	2.50%	*7545*
	2 to 4	0.83%	0.07%	0.09%	0.94%	*4593*
	4 to 6	1.31%	0.15%	0.09%	1.44%	*4586*
	6 to 8	2.16%	0.23%	0.15%	2.35%	*4811*
	>8	15.25%	4.30%	1.56%	18.25%	*25671*

	Distress Type	Patching on Pavement				
	Severity	L	M	H	Mixed	*Total Number of Sections*
Age of Pavement (year)	0 to 2	1.35%	0.61%	0.46%	2.01%	*7545*
	2 to 4	1.09%	0.20%	0.07%	1.28%	*4593*
	4 to 6	1.81%	0.46%	0.15%	2.29%	*4586*
	6 to 8	2.97%	0.52%	0.33%	3.53%	*4811*
	>8	8.65%	5.41%	2.59%	13.43%	*25671*

	Distress Type	Slippage Cracking				
	Severity	L	M	H	Mixed	*Total Number of Sections*
Age of Pavement (year)	0 to 2	0.03%	0.00%	0.00%	0.03%	*7545*
	2 to 4	0.00%	0.00%	0.00%	0.00%	*4593*
	4 to 6	0.02%	0.00%	0.00%	0.02%	*4586*
	6 to 8	0.00%	0.00%	0.00%	0.00%	*4811*
	>8	0.10%	0.00%	0.01%	0.11%	*25671*

	Distress Type	Weathering and Raveling				
	Severity	L	M	H	Mixed	*Total Number of Section*
Age of Pavement (year)	0 to 2	0.23%	0.12%	0.07%	0.36%	*7545*
	2 to 4	0.15%	0.04%	0.00%	0.17%	*4593*
	4 to 6	0.83%	0.04%	0.04%	0.89%	*4586*
	6 to 8	1.35%	0.10%	0.06%	1.43%	*4811*
	>8	2.32%	0.72%	0.34%	2.80%	*25671*

Figure 3-3 Distribution of other types of distresses reported in PIF

3.2 Statistics of Studied Test Sections

The following graphs show the extent of the observed distresses for the on-site performance survey results conducted by the research team on the 30 studied sections. Based on the results, it was found that there is a discrepancy between PIF and research group surveys. However, both measurements confirmed that the dominant distresses in the field are still the four discussed distresses namely rutting, alligator, longitudinal and transverse cracking. The following graphs are showing their distribution and severity.

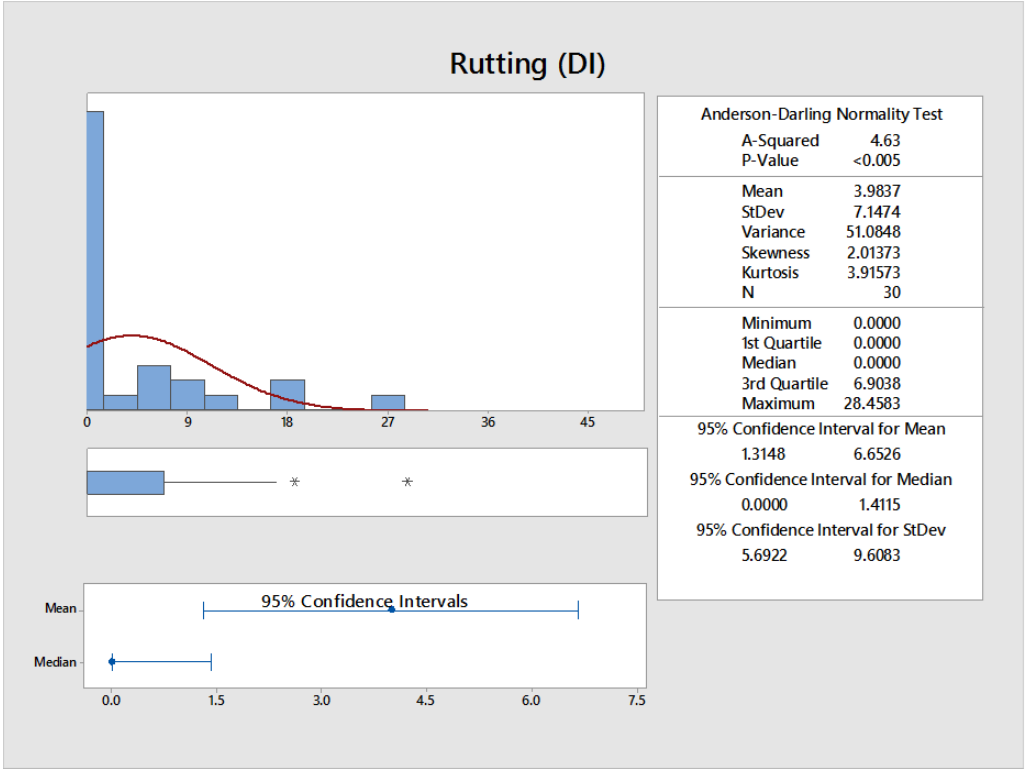

Figure 3-1 Rutting distribution within the investigated sections

The rutting distribution in Figure 3-4 shows that most of the sections have minimal rutting problems. The 95% confidence interval for the 30 investigated sections is between DI values of 1.2 to 6.7. These values are in line with the observed network performance, indicating that rutting is not a major performance issue for Wisconsin, but it may be observed occasionally.

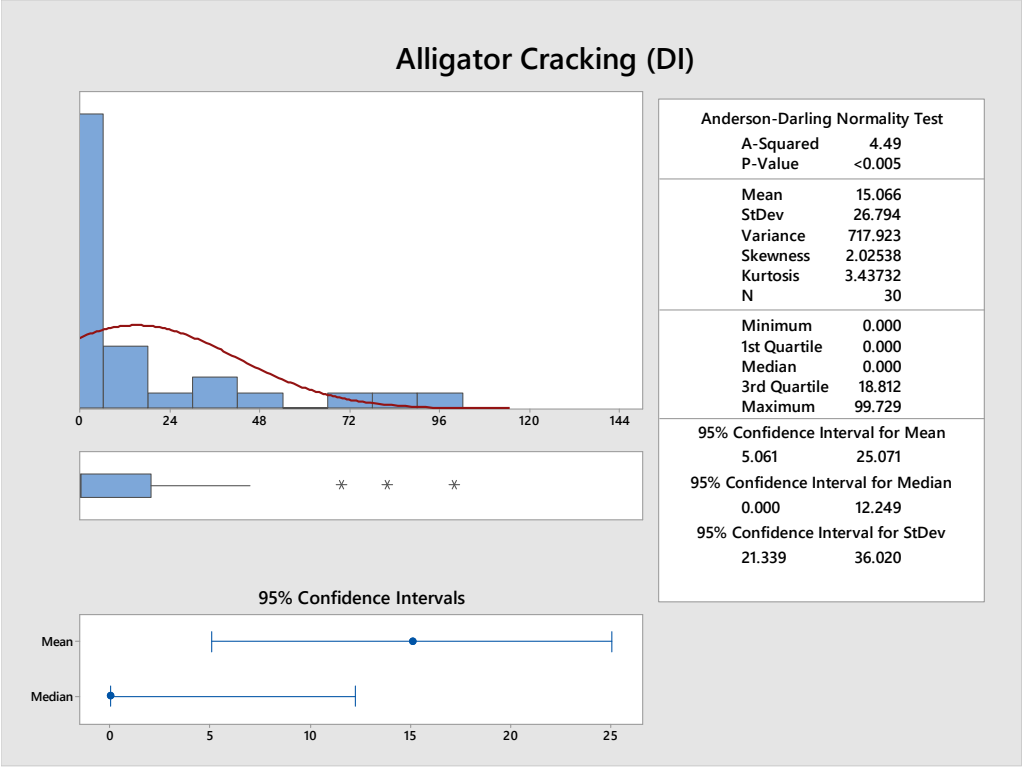

Figure 3-2 Alligator cracking distribution within the investigated sections

The alligator cracking distribution shows a 95% confidence interval on the mean alligator DI of 5.1 to 25.2. This indicates that some sections may have a high level of the distress, but the majority are still higher than the fair rating. This matches with the network analysis. However, a closer investigation of the factors contributing to this distress is needed.

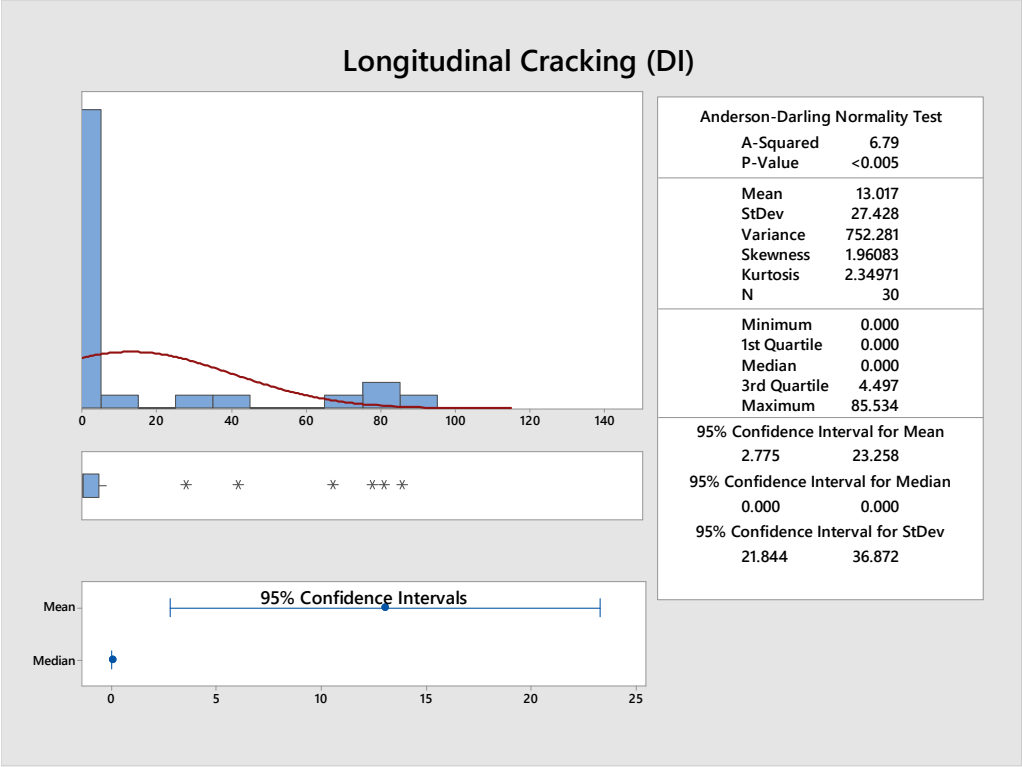

Figure 3-3 Longitudinal cracking distribution within the investigated sections

Longitudinal cracking, as shown in Figure 3-6, follows the same distribution as the alligator cracking. Yet, for longitudinal cracking the majority of the observed cracking are joint longitudinal cracking. Therefore, the analysis conducted on factors influencing this distress only focused on observed in-lane cracks.

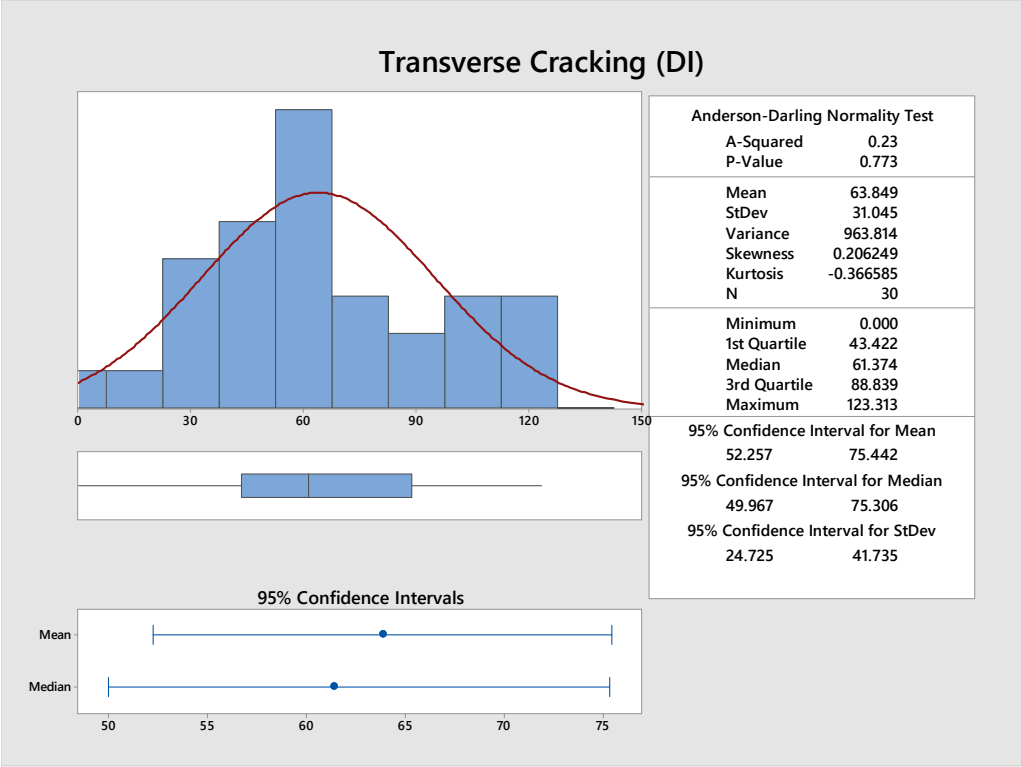

Figure 3-4 Transverse cracking distribution within the investigated sections

For the transverse cracking, the test sections also matched the network distribution. In fact, all test sections exhibited transverse cracking. The confidence interval of the mean cracking DI for the test sections ranged from 52.3 to 75.5. This is a high level of deterioration for this distress given the ages of the pavement sections investigated. In addition, the median of the DI values overlaps with the mean indicating a balanced distribution of this high level of transverse cracking.

3.3 Distribution of Quality Control Indicators

This section presents the distribution of the sampled data used in this research study. It is important to study the distribution of quality measures to understand the boundaries of the analyses that follow. In addition, the distribution provides an overview of the variability and conformity of the quality indicators at the global level. The 30 studied pavement sections can be considered a sample of the Wisconsin roadway network since they cover 16 unique mix designs and distributed across the state. Furthermore, the performance of these sections matches that of the network as illustrated in section 3.2.

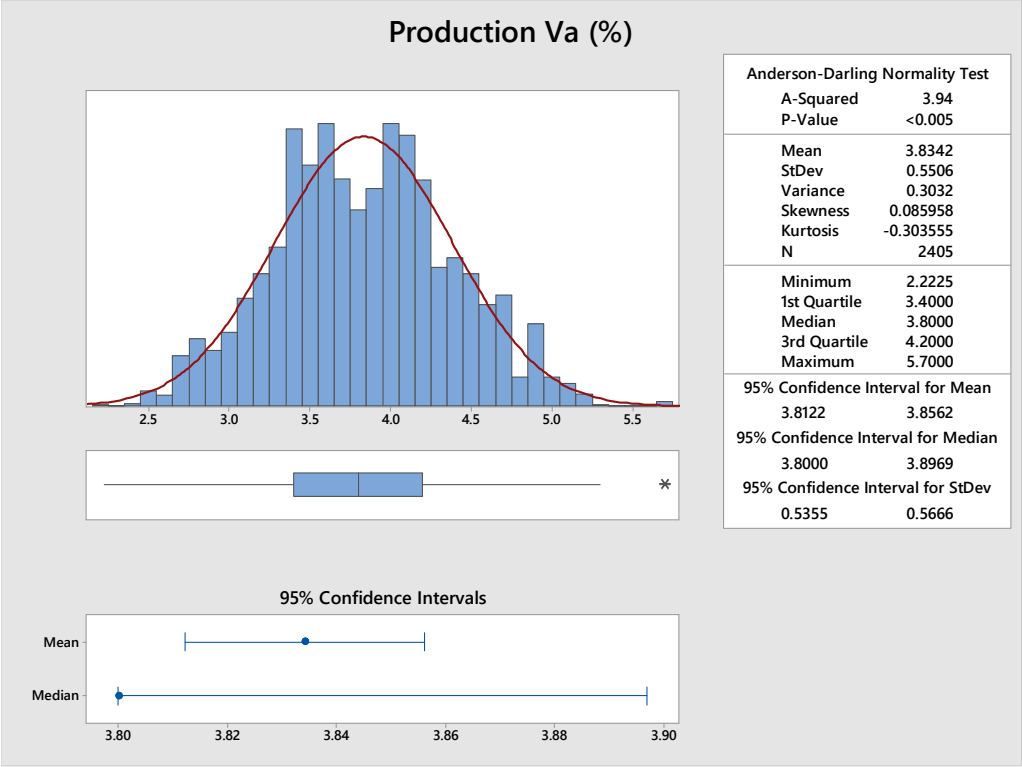

Figure 3-5 Distribution of mix air voids during production

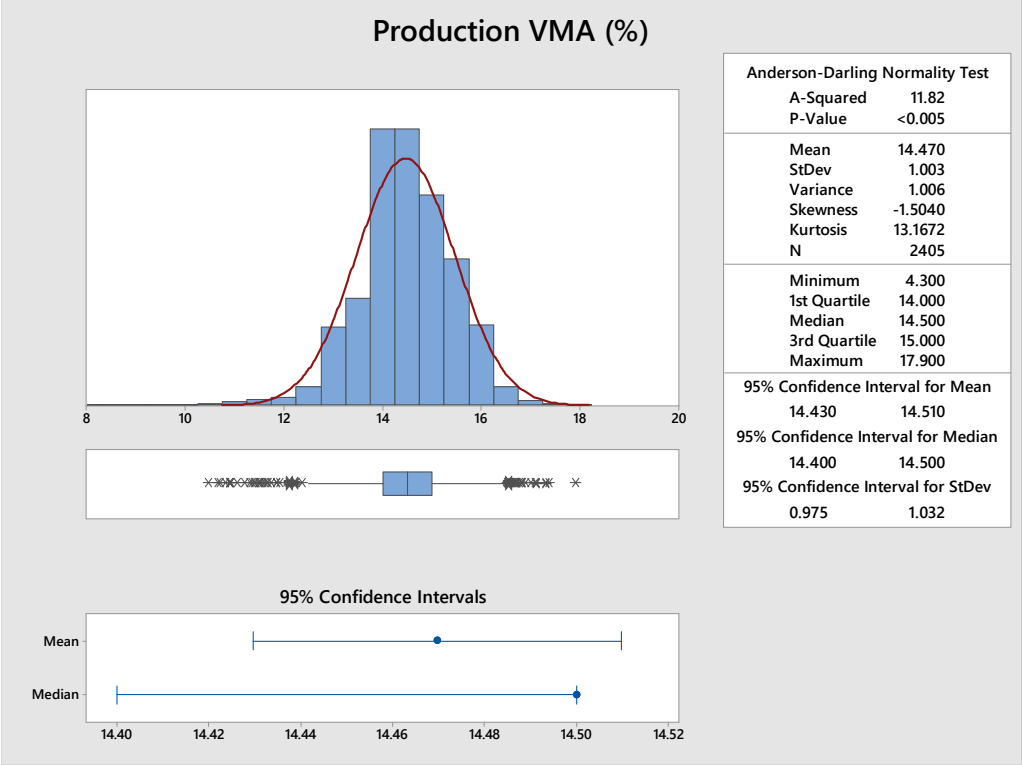

Figure 3-6 Distribution of mix VMA during production

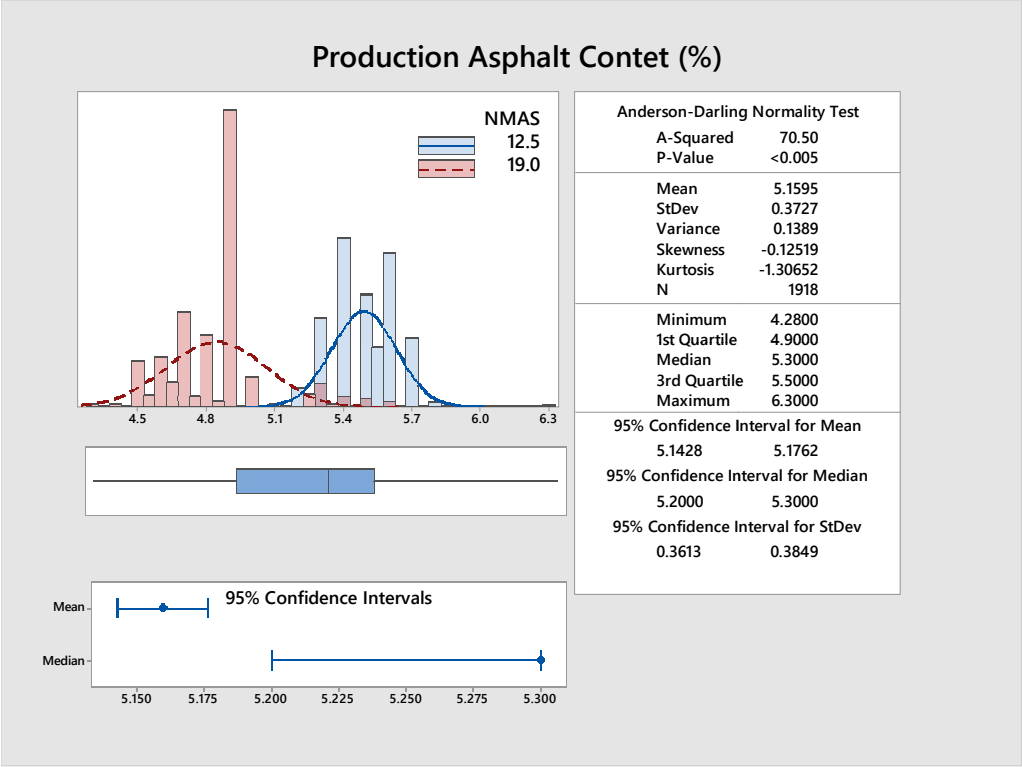

Figure 3-7 Distribution of asphalt content during production

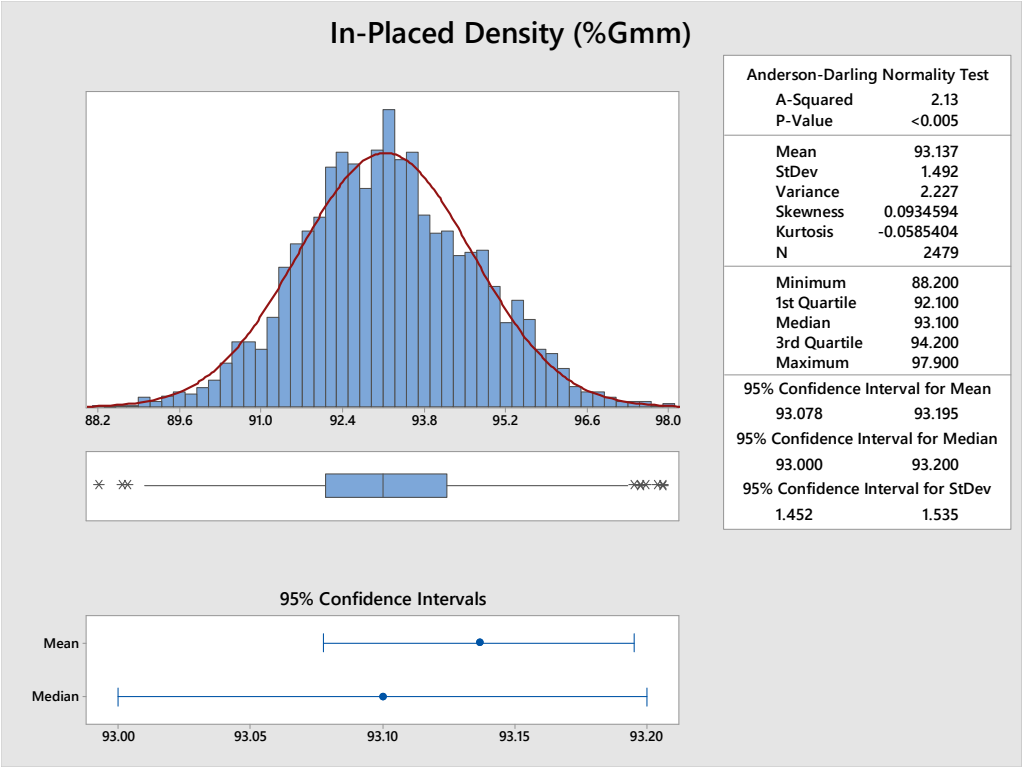

Figure 3-8 Distribution of placement density during construction

The distributions shown in Figure 3-8 to Figure 3-11 illustrate the high conformity of the production and construction quality measures to the Wisconsin specifications. Also, the distributions show a relatively narrow range for quality measures variability.

3.4 Per Project Evaluation

For each of the highways investigated in this study, a summary of the collected production, construction and performance data is presented. Please note that some of the highways did not demonstrate any distresses according to the PIF data. The performance graphs are based on the recorded performance measurements in 2017 version of the PIF.

3.4.1 STH 11 (Designation: Premature Failure)

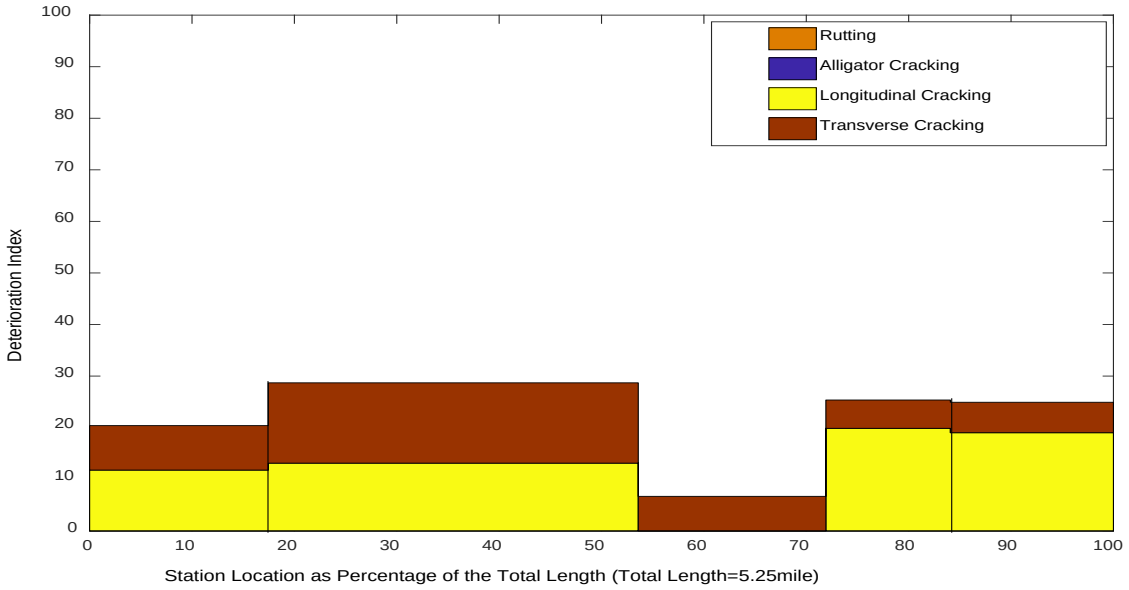

Figure 3-9 STH 11 distress distribution over the length of the project

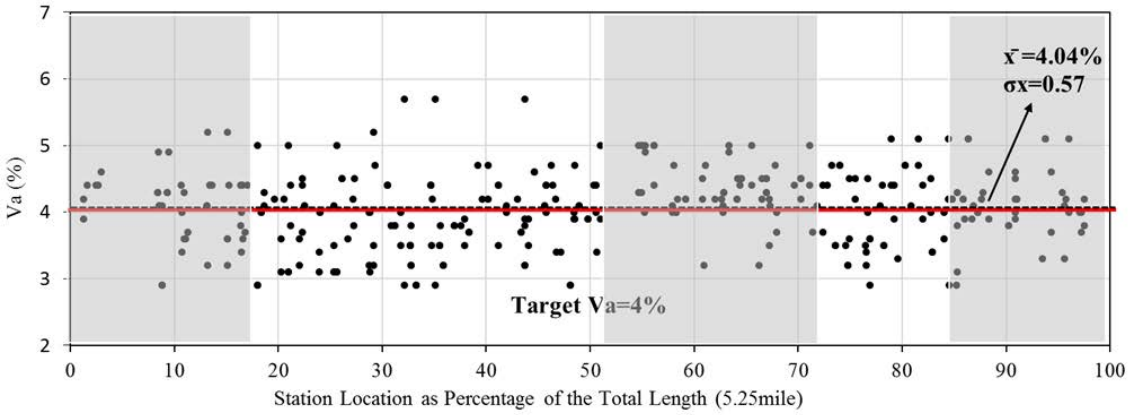

Figure 3-10 Va reported values during production

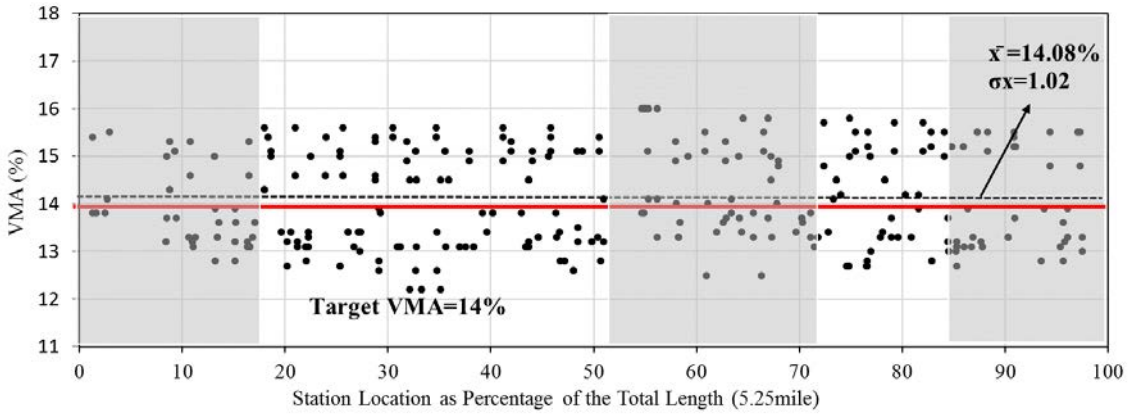

Figure 3-11 VMA reported values during production

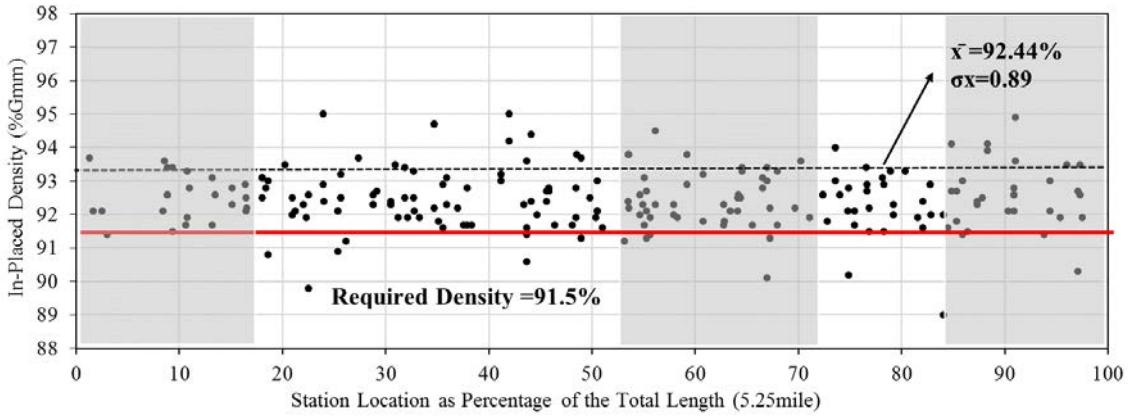

Figure 3-12 Placement density during production

This particular pavement was labeled as a premature failure roadway. The distress data recorded on the PIF shown in Figure 3-12 were recorded at the age of 14. The entire length of the project is showing a consistent level of transverse cracking and longitudinal cracking.

The distress distribution shown in Figure 3-12 indicates that despite the age of pavement, the severity of the recorded distresses is not high. Quality indicators are showing that construction quality is highly conforming to the specs while production is showing a high variability. The production Va ranges from a high of 5.8% to a low of 2.9%. The same observation can be made for the production VMA, which ranges from 12.5 to 16%.

3.4.2 STH 13 (Designation: Air Void Regression)

- No Distress

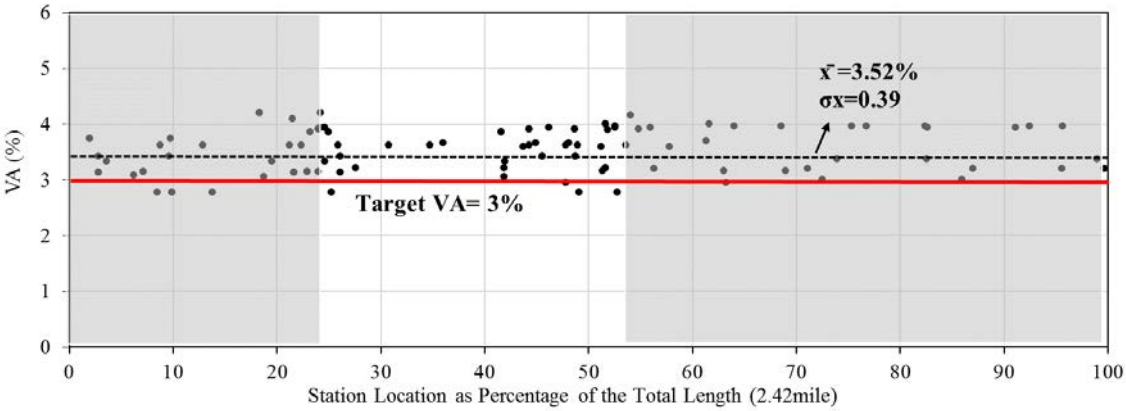

Figure 3-13 Va Reported values during production

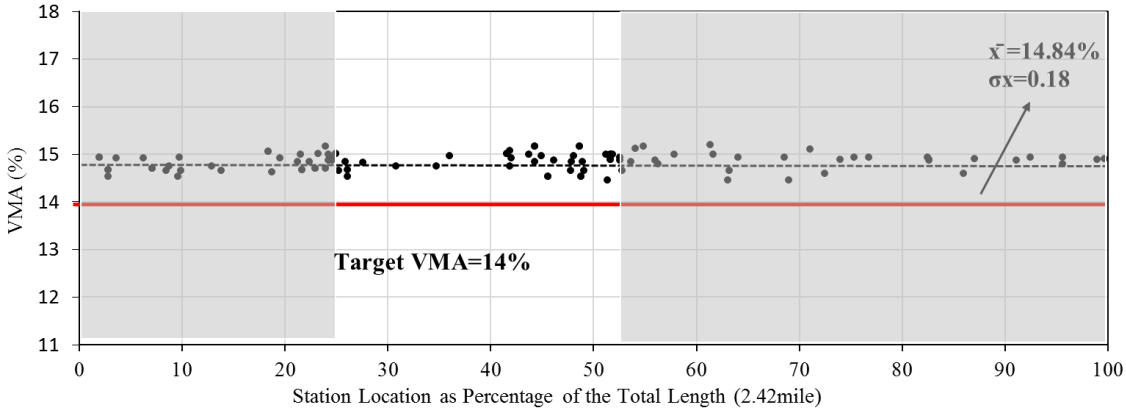

Figure 3-14 VMA reported values during production

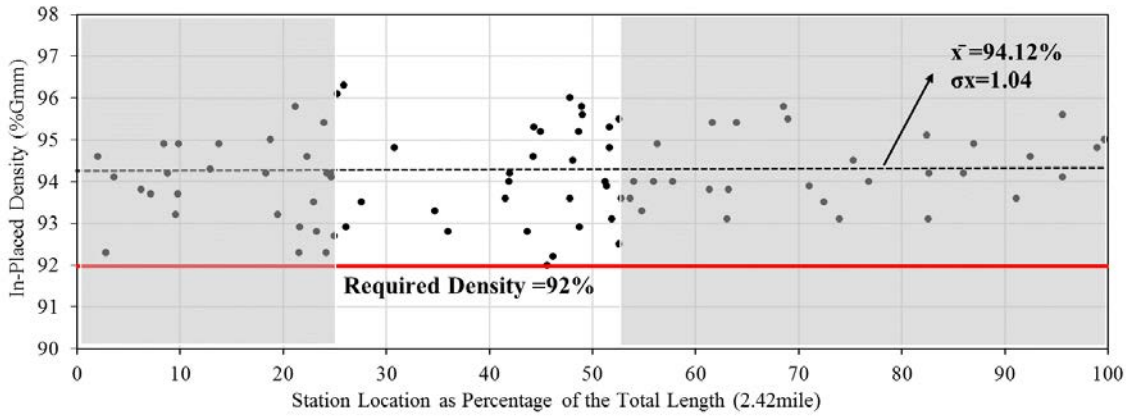

Figure 3-15 Placement density during construction

This project was only two years old at the time of this research. According to PIF, no distresses were recorded. The quality indicators are highly conforming with a low level of variability. While

this project was designed for regressed air void content, average Va is 3.52% with a range of 2.9 to 4.2%. For the air void regression project, this range of Va is similar to other production data for mixes targeting the 4% Va.

3.4.3 STH 17 (Designation: Perpetual Pavement)

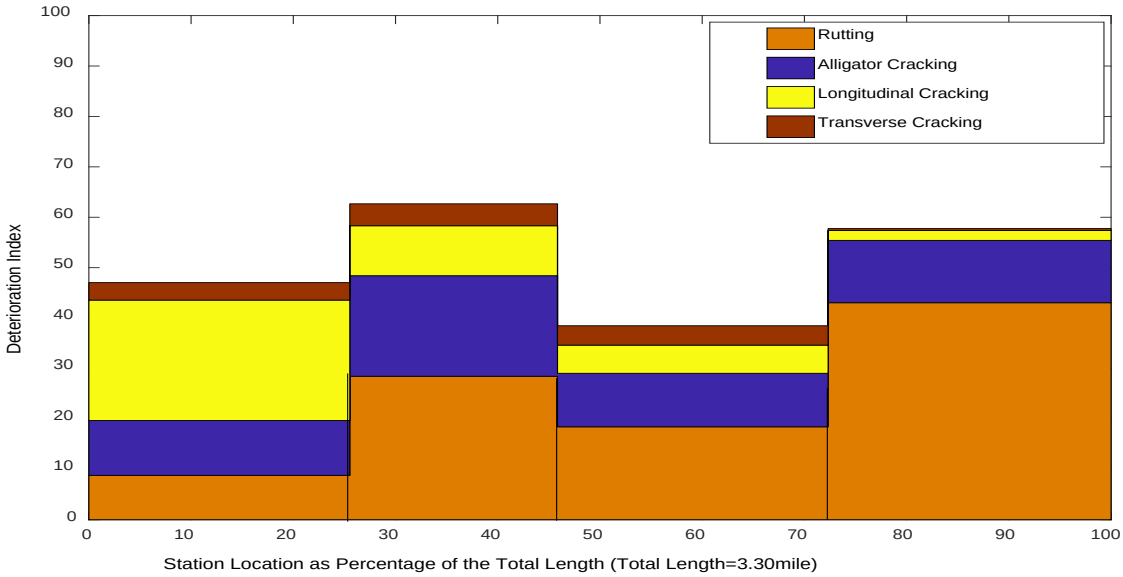

Figure 3-16 STH 17 distress distribution over the length of the project

This project was 14 years old at the time of the latest recorded distresses in the PIF. The distress distribution is shown in the above Figure 3-19. It shows a significant level of rutting compared to the network distribution. The other distresses recorded (Longitudinal, Alligator, and Transverse) are less than or comparable to other projects of the same age.

Due to the unavailability of construction placement data, positioning of Va and VMA is not possible. Therefore, the distribution graphs are presented here based on overall data without geo-referencing.

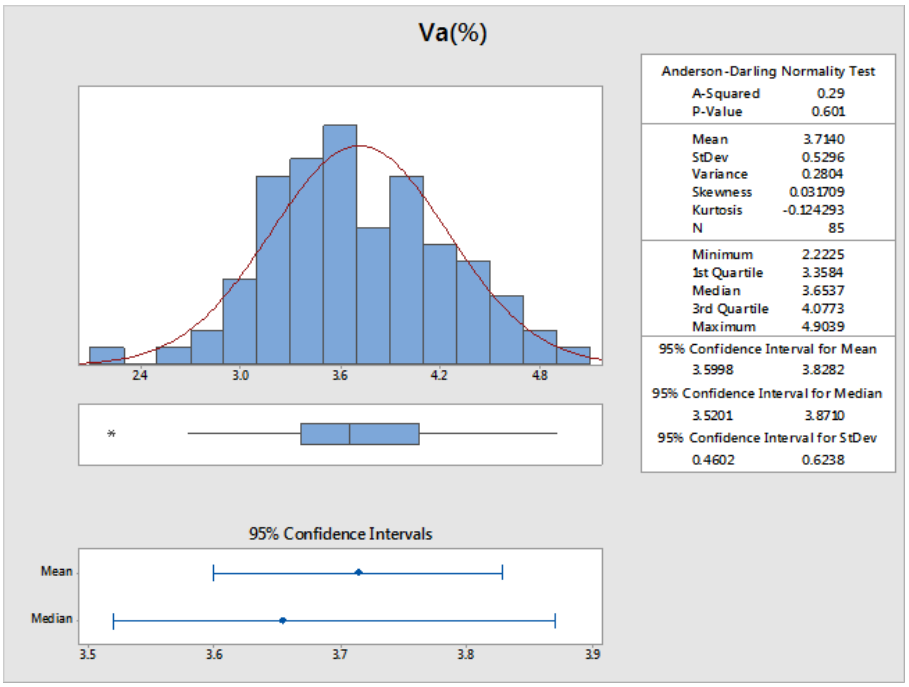

Figure 3-17 Va reported values during production

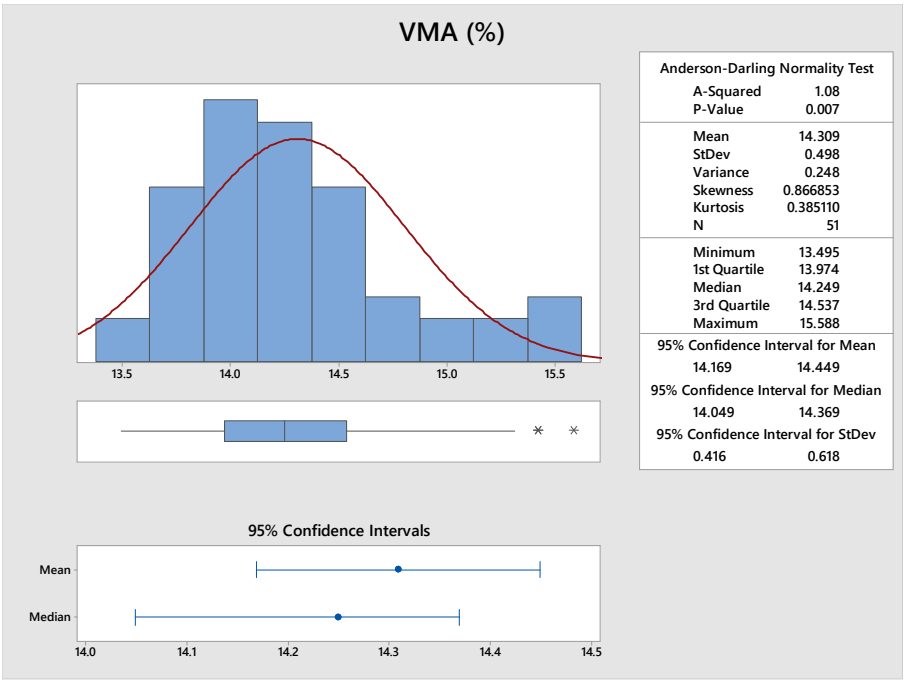

Figure 3-18 VMA reported values during production

The production data show a wide range of Va values (2.2-4.9%) with the majority of the tested lots having a Va under 4%. Yet the 95% confidence interval for Va is between 3.6% and 3.8%, which demonstrates consistency in production. The level of variability in the VMA follows the same trend.

3.4.4 STH 178 (Designation: Premature Failure)

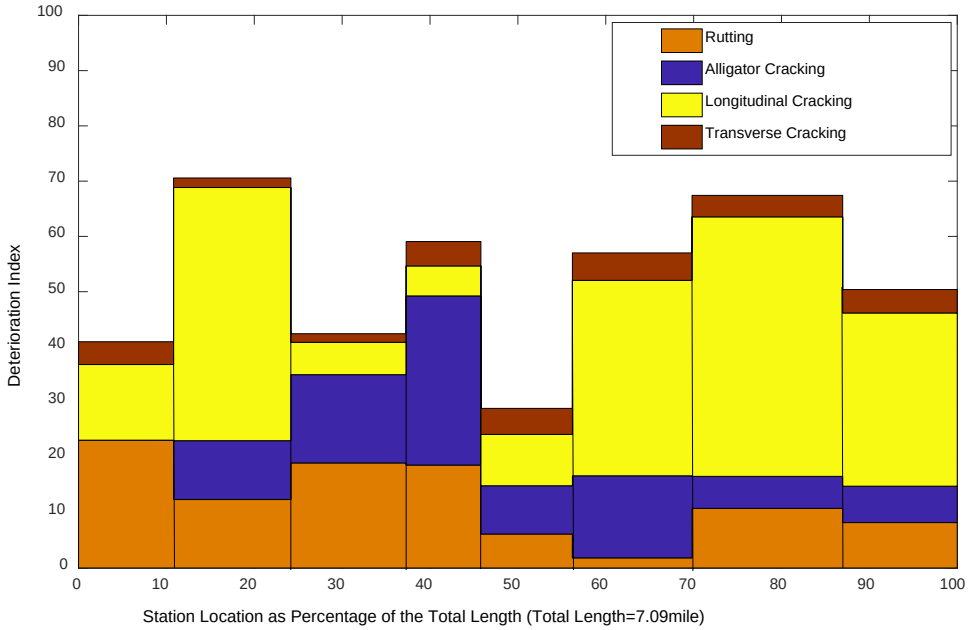

Figure 3-19 STH 178 distress distribution over the length of the project

This project was constructed in 2003. After 14 years is it showing a high level of rutting and alligator cracking compared to the network averages for this age. It is also showing a significantly high level of longitudinal cracking compared to the network. On the other hand, the transverse cracking is lower than the averages for this age.

Due to the unavailability of construction placement data for this project, positioning of Va and VMA is again not possible. Therefore, the distribution graphs are presented here.

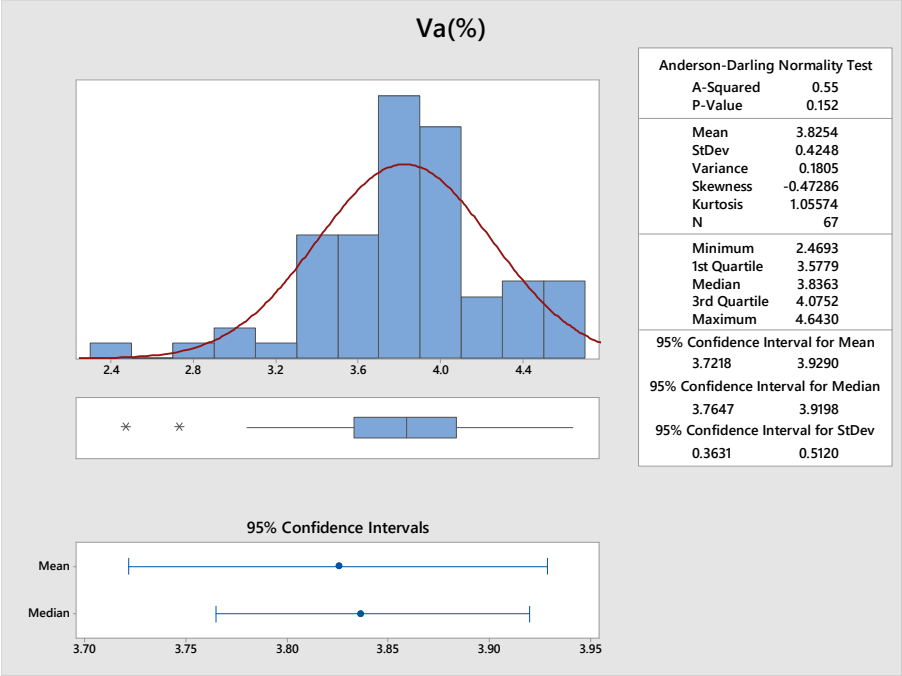

Figure 3-20 Va reported values during production

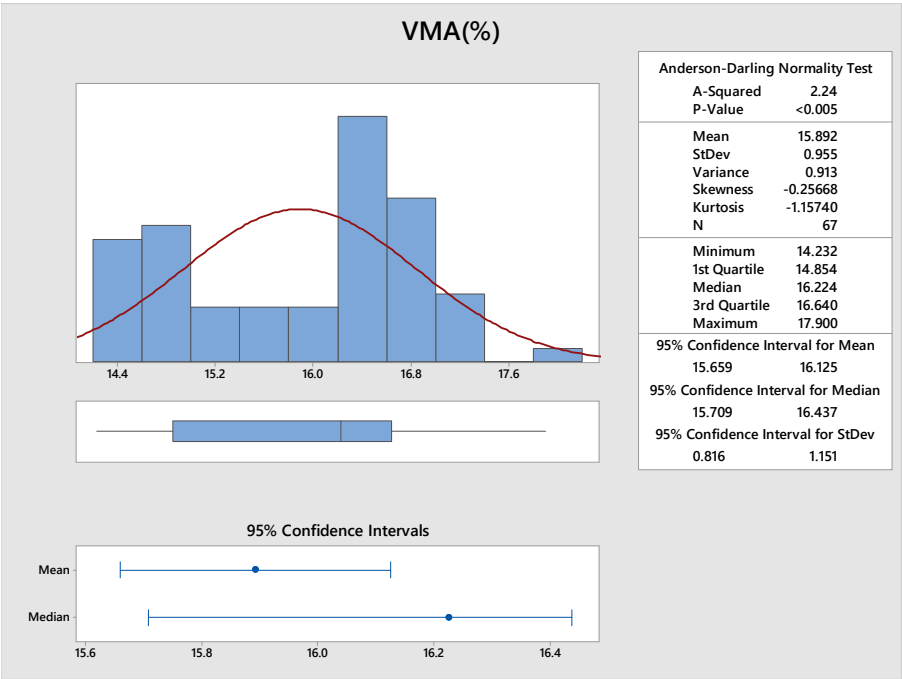

Figure 3-21 VMA reported values during production

The production data shows a wide range for Va, however, the range is still conforming for the most part, to specification limits with a narrow 95% confidence interval. The same is applicable to VMA.

3.4.5 STH 21 (Designation: FHWA Density Demonstration)

- Zero Distress

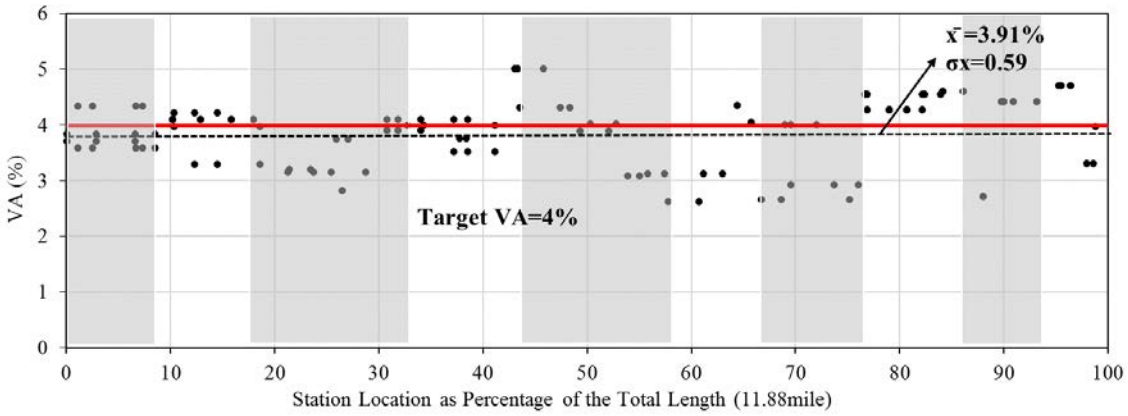

Figure 3-22 Va reported values during production

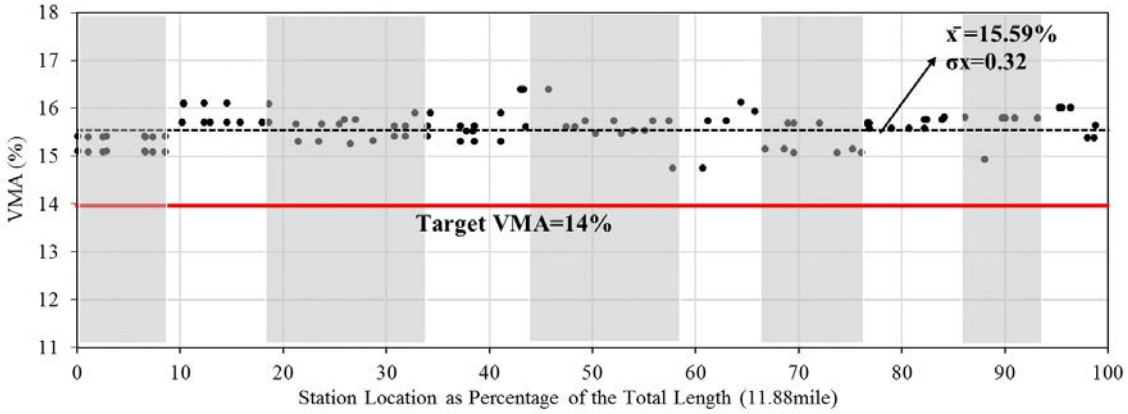

Figure 3-23 VMA reported values during production

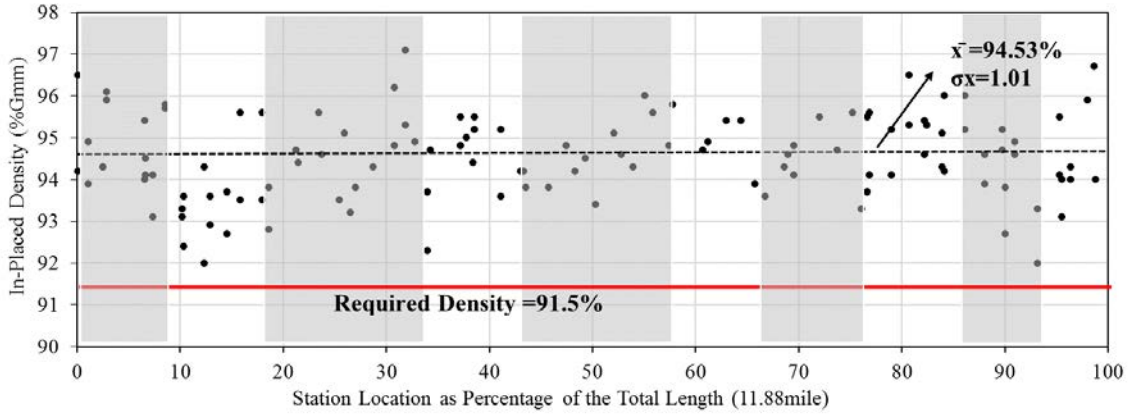

Figure 3-24 Placement density during construction

This project was constructed in 2015. It is showing no distresses according to PIF. As expected, the average placement density is higher than the specification requirements by more than 3%. Production quality is highly conforming with minimal variability.

3.4.6 STH 26 (Designation: High Recycled Project)

Zero Distress

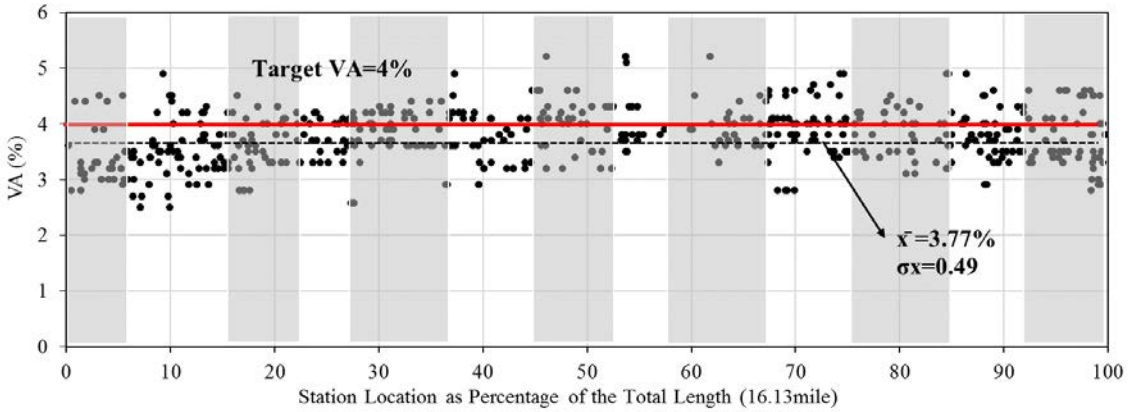

Figure 3-25 Va reported values during production

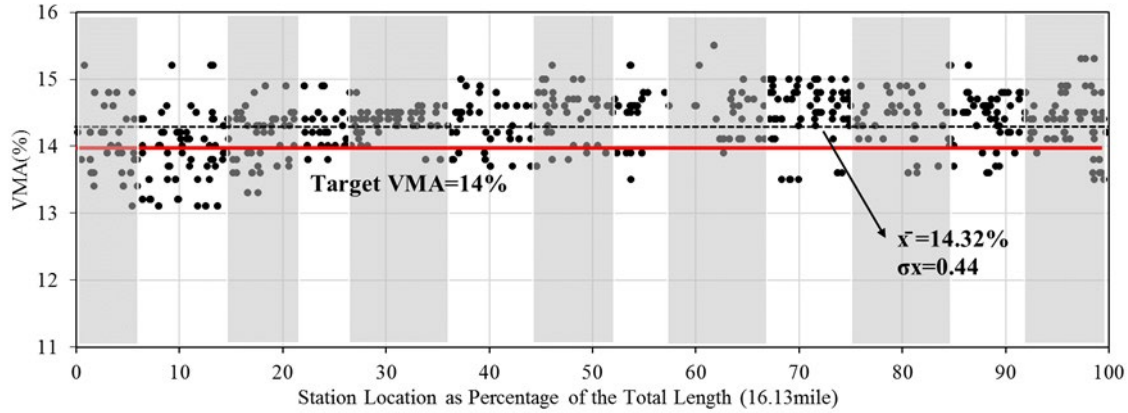

Figure 3-26 VMA reported values during production

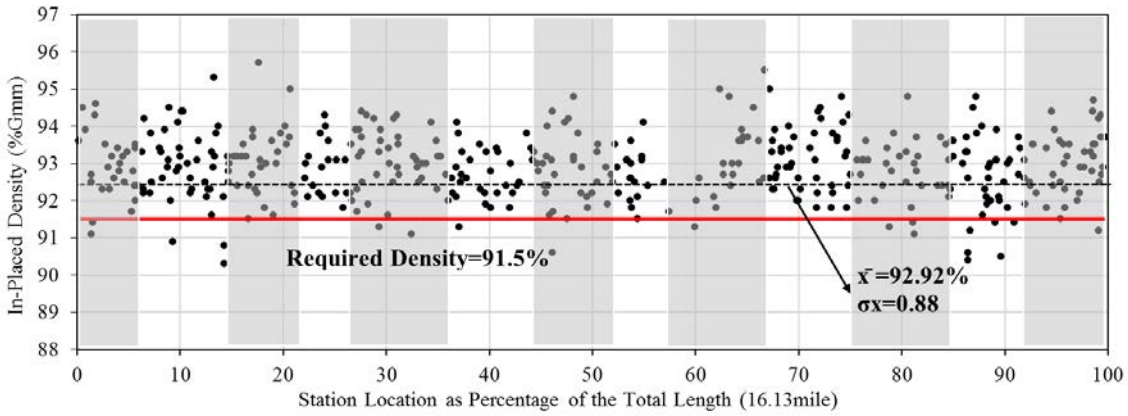

Figure 3-27 Placement density during construction

This project was constructed in 2015. No distresses are recorded in PIF. Few lots are falling outside of the specifications limit for Va and in-place density. But the overall production and construction are consistent. It is important to note that in-place density distribution shows a wide variety within each sequence number. This may be caused by the RAP content in the mix. However, no information regarding the amount of RAP present in the mix and at which lift was found with respect to this pavement.

3.4.7 STH 36 (Designation: High-recycle NCHRP)

- Zero Distress

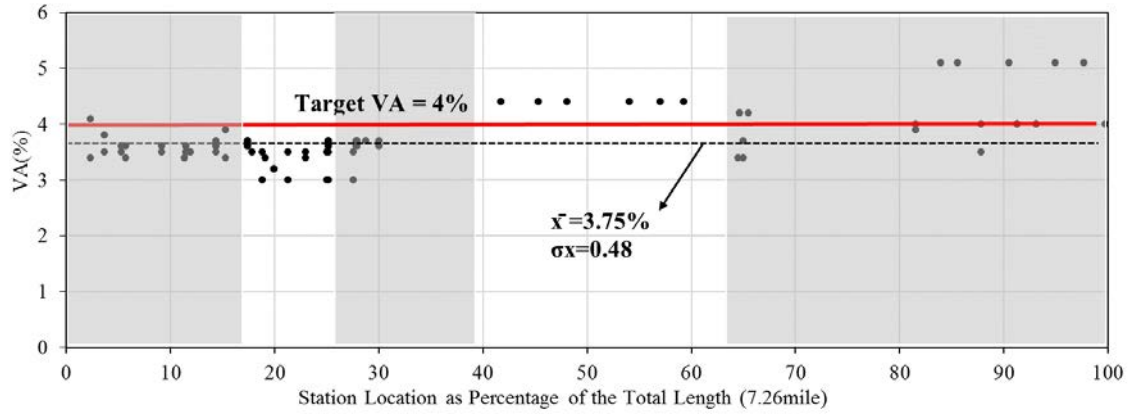

Figure 3-28 Va reported values during production

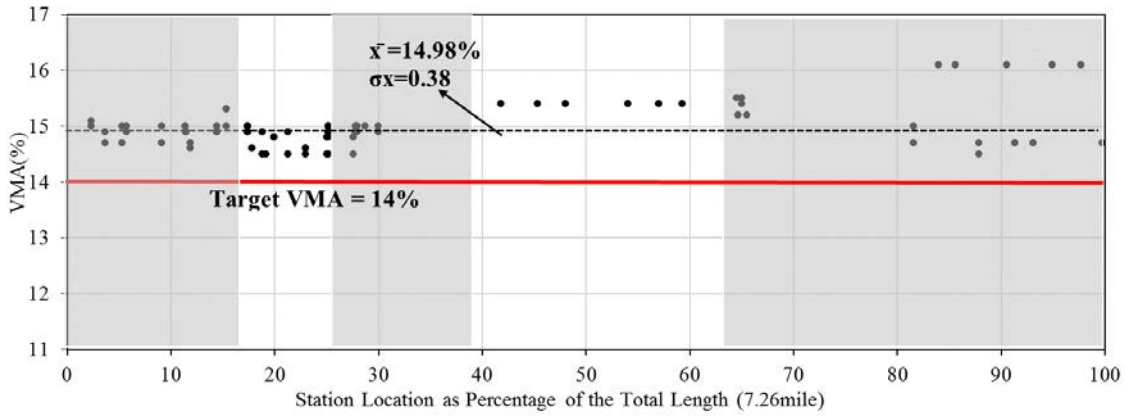

Figure 3-29 VMA reported values during production

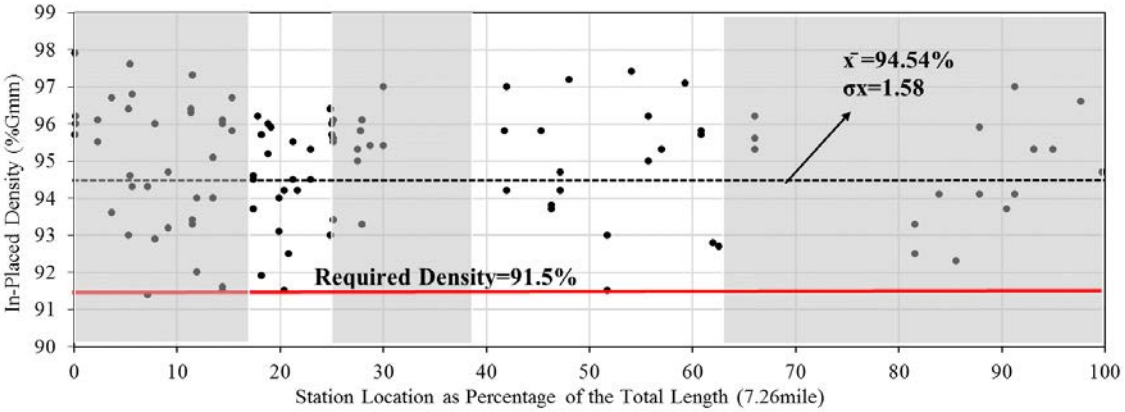

Figure 3-30 Placement density during construction

This project was constructed in 2015. No distresses are recorded in PIF. Production data are conforming to specifications with minimal variability. Placement data is conforming but highly variable. Similar to STH 26, such variability could be influenced by the RAP content. This project was constructed with an asphalt mix with a 31% binder replacement.

3.4.8 STH 73 (Designation: High Recycled Project)

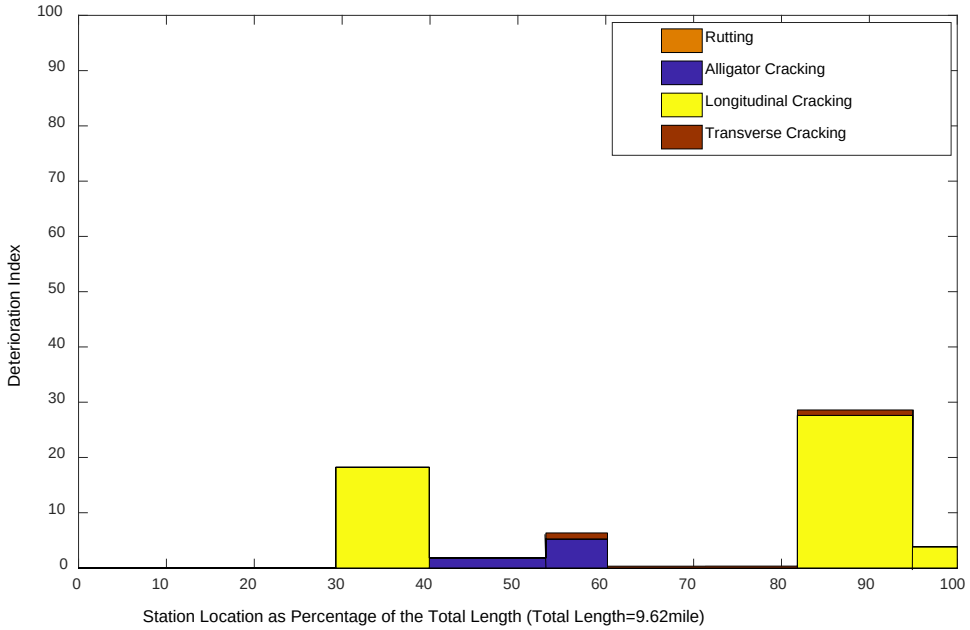

Figure 3-31 STH 73 distress distribution over the length of the project

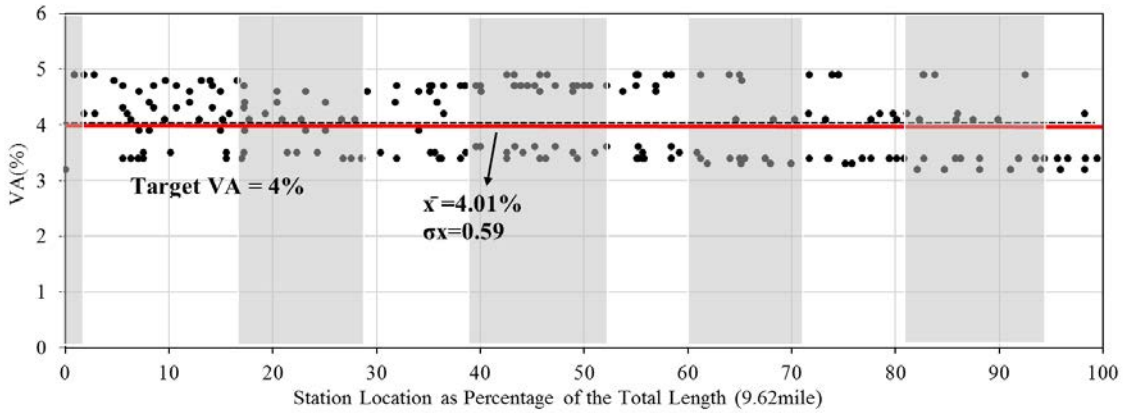

Figure 3-32 Va reported values during production

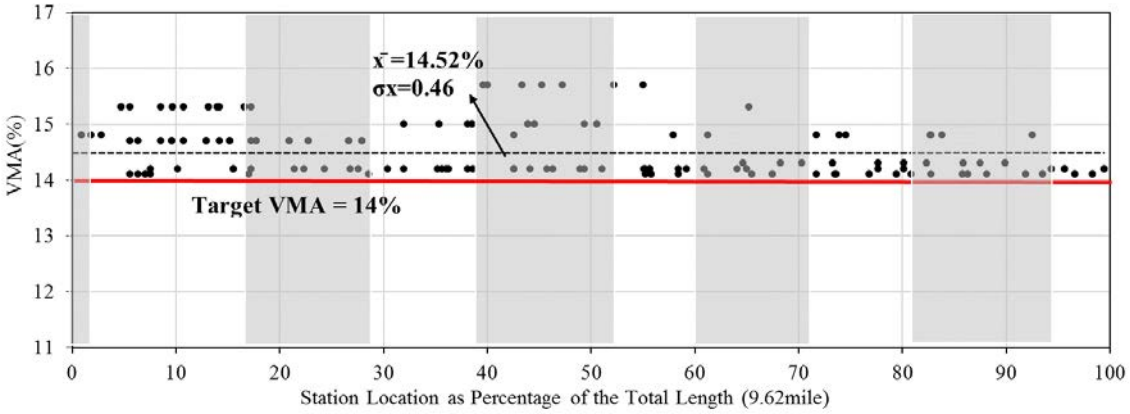

Figure 3-33 VMA reported values during production

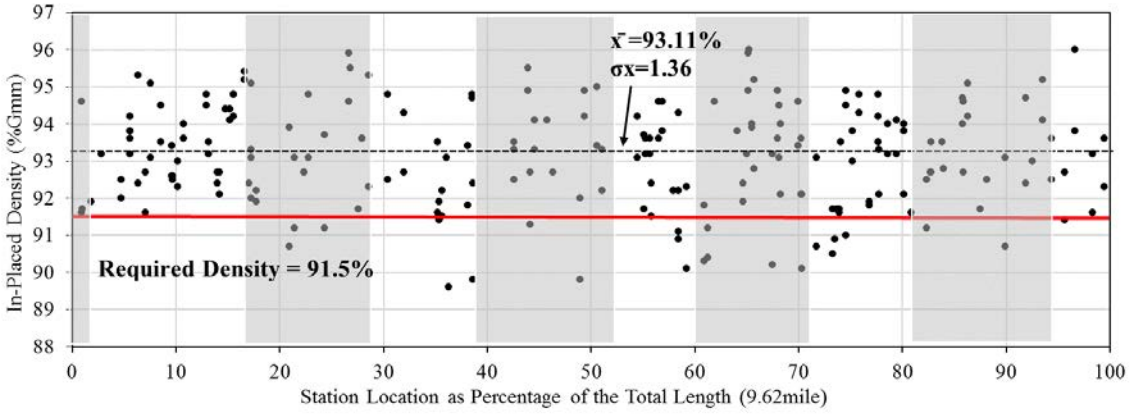

Figure 3-34 Placement density during construction

This project was constructed in 2014. It is showing minimal distresses according to PIF. Two of the segments within the project are showing a moderate level of longitudinal cracking. This project continues the trend of high RAP projects with a wide range of in-place density. No information was found regarding the RAP utilization in the mix of this pavement.

3.4.9 STH 77 (Designation: High Recycled Project)

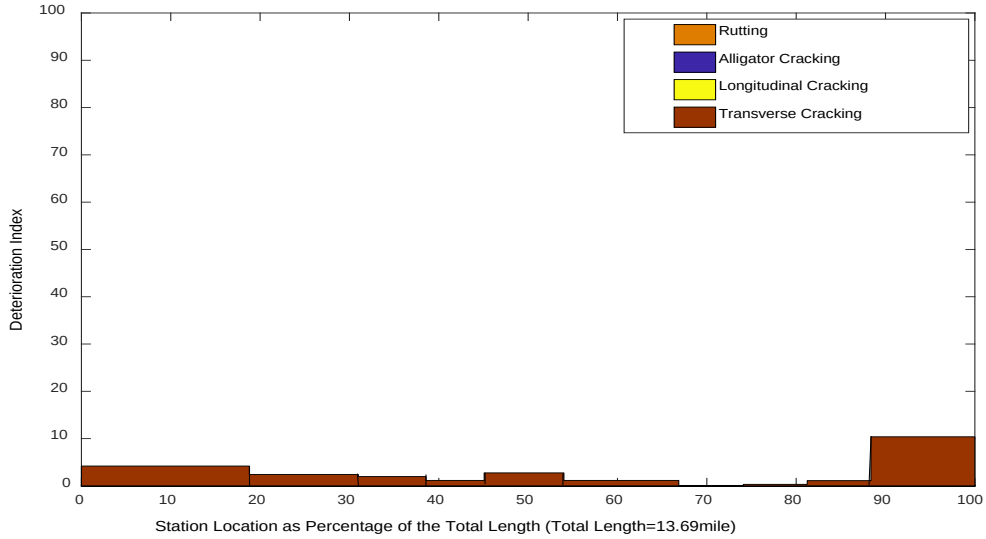

Figure 3-35 STH 77 distress distribution over the length of the project

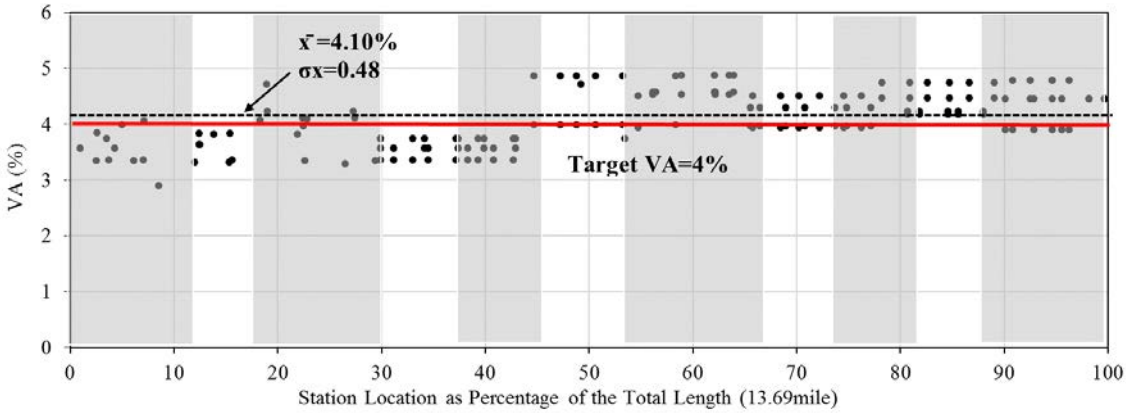

Figure 3-36 Va reported values during production

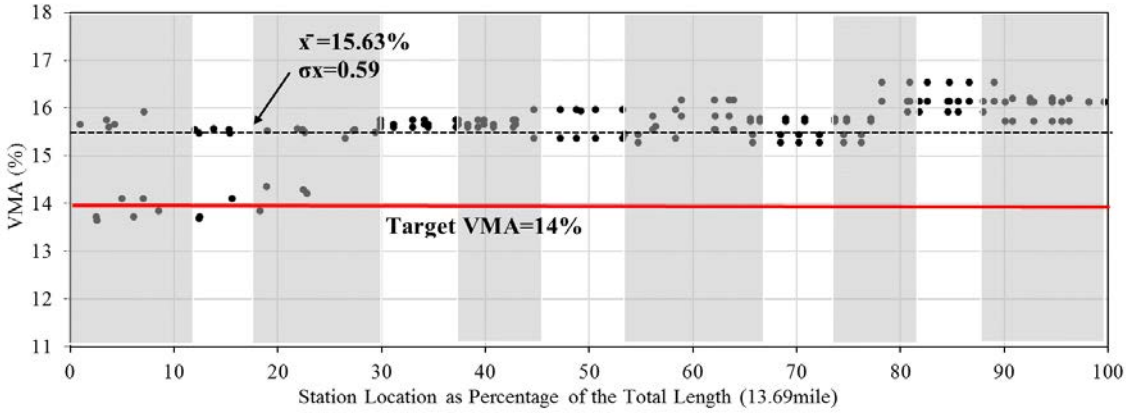

Figure 3-37 VMA reported values during production

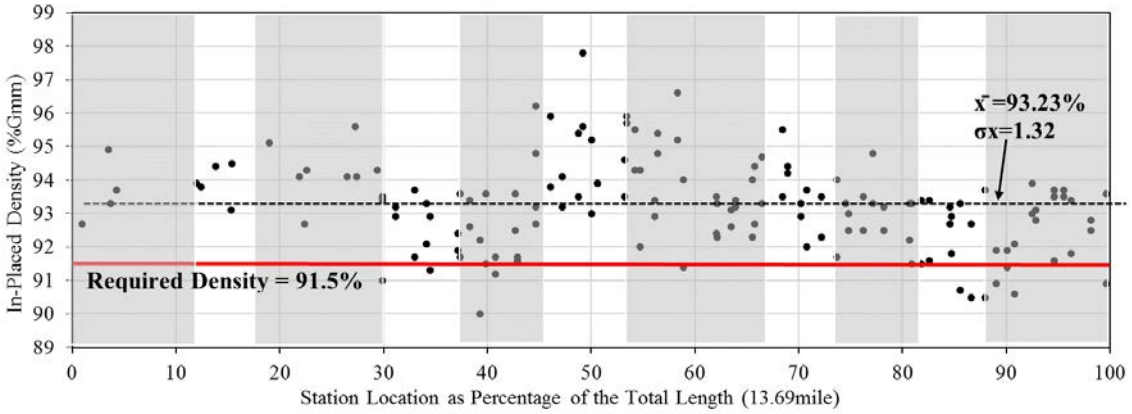

Figure 3-38 Placement density during construction

This project was constructed in 2014. It is showing minimal transverse cracking according to PIF. The in-place density is showing a wide range within some of the sequence numbers. In some cases, the minimum on-site compaction was not achieved. This can be attributed to the RAP content. Furthermore, due to the lack of distresses, it is difficult to assess if this high variability poses a detrimental influence on pavement performance. None of the high RAP projects are showing enough distresses to further investigate the relationship between RAP, in-place density, and performance. This pavement was constructed with a mix containing 33% RAP.

3.4.10 STH 80 (Designation: Thin overlay project)

Zero Distress

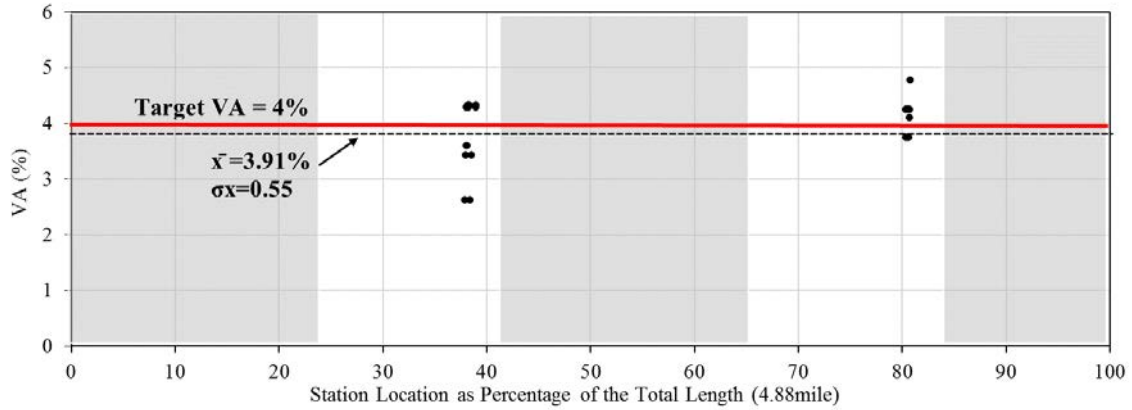

Figure 3-39 Va reported values during production

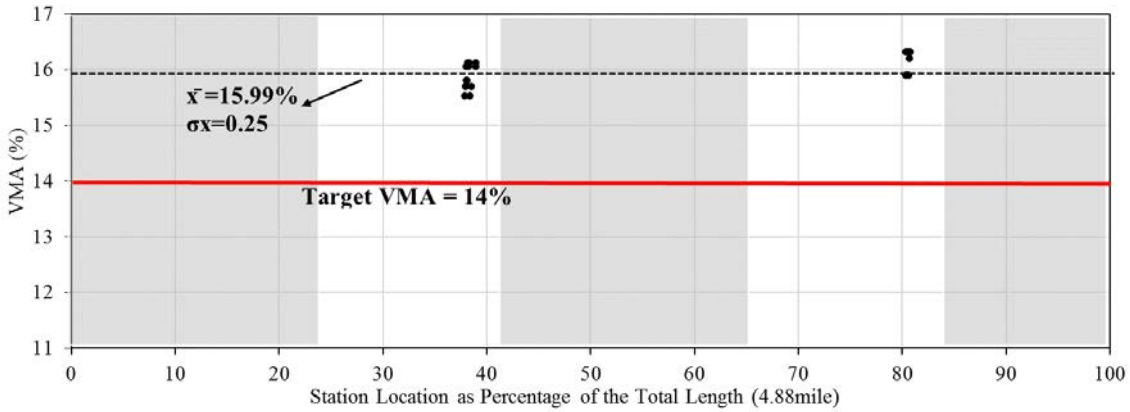

Figure 3-40 VMA reported values during production

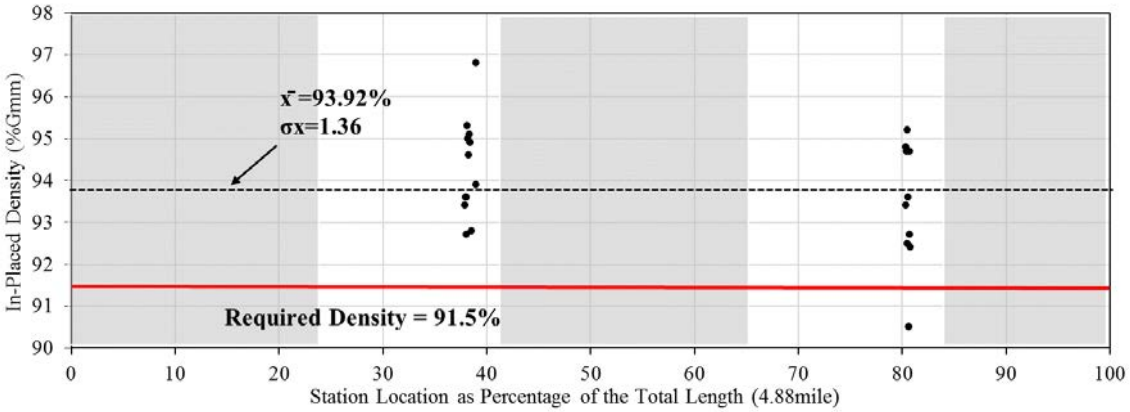

Figure 3-41 Placement density during construction

This project was constructed in 2014. It is showing no distresses according to PIF. The quality data retrieved is incomplete.

3.4.11 USH 141(Designation: High Recycled Project)

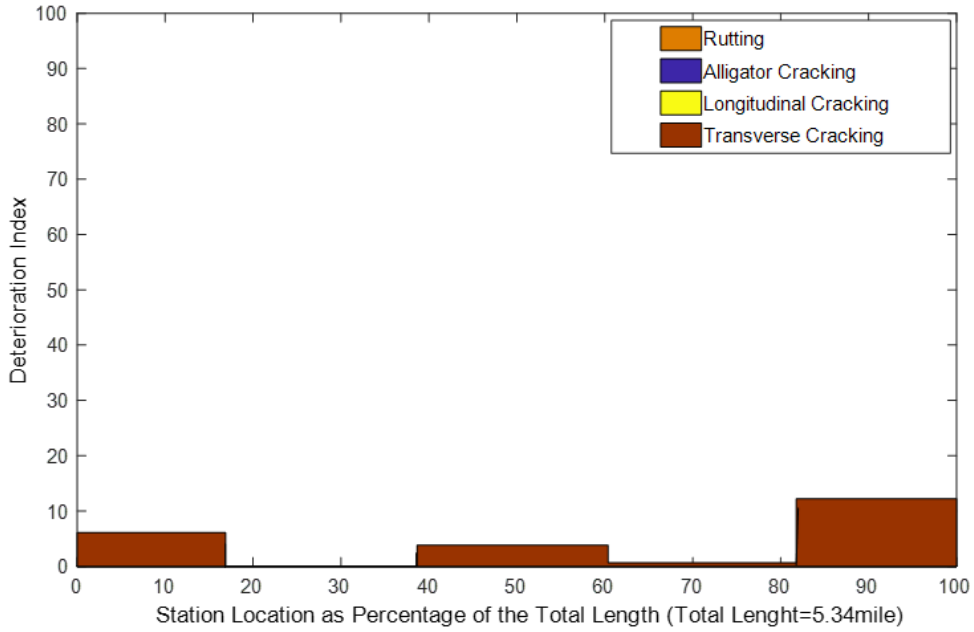

Figure 3-42 STH 141 distress distribution over the length of the project

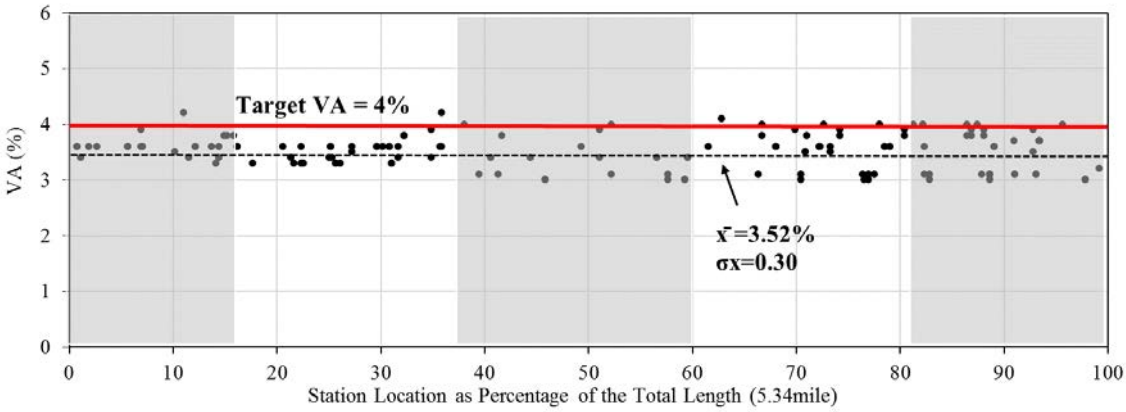

Figure 3-43 Va reported values during production

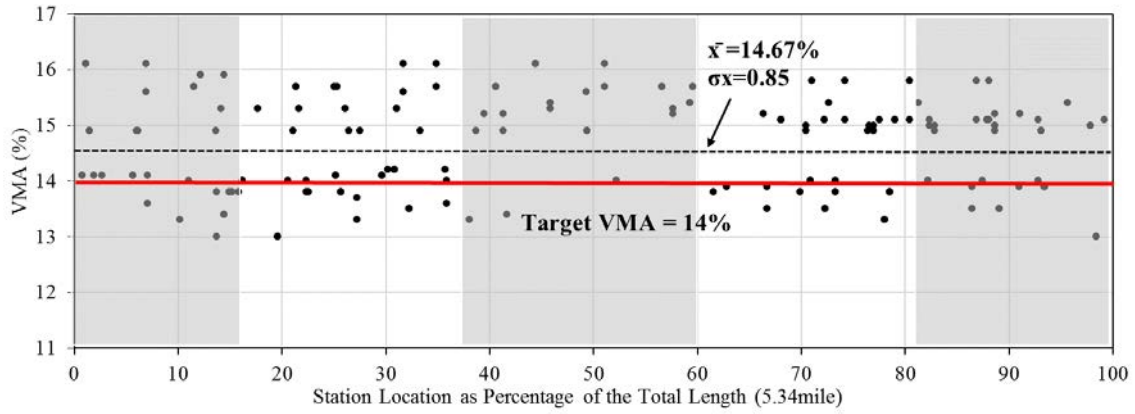

Figure 3-44 VMA reported values during production

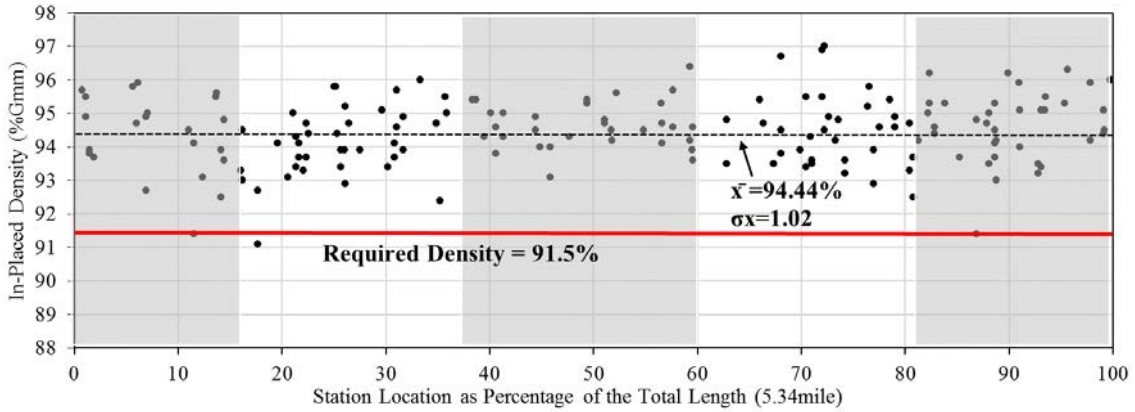

Figure 3-45 Placement density during construction

This project was constructed in 2013. It is showing minimal transverse cracking according to PIF. The production Va data is highly conforming with minimal variability. The VMA is not conforming in multiple sections with a high level of variability. Construction in-place density data exceed the minimum limit for the majority of sections. Unlike other high RAP pavements, this one does not exhibit the high variability in compaction density. The percent RAP utilization in this mix was not found. But it could be speculated that RAP was used in the binder lift rather than the surface lift, which contributed to the consistent in-place density during construction.

3.4.12 USH 8 (Designation: Thin Overlay Project)

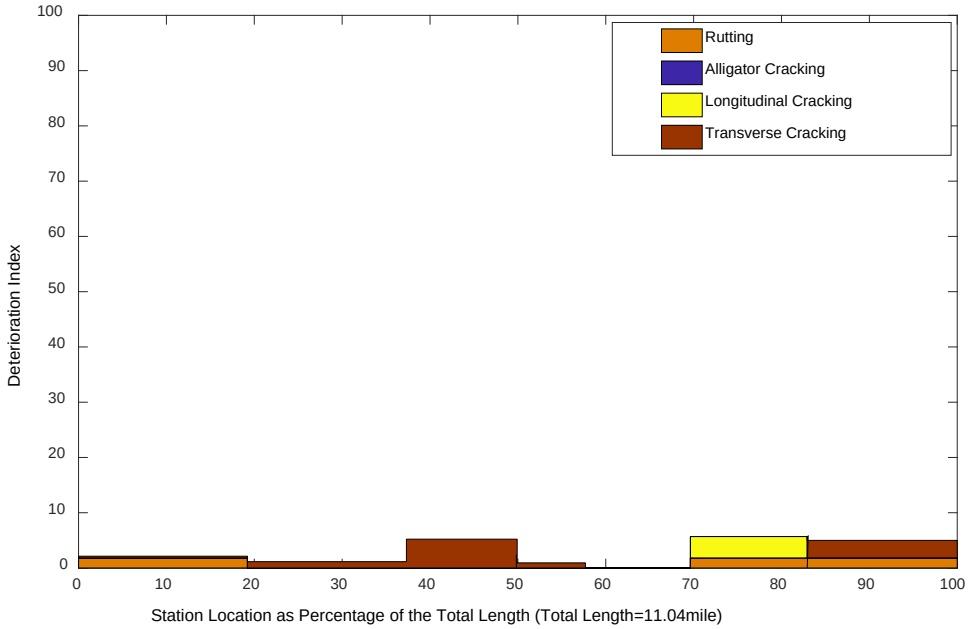

Figure 3-46 USH 8 distress distribution over the length of the project

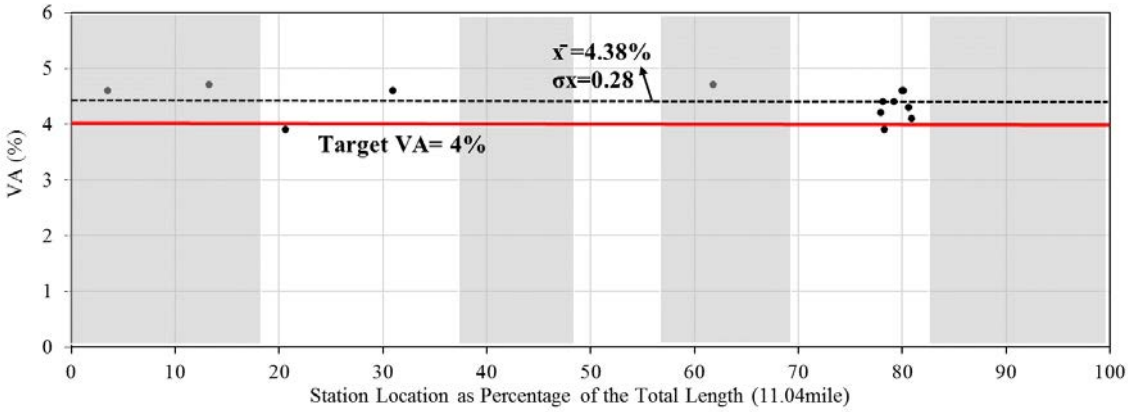

Figure 3-47 Va reported values during production

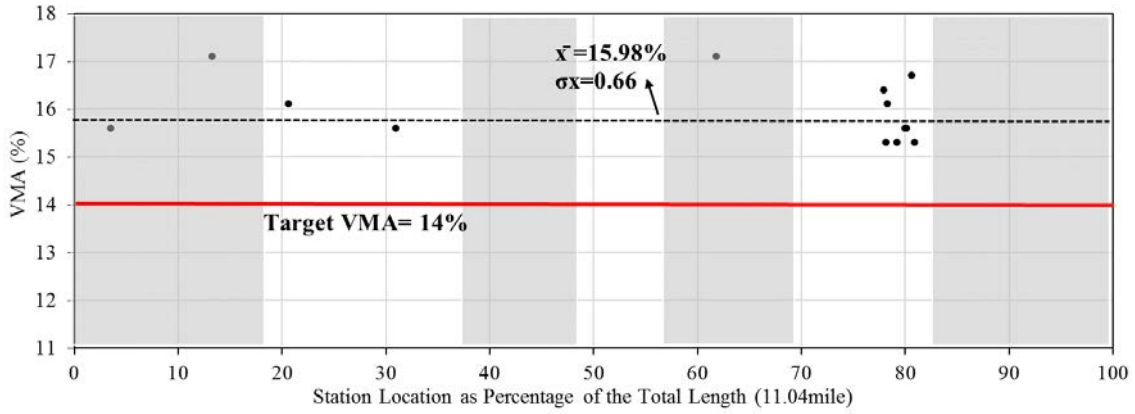

Figure 3-48 VMA reported values during production

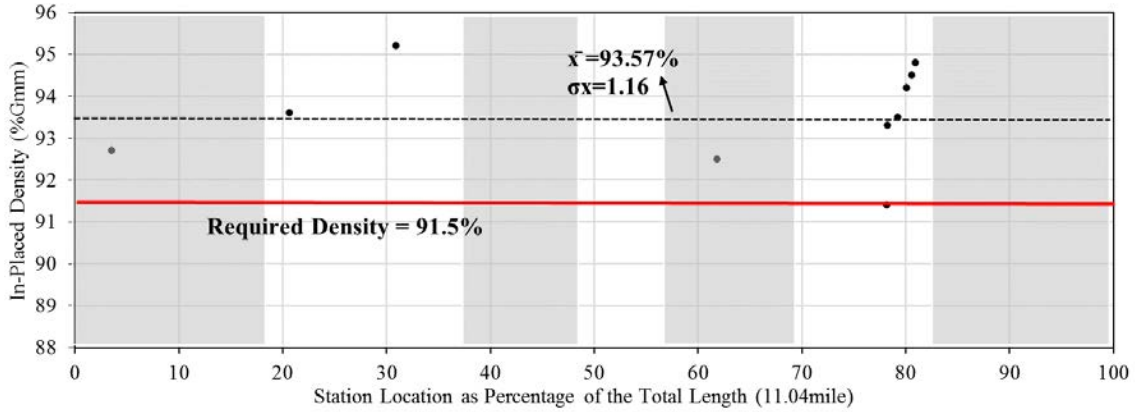

Figure 3-49 Placement density during construction

This project was constructed in 2014. PIF is showing minimal distresses. Quality data is incomplete.

3.5 Summary

- Five out of the twelve studied projects showed zero distress. Projects STH 26, STH 21, STH 13, STH 36, and STH 80 are the projects with no signs of rutting, alligator, longitudinal or transverse cracking problems.
- Geo-tagging the data was not possible for two of the studied projects, STH 17 and STH 178. Also, for STH 80 and USH 8, there were limited data points.
- Projects STH 77, USH 141, and STH 73 showed low deterioration. While the main performance problem for STH 73 was longitudinal crack, with low severity, the USH 141 only showed transverse cracking problems.

- For STH 77, the high recycle project, no significant performance differences were observed between the high RAP and normal HMA sections.
- STH 11 is labeled as a premature failure project. However, the detailed analysis showed that the deterioration of this project at the age of 14 is not high. An overall good conformation to the specs was observed for the quality data of this project.
- It was noticed that STH 13, known as the Air Void Regression project has no sign of distress after 2 years of construction. Also, the range of Va was comparable with the other product data for mixes targeting 4% Va.
- Project STH 178 has the highest deterioration rate among the 12 studied projects. This project was designated as a premature failure project. In particular, the level of longitudinal cracking was observed to be higher compared to the average of the network. On the other hand, the transverse cracking was lower than the network average.
- STH 21 showed no distress with a relatively high in-placed density. The average in-place density of this project is about 3% more than the specification targets.
- Similarly, more than 16 miles of project STH 26 showed no sign of distress at age 2. While there are few lots in this project that have lower Va and in-place densities than the specification limits, the overall production and construction are conforming to the specifications. It is also observed that the presence of RAP did not cause an early deterioration in this project.
- STH 36 has no recorded rutting, longitudinal, alligator, and transverse cracking at age 2, according to the PIF database. This is the high recycle NCHRP project. The placement density shows high variability, that might have been caused by the presence of the RAP content.
- STH 73, with a minimal deterioration at age 3, has a wide range of in-place density.
- Some of the sections in STH 80 did not meet the in-place density specification targets. However, the project has shown to have only minimal transverse cracking at age 3. This project has also used RAP materials, and yet no meaningful correlations with distresses were found.
- There was not much information about STH 80 regarding the quality of construction and production. Also, there is not any type of distress in this project, according to the PIF.

- Minimal transverse cracking was observed for USH 141, according to the PIF. While VMA is highly variable in this project, the in-place density and Va are showing good conformation to the specifications. The average in-place density of this project is about 3% higher than the specification targets, with a narrower range of variability compared to the other high RAP projects.
- Project USH 8 has minimal rutting and cracking problems at age 3, according to the PIF. The quality data is incomplete for this project, which makes it difficult to make any conclusion regarding the effects of construction and production quality on the performance.

4. Exploratory Analysis

This chapter serves to investigate the potential influence of individual parameters on in-service performance. This is critical to isolate potential colinearities and understand direct correlations before further levels of analyses are conducted. The investigation conducted in this chapter is based on the information gained from the on-site distress surveys, core testing. As can be noted, the PIF data under-represented the distresses experienced by the pavements. All test sections exhibited some form of distresses, while the PIF reported no distresses or distresses at the much lower extent.

4.1 Description of Sections' Measured Performance

In addition to the field coring, performance measurements were also conducted on the investigated projects. In this regard, different pavement sections were selected at each highway project, in a way that each project had at least two representative sections. For some of the projects, due to the possibility of having multiple mix designs according to the original mix design documents, more than two pavement sections were chosen. The performance per section is shown in Figure 4-1. This figure shows the DI value of each distress for all studied pavement sections.

The performance recorded for the different sections belonging to the same highway was comparable. STH 17, STH 178, and STH 80 demonstrated different performance between the sections. The graph shows that all roadways experienced different levels of transverse cracking. The previous chapter showed that all the projects were constructed at a high level of conformity for the most part. It was found that all four types of distresses exist in the studied projects. Among all distresses, transverse cracking was found to be the predominant type. Field observations indicated that transverse cracking is not believed to be a construction-related issue. There was also no indication that the other distresses could be related to systematic construction or production deficiencies. The following sections attempt to investigate possible correlations between material, loading, and environmental factors to the observed performance.

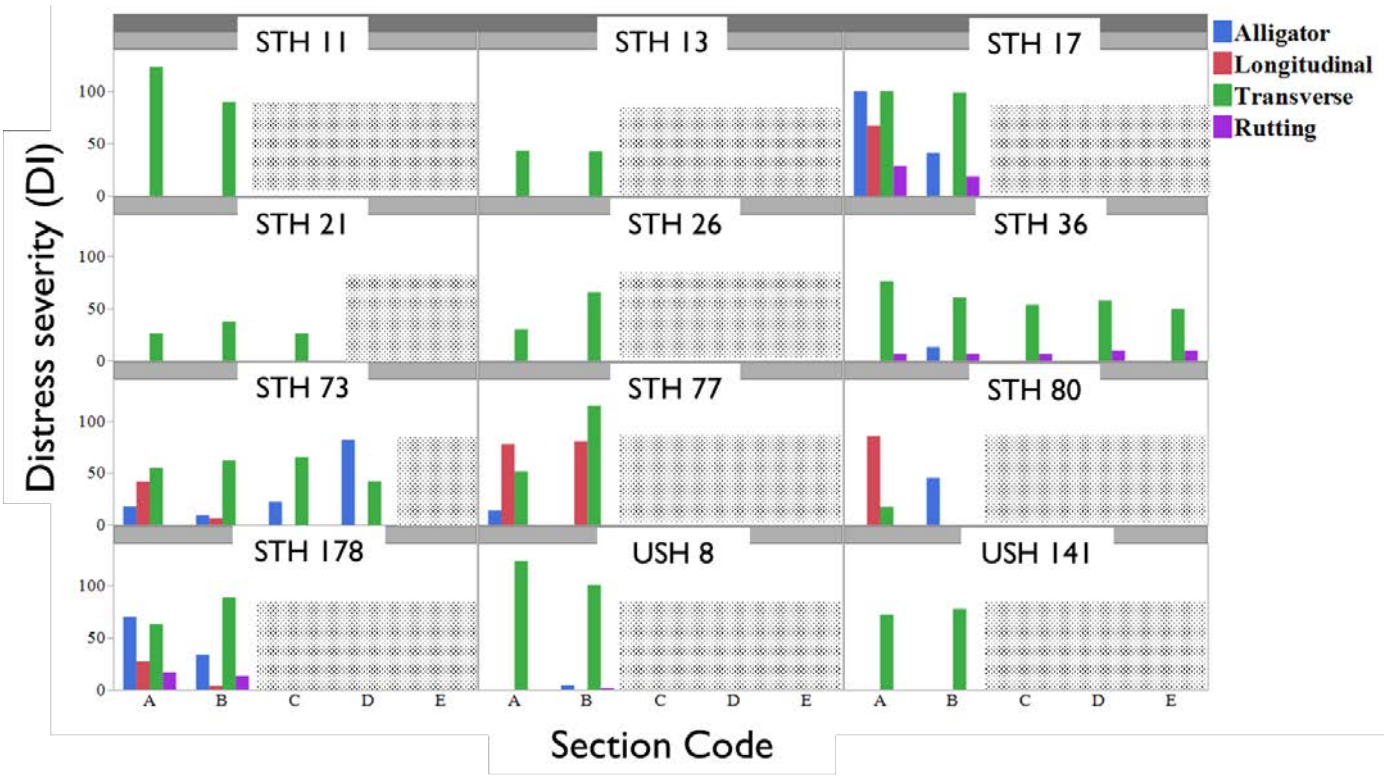

Figure 4-1 Distribution of distresses in 30 studied sections

The measured distresses shown in Figure 4-1 do not appear to be related to construction quality or project designation. Therefore, the analysis approach will proceed by investigating the relationship between the data population with other potential parameters.

4.2 Performance Comparison of "Wheel Path" (WP) and "Between Wheel Path" (BWP) Cores

The coring plan includes separating cores into two groups; wheel path (WP), and between wheel path (BWP) cores. Before proceeding with the analysis, it is important to investigate if the core location should be incorporated as a variable. Therefore, cores collected from the sections are evaluated to quantify the difference in performance within a section based on the location: WP vs. BWP. Mechanical evaluation of the cores as well as testing of the extracted binder is used as criteria for establishing the variation in performance between BWP and WP cores.

The results showed in Figure 4-2 clearly demonstrate that the consistency in the performance of the core is independent of the wheel path. The comparison is conducted at the core mixture level through comparing the core cracking potential using the IDEAL test, and at the binder level

through capturing the continuous intermediate grade of the extracted binders (Temperature at which the G*.sinδ is 5000 kPa). Figure 4-2 shows a comparison of the test results for both groups of cores.

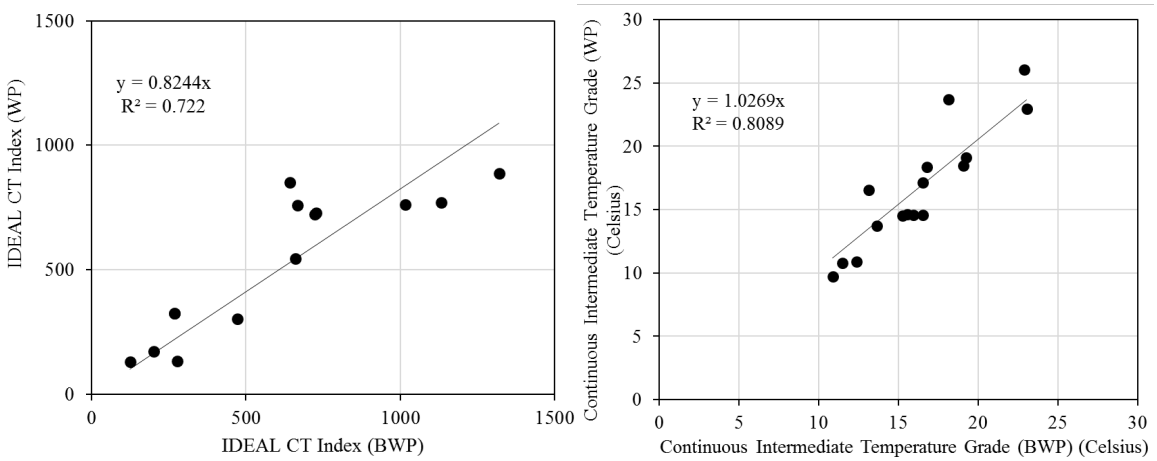

Figure 4-2 Correlation between BWP and WP samples in mixture and binder tests

As shown in Figure 4-2 the IDEAL CT and binder testing agree that the WP and BWP cores are the same. The slope of the fit line is very close to equality (1.0) at a high coefficient of correlation (R^2). Therefore, the core location will not be included in the analysis as a separate variable.

4.3 Effects of Mix Properties on Performance

This section intends to show the individual correlations between the mix properties and the studied distresses. As-produced properties such as Va (%) and VMA (%), as-constructed properties including placement density (%Gmm) and Thickness, cores mechanical testing, extracted binder testing, and extracted aggregate gradation are all evaluated. The correlations are evaluated based on their strength (R^2) and trend. It is important to note that the pavements studied in this research have different ages. The correlations presented here are for deterioration rates rather than accumulated distresses. This way, the comparison between different projects is adequate and independent of age. However, for comparing core mechanical testing and extracted binder performance, the correlations rely on the accumulated deterioration. This is because the comparison is now between variables of the same age.

It is important to note that the correlations presented in this chapter investigate a singular association between performance and a given variable. It is understandable that the performance

is dependent on a group of variables rather than a single variable. Therefore, a multivariate analysis is included in chapter 5.

4.3.1 Pavement Thickness

The thickness information evaluated in this section is the surface layer thickness. The correlation of the thickness against the on-site measured distresses is shown in Figure 4-3.

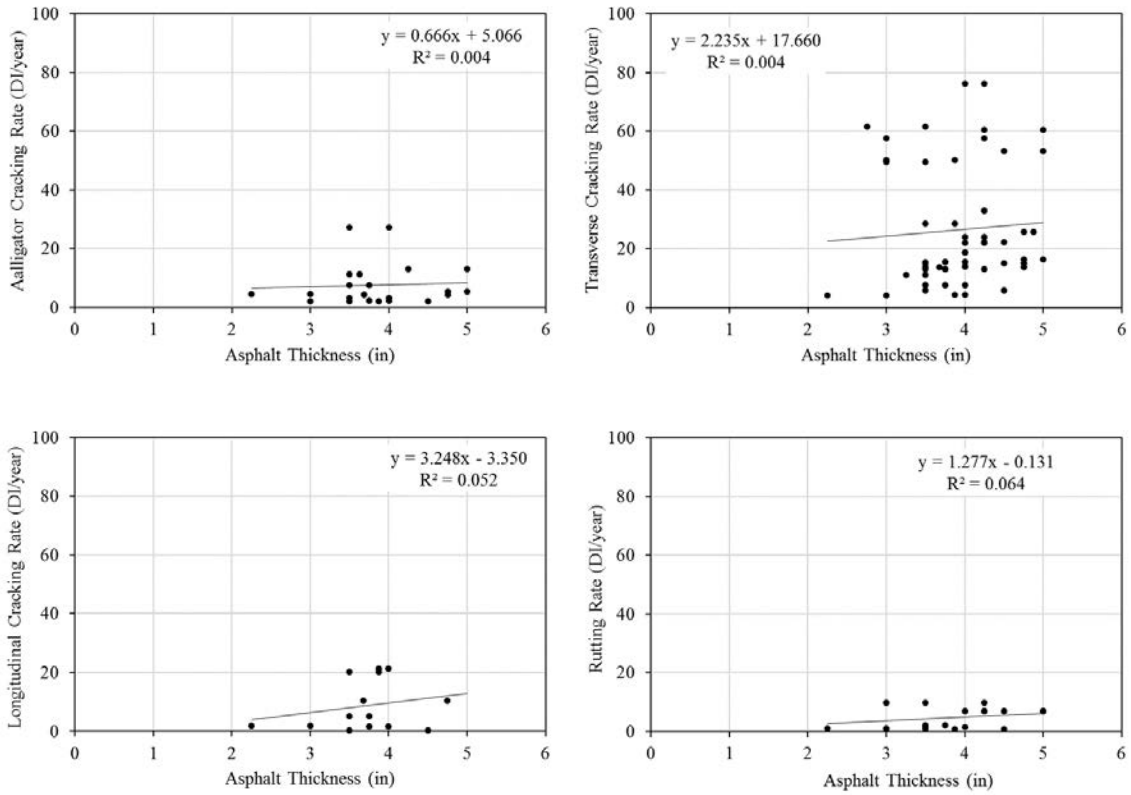

Figure 4-3 Correlation between asphalt thickness and four studied performance indicators

The results show no association between the surface layer thickness as measured from the cores and any of the distresses.

4.3.2 Asphalt Content

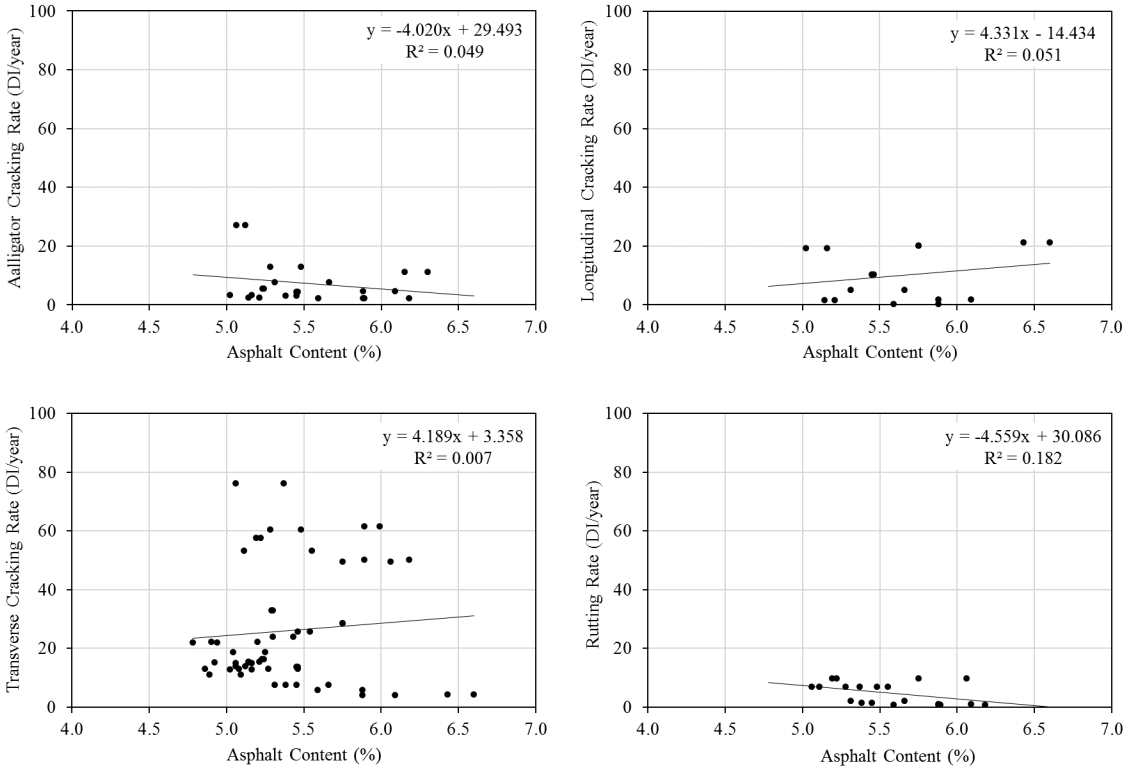

Figure 4-4 Correlation between asphalt content and four studied performance indicators

The data are showing that there is no direct association between the AC% of the surface layer with the distresses observed. This is an interesting observation, as the AC% is believed to directly correlate to performance. It is important to note that AC% refers to the content measured from the extracted cores.

4.3.3 Placement Density (%Gmm)

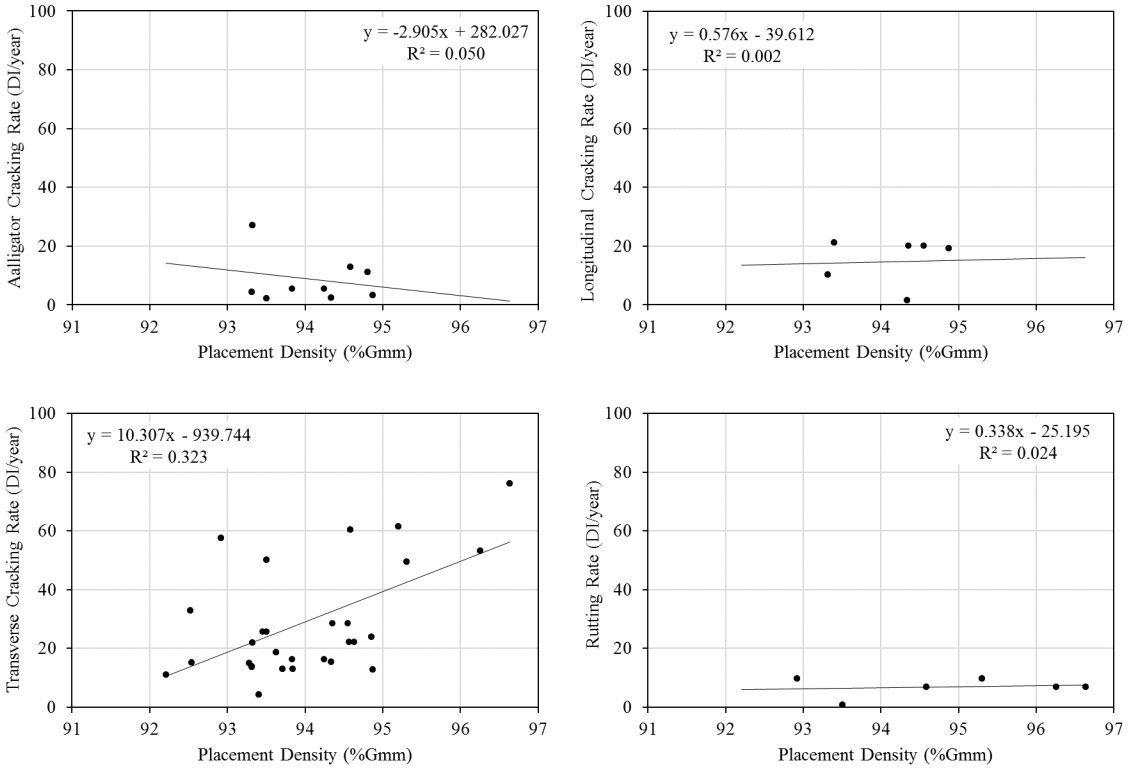

Figure 4-5 Correlation between placement density and four studied performance indicators

The trends shown above, suggests that there is a positive correlation between the placement density with transverse correlation. As the average density of the 500 ft sections increases, the recorded transverse cracking rate increases. This could be due to thermal diffusion and specific heat capacity differences between air and mixture. However, further study on this issue is necessary before any postulations can be made.

4.3.4 Production Va (%)

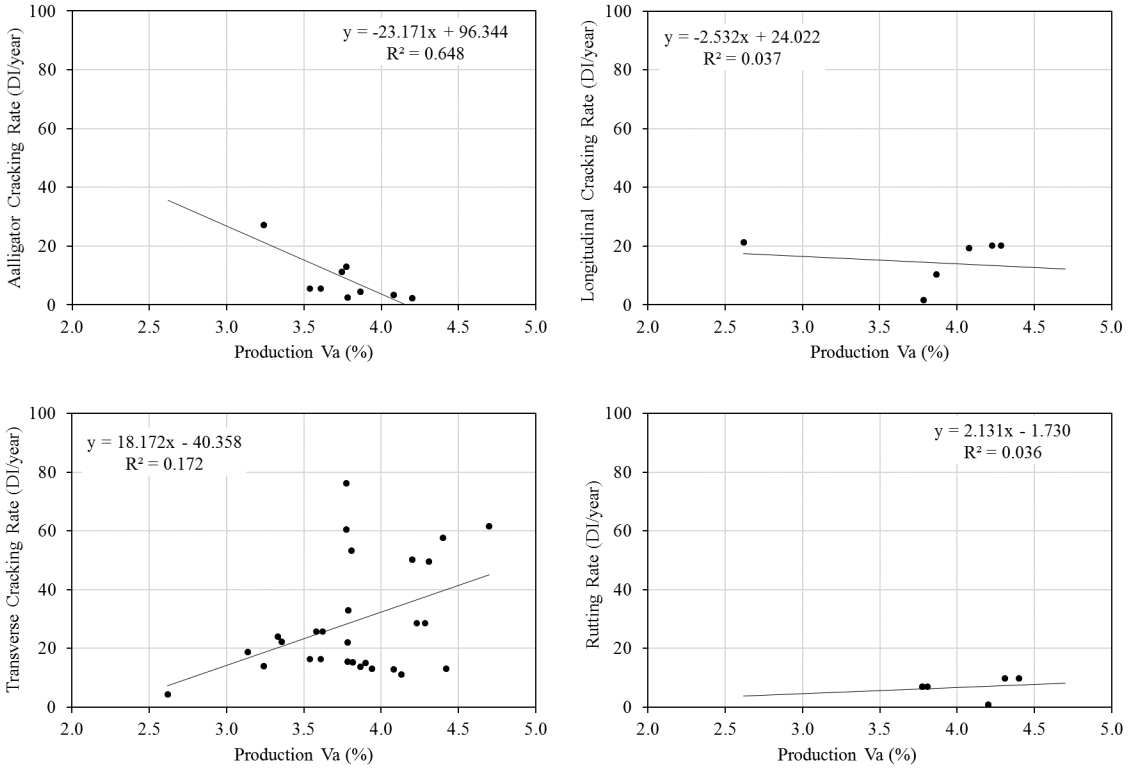

Figure 4-6 Correlation between Va and four studied performance indicators

The correlations show that the higher the average Va the lower the alligator cracking rate of deterioration. On the other hand, the higher the Va, the higher the rate of transverse cracking. This could be speculated that when mixes during production are harder to compact, they have higher mechanical stability, thus higher resistance to load related alligator cracking. But for the transverse cracking, it is more difficult to speculate a physical reason for this correlation.

4.3.5 Production VMA (%)

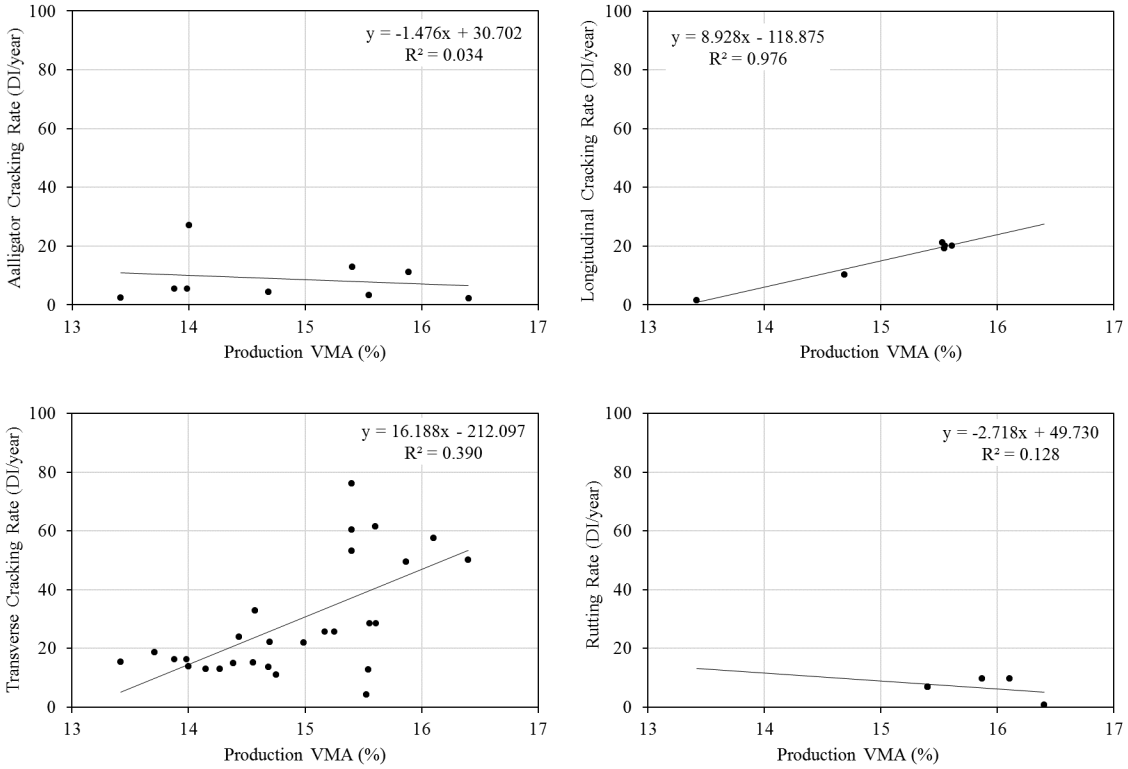

Figure 4-7 Correlation between VMA and four studied performance indicators

There is a strong correlation between longitudinal cracking rate and VMA. However, this correlation is based on 5 data points, with three of the data points clustered together. Therefore, this correlation is based on three unique values for VMA. It is difficult to reach a conclusion using such a low number of data points, especially knowing that it is believed in the field that higher VMA corresponds to higher mechanical stability. With respect to the transverse cracking rate, there is a positive correlation between the VMA and the rate. This correlation mirrors that of transverse cracking and Va.

4.3.6 Dust/Binder Ratio

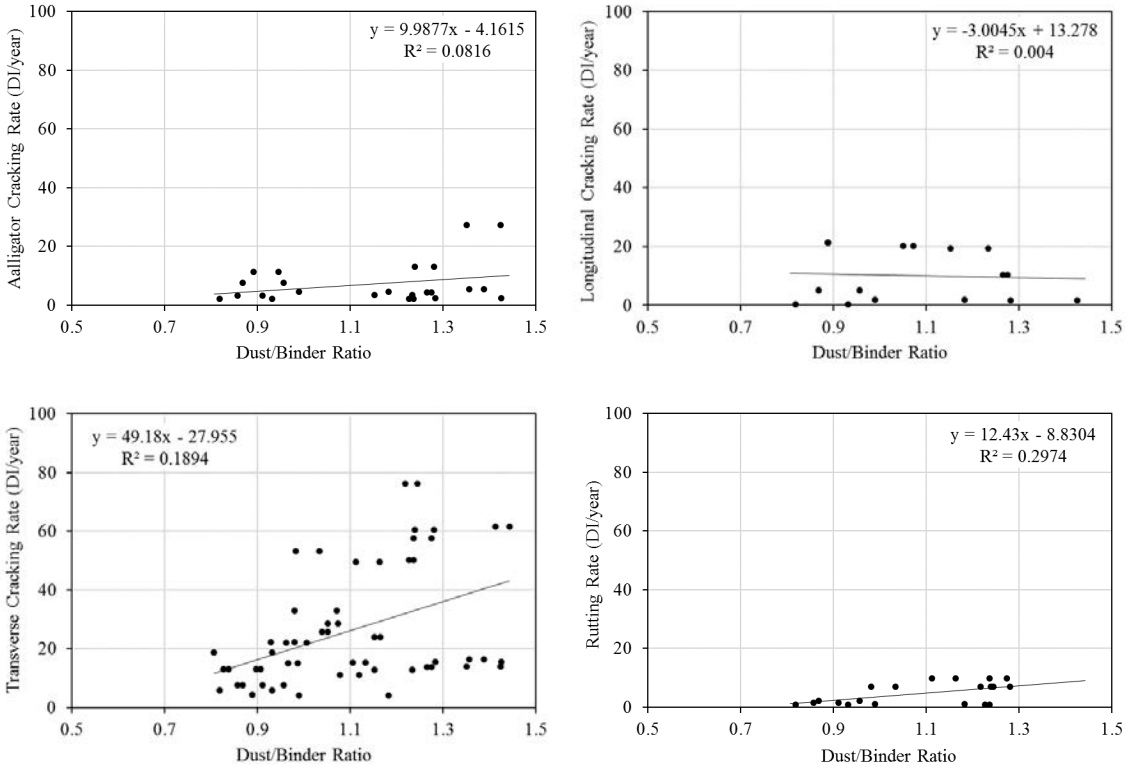

Figure 4-8 Correlation between dust/binder ratio and four studied performance indicators

The results show some weak correlation between D/B and transverse cracking and rutting. For transverse cracking, the relationship could be influenced by the stiffening effect of the fines on the binder. For rutting, the higher D/B could be correlated with a higher rate by extending the binder. This stipulation requires further in-depth analysis of the nature of the filler within the mix along with its physicochemical properties. Such an analysis is beyond the scope of this project.

4.3.7 Aggregate Uniformity Coefficient - Cu

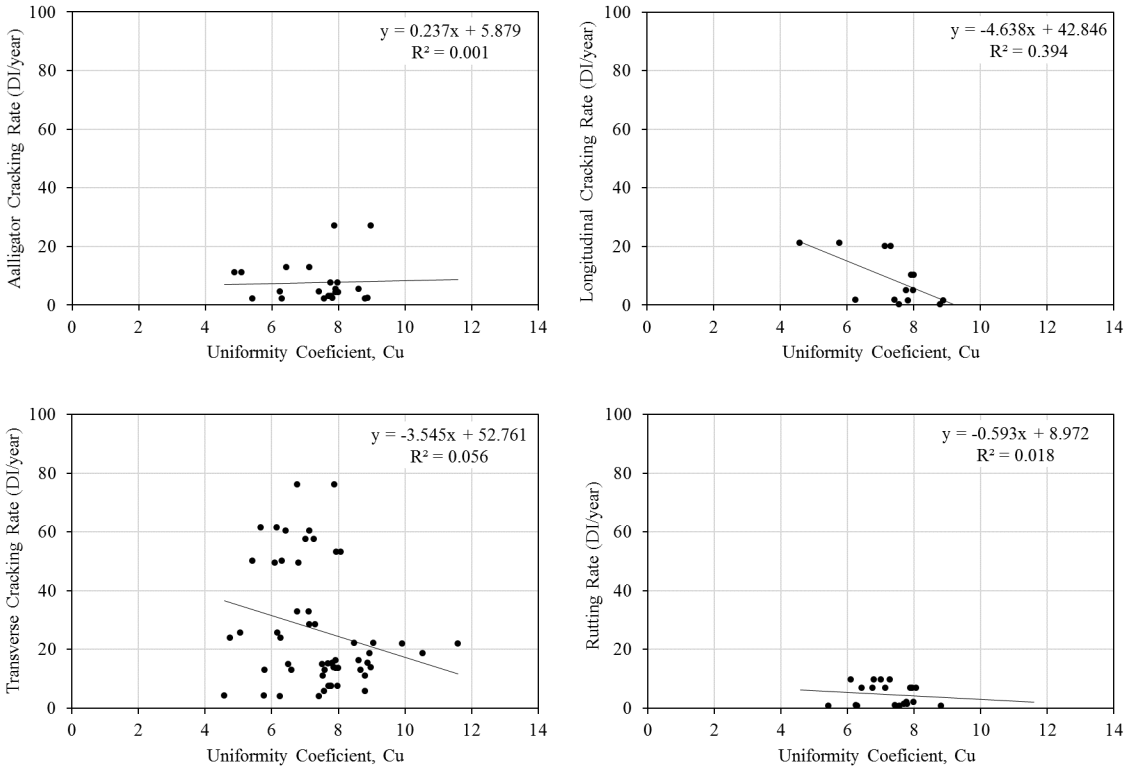

Figure 4-9 Correlation between Cu and four studied performance indicators

There appears to be a negative correlation between the aggregate gradation uniformity coefficient (Cu) and longitudinal cracking. A higher Cu indicates a well-graded aggregate gradation, which leads to better packing. The results suggest that such packing is beneficial for longitudinal cracking.

4.3.8 Aggregate Coefficient of Curvature - Cc

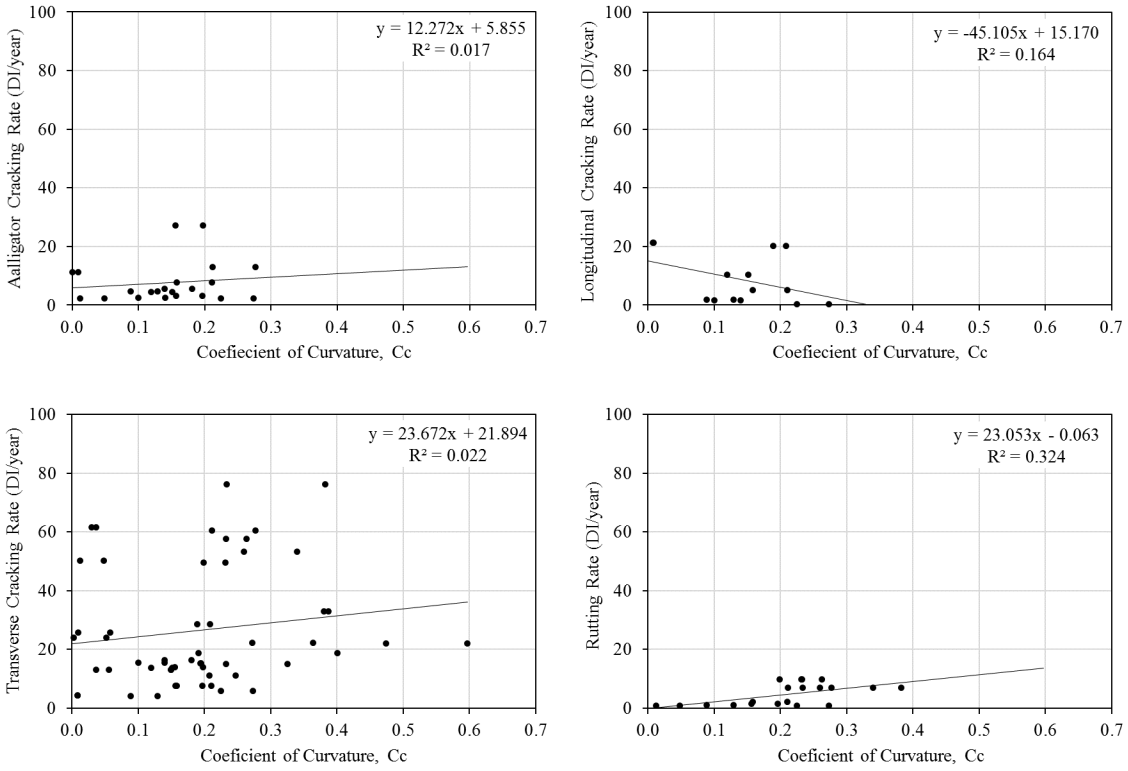

Figure 4-10 Correlation between Cc and four studied performance indicators

The plots are showing a positive correlation between the coefficient of curvature (Cc) and rutting rate, and a negative correlation with longitudinal rate. Yet the scatter shown for these plots indicates the dependency of the performance of the Cc is not reliable.

4.4 Correlation of Core Binder and Mixture Testing with In-Service Performance

4.4.1 Mixture Testing

This section investigates the correlations of the conducted mixture testing on field samples with the on-site performance measurements.

4.4.1.1 *Rutting*

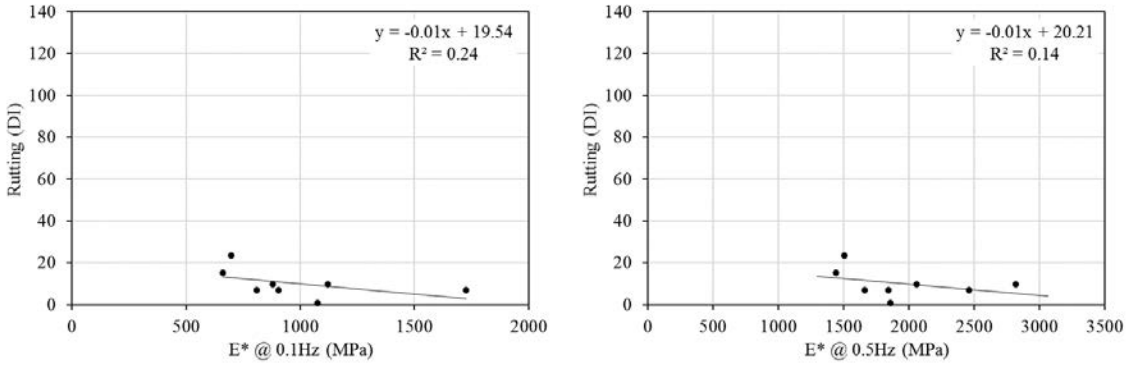

Figure 4-11 IDT dynamic test correlation with rutting

There is a negative correlation between the accumulated rutting and the E*@25C and 0.1 and 0.5 Hz. This is a logical trend. Because at a lower frequency of testing the higher modulus correlates with lower permanent deformation. Higher E* at lower frequency indicates higher mix mechanical stability.

4.4.1.2 *Alligator Cracking*

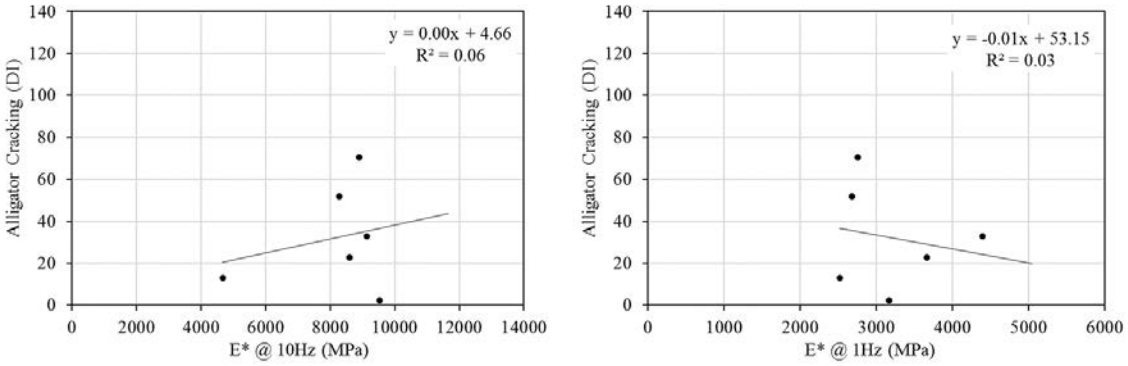

Figure 4-12 IDT dynamic test correlation with alligator cracking

The correlation between the E* at a higher frequency and the alligator cracking shown in the above figure is unclear. However, the correlation using the IDEAL test, as shown below, is apparent and logical.

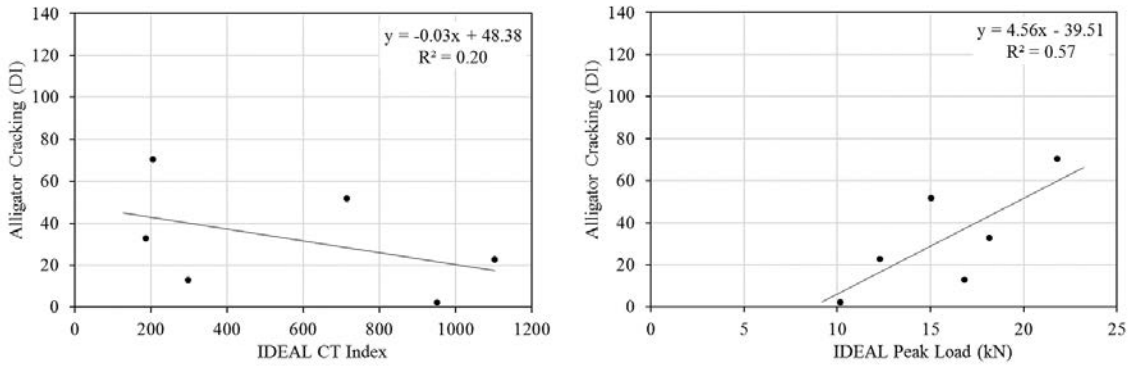

Figure 4-13 IDEAL test correlation with alligator cracking

The figure shows that the higher cracking index, alligator cracking is reduced. On the other hand, peak load for mixtures correlates at a stronger level with in-service cracking. A higher peak load indicates a higher level of alligator cracking. This is an indication that for increased stiffness in mixes, cracking potential increases.

4.4.1.3 *Longitudinal Cracking*

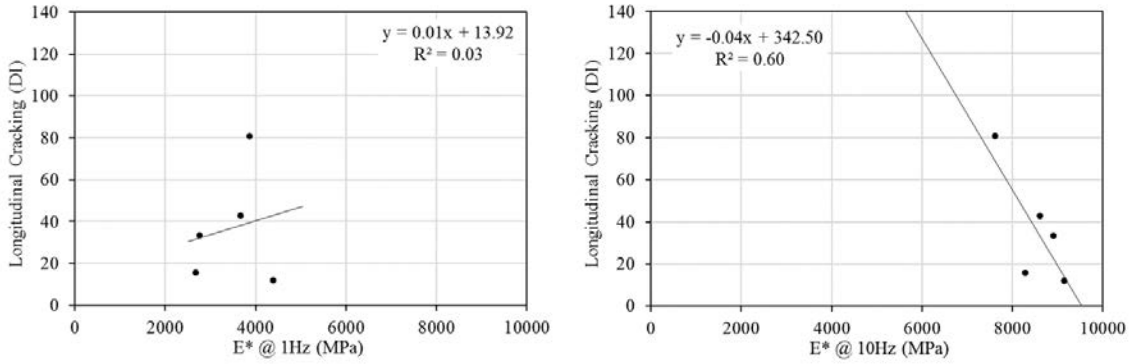

Figure 4-14 IDT dynamic test correlation with longitudinal cracking

The longitudinal cracking is negatively correlated with E* at 10Hz at a relatively high correlation coefficient. The trend is opposite to that observed at a lower frequency level of 1 Hz. This is logical and follows fundamental rheological principals for stress-controlled fatigue failure. However, the number of data points available for this correlation is low to trust the universality of this correlation.

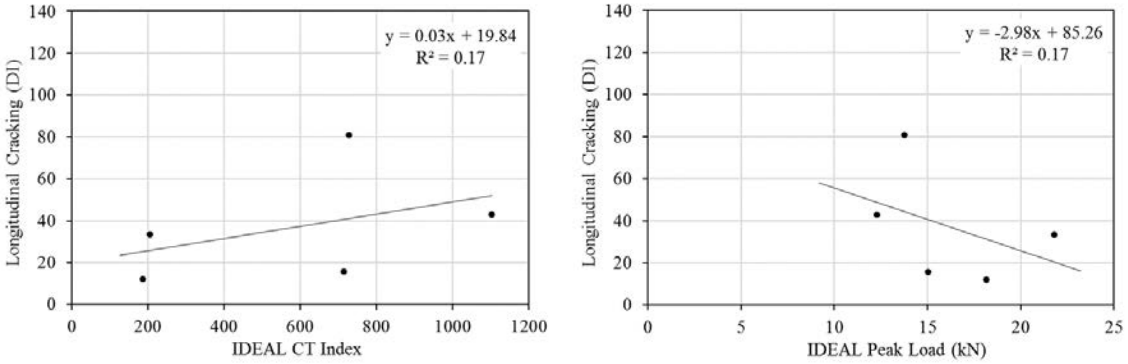

Figure 4-15 IDEAL test correlation with longitudinal cracking

For the IDEAL test, the higher CT index is positively correlated (at low R^2) with higher longitudinal cracking. On the other hand, higher core stiffness is correlated with lower longitudinal cracking. This is logical for this type of distress and follows the expected trend for strain-controlled failure in viscoelastic materials.

4.4.1.4 *Transverse Cracking*

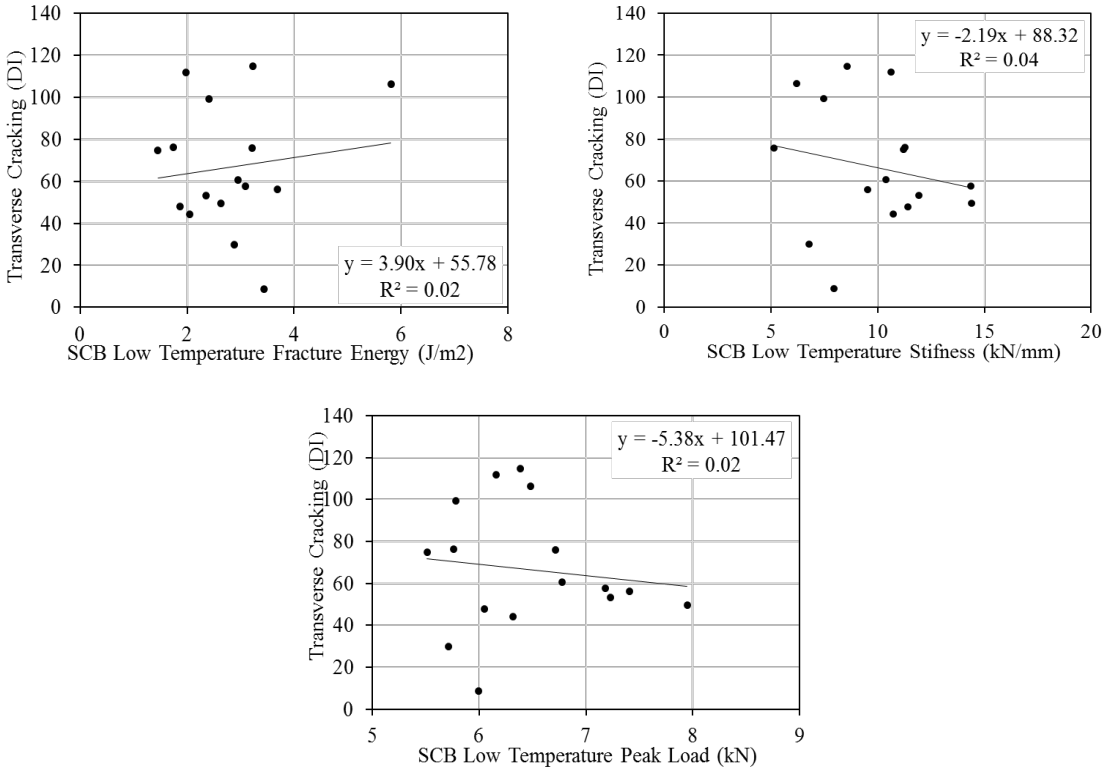

Figure 4-16 Mixture testing correlation with transverse cracking

Field cores testing using the SCB set up at -18ºC show no correlation with transverse cracking. This could be due to the different mechanisms of failure between the pavements and SCB samples.

This could also be due to the inability of the SCB alone to characterize the pavement low-temperature performance where the interaction of the SCB parameters and other mix parameters need to be considered. This possibility is examined in Chapter 5 of this report.

4.4.2 Extracted Binder Testing

This section investigates the correlations of the conducted binder testing on the extracted binders from the field samples with the on-site performance measurements.

4.4.2.1 *Alligator Cracking*

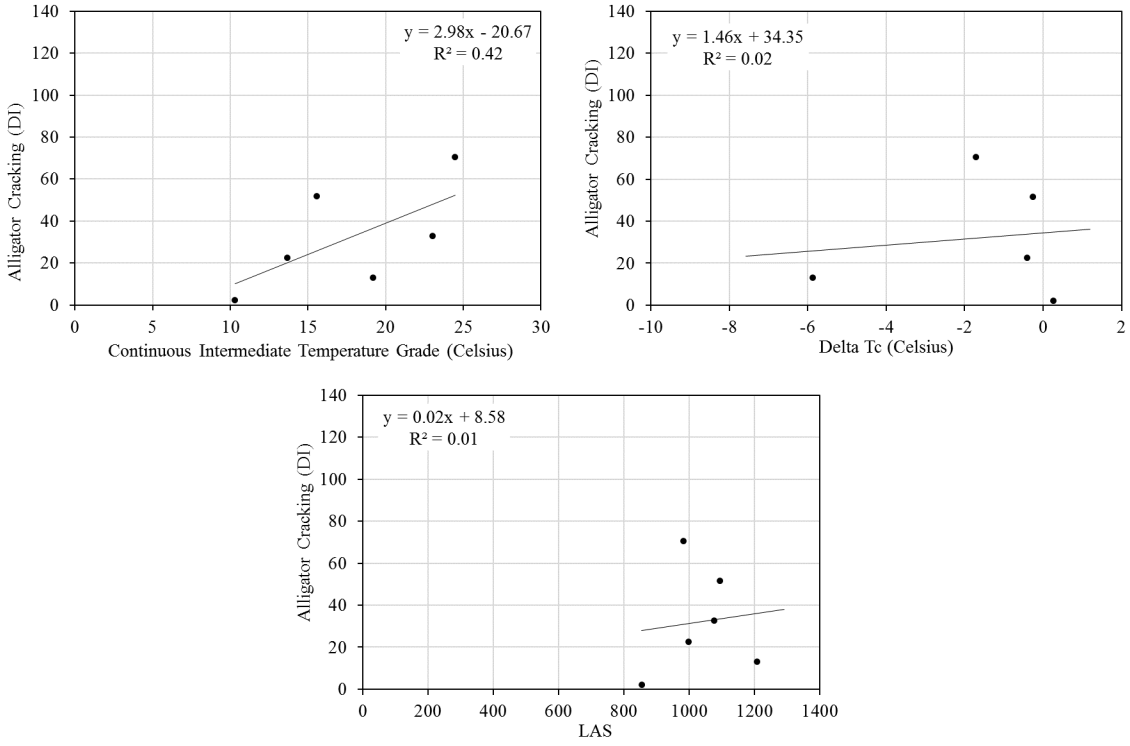

Figure 4-17 Correlations between alligator cracking and binder properties

Alligator cracking is only correlated with the continuous binder intermediate grade. This is the temperature at which the extracted binder complex modulus (G*) reached 5000 kPa. The trend of the correlation is logical and follows the expected trend. This trend also aligns with the mixtures where higher stiffness is correlated with higher fatigue cracking damage.

4.4.2.2 *Longitudinal Cracking*

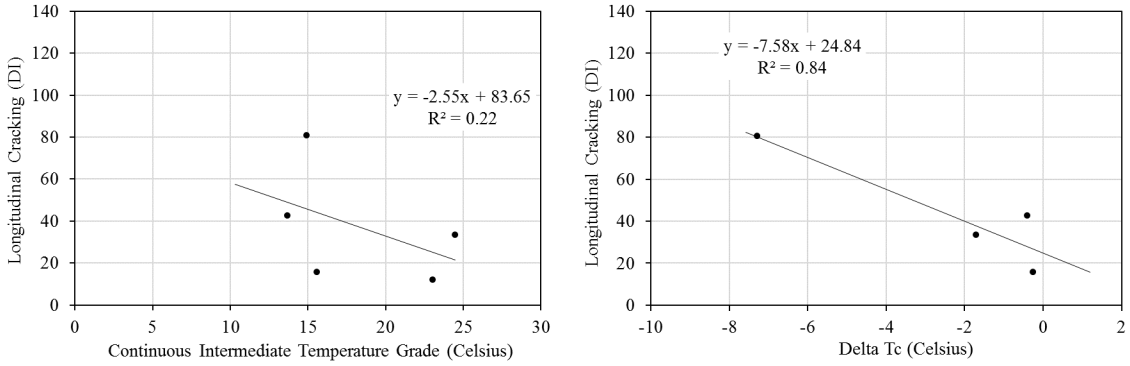

Figure 4-18 Correlations between longitudinal cracking and binder properties

The trend of the correlation between the binder continuous intermediate grade and the longitudinal cracking matches that of the core mixture testing. The higher the stiffness of the binder the lower the cracking. While the correlation between the ΔT_c and cracking is strong, it is based on only a few data points. Therefore, it is difficult to make a statement at this stage. It is important to note that this trend is similar to that observed for mixtures, where higher stiffness correlated with lower longitudinal cracking damage.

4.4.2.3 *Transverse Cracking*

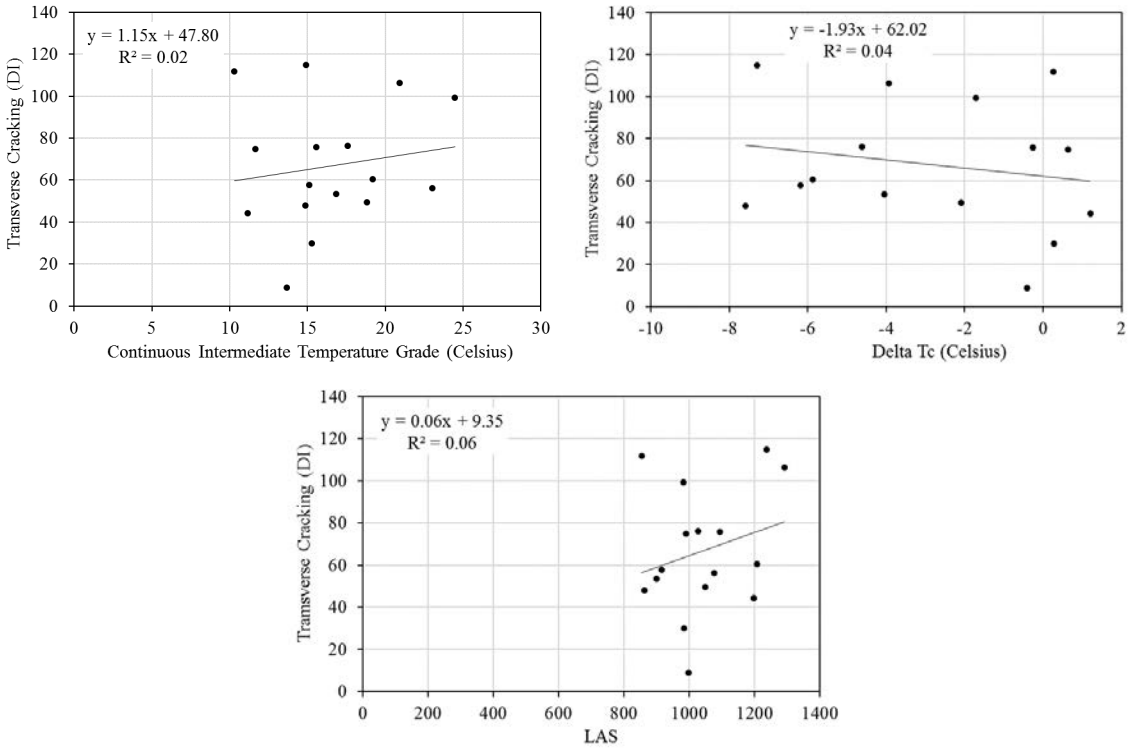

Figure 4-19 Correlations between transverse cracking and binder properties

Transverse cracking does not show a significant correlation using binder testing. The multivariate analysis included in the next chapter will investigate the dependency of this distress and other distresses to a combination of factors.

4.5 Correlation of Traffic Loading with Performance

The effects of the cumulative traffic load on the performance are provided in this section. The X-axis of the graphs are the cumulative passing traffic loads on the pavement during the life of the pavement.

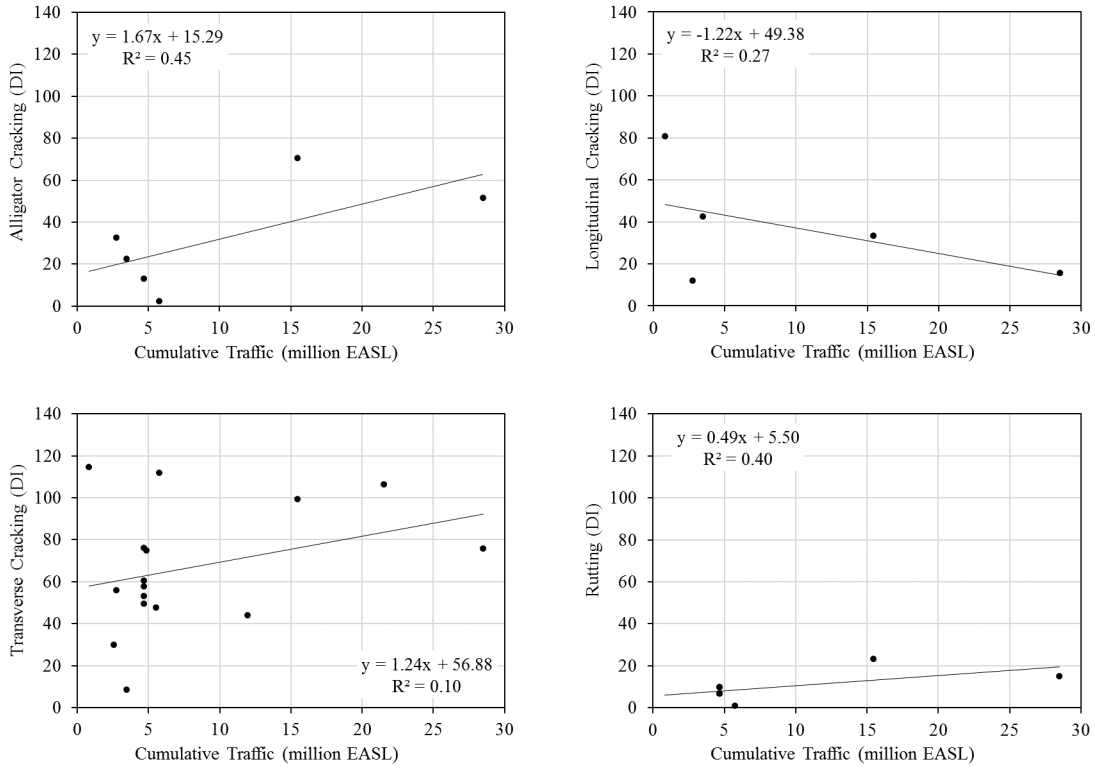

Figure 4-20 Effects of traffic load on four studied distresses

The correlations between the cumulative traffic and the distresses are not very clear given the distribution of the scatters. The correlation between traffic load and rutting is the only trend that is showing to be consistent and logical. Yet, the number of rutting occurrences is too few to establish

4.6 Correlation of Climate with Performance

4.6.1 Rutting

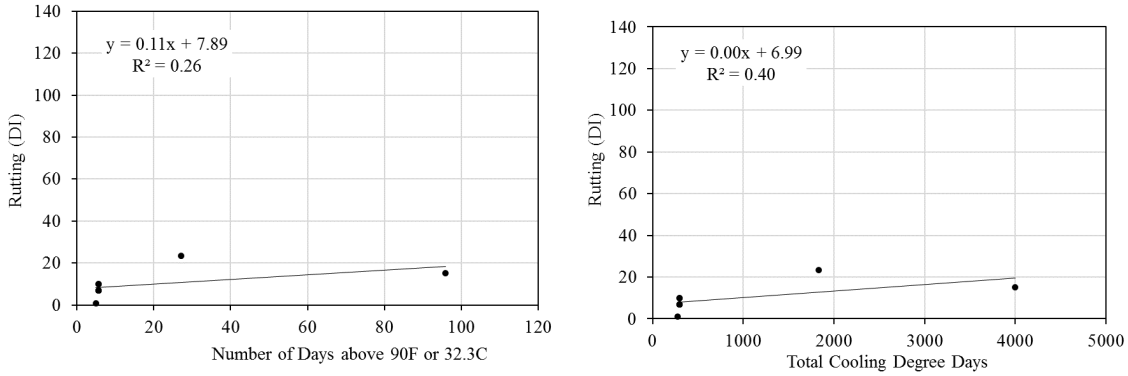

Figure 4-21 Effects of climate on rutting

4.6.2 Alligator Cracking

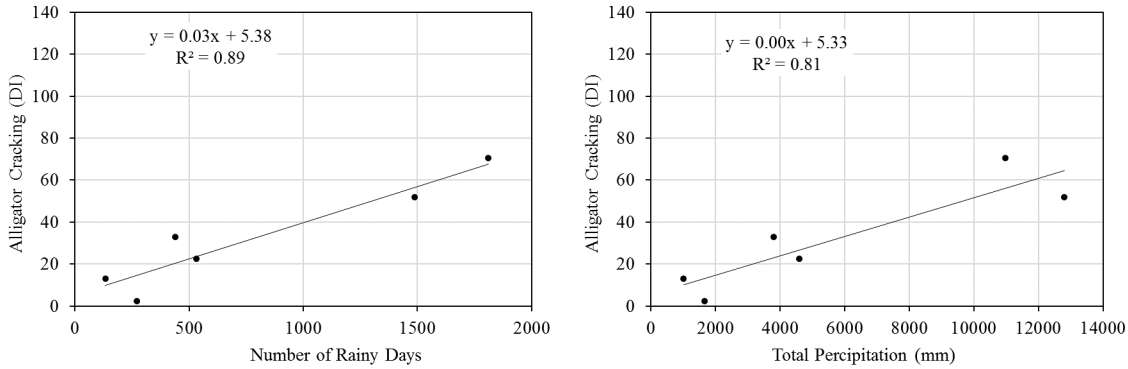

Figure 4-22 Effects of climate on alligator cracking

4.6.3 Longitudinal Cracking

No logical correlations were found.

4.6.4 Transverse Cracking

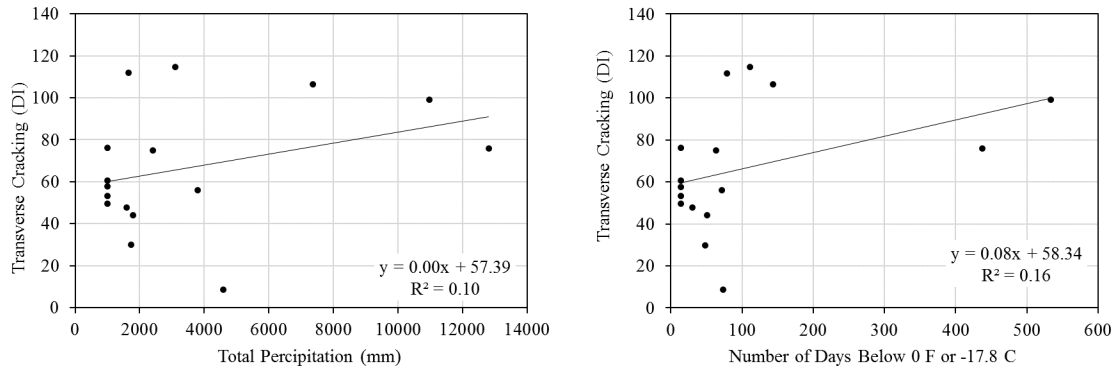

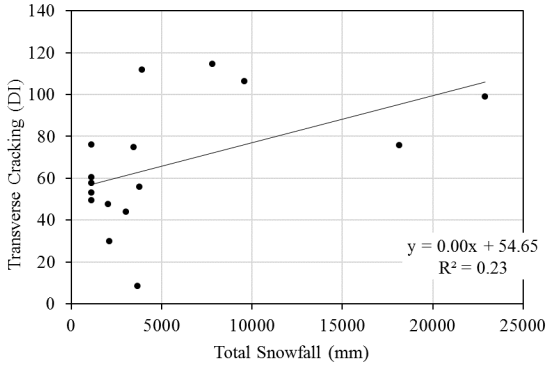

Figure 4-23 Effects of climate on transverse cracking

Summary of the effects of climate variables on performance measurements:

- There is some correlation between the number of days above 32.3°C and rutting.
- Alligator cracking is highly correlated with the precipitation related indicators.
- No logical direct correlations between longitudinal cracking and climate indicators.
- Weak logical correlations between cold weather indicators and transverse distress.

4.7 Comparison between IDEAL and SCB Tests

In this section, a comparison between measured IDEAL results against SCB results at 25ºC is conducted. Because the WP and BWP groups for cores were combined, the additional cores were used to test the cores for IDEAL and SCB. The comparison plots shown below include the overall indices and peak loads.

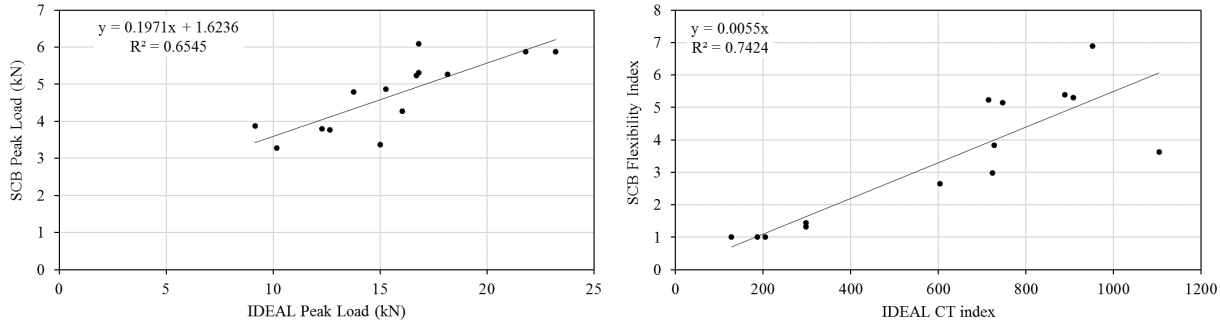

Figure 4-24 Comparison between IDEAL and SCB tests

The comparison presented above shows a very strong correlation between the IDEAL test results and the SCB. This means that both tests characterize the mixes similarly. They can be used interchangeably. Given the ease of use and simpler sample fabrication, the IDEAL appears to be a more suitable candidate for adopting.

4.8 Summary

- The distress survey revealed that transverse cracking has the highest severity and abundance. It was also observed that the rutting has the least deterioration index values compared to the other types of distresses.
- The results of the mixture and binder testing showed that there is no meaningful difference between the WP and BWP samples.
- No direct correlations between the asphalt layer thicknesses and AC with the performance were observed.
- Increasing the in-place density is associated with higher transverse cracking.
- The higher Va is associated with the lower alligator cracking and higher transverse cracking.
- The higher VMA is associated with higher longitudinal and transverse cracking.
- Some weak correlations were observed for high D/B ratio to the higher transverse and rutting, but this needs to be further studied.
- Aggregate uniformity coefficient, Cu, is correlated with the longitudinal cracking. The better the aggregate gradation packing the lower the longitudinal cracking.
- The coefficient of curvature, Cc, is correlated with the rutting and longitudinal rate. Although the data are highly scattered around the trend line. The increase in Cc value is around with the higher rutting and a lower longitudinal rate.
- The IDT dynamic test showed that lower rutting DI is correlated with a higher E* at the rates of 0.1 and 0.5.
- The IDEAL test results showed meaningful correlations with the alligator cracking. The lower CT index and higher peak load are associated with the higher alligator cracking. The opposite trend is observed for longitudinal cracking, whereas the high peak load and lower CT index is associated with a lower longitudinal cracking problem.
- The SCB low-temperature test results were observed to be not correlated with the measured transverse cracking.
- Alligator cracking is correlated with the continuous binder intermediate grade. The higher the grade the higher alligator cracking DI was observed.

- Unlike alligator cracking, the higher continuous intermediate grade of the binder is correlated with a lower longitudinal cracking DI problem.
- The climate data revealed that there is some correlation between the number of days above 32.3^{o} C and rutting and between alligator cracking and precipitation related indicators. However, there were weak correlations between cold weather indicators with the transverse cracking and no correlations between longitudinal cracking and climate indicators.
- There is a very strong correlation between SCB and IDEAL test results. Due to the simplicity of the coefficient IDEAL test, it can be a better substitute for the SCB test in the field.

5. Connecting Mix-Design Parameters to In-Service Performance

This regression analysis was conducted to evaluate in-place factors that may be influencing the performance of the sections under study. These factors include core properties, extracted binder properties, core aggregate properties, traffic experienced by the pavement sections, or climate during the in-service life. Therefore, the regression models provide the connection between mix design and laboratory testing with in-service performance. these models are expected to serve the DOT in its efforts towards developing performance engineered mix design.

The models cover Alligator, Rutting and Transverse Distresses only. Longitudinal cracking was not included due to the small number of sections reporting this distress (5 sections only). It is important to note that transverse cracking is reported in all pavement sections. This analysis was conducted such that the least number of variables can be included in the model given, provided that they are statistically significant, and follow the laws of physics. The developed models provide guidelines for future mix-designs to be engineered for targeted performance levels with respect to the studied distresses.

In pursuing the iterative process of determining the best model, the analysis was conducted without allowing to fit an intercept in the regression model. This is because of the fact that in multivariate fitting, the intercept can act as a balancing measure to achieve higher R^2. The regression fitting was conducted using mixed (backward and forward) fitting with a cutoff p-value of 0.1 for all the independent variables. Then engineering experience was used to select the appropriate variable from the physical point of view. This is in addition to limiting the number of variables to four for alligator cracking and rutting due to the small number of sections exhibiting these distresses (under 12), while the variable used for transverse cracking modeling was increased to 5 since all sections experienced transverse cracking.

5.1 Alligator

For this distress, the regression analysis reveals that it is highly correlated to the continuous intermediate grade of the extracted binder, the age of the pavement, and the core cracking index measured used the IDEAL test. The regression results are shown in the following table.

Table 5-1 Results of the alligator cracking regression multivariate analysis

Term	Estimate	Std Error	t Ratio	Prob>|t|
Continuous Intermediate Grade	0.945	0.180	5.26	0.0005
Age	3.353	0.361	9.28	<.0001
CT_{index}	-0.010	0.004	-2.75	0.0226

The table shows the significance of the three-independent variable. To validate the model, it is important to assure there is no bias in the model. This is done by comparing the order against the residual of the fit. Figure 5-1 shows that the scatter has a random distribution and not any apparent bias. The following plot shows the data order against the residual.

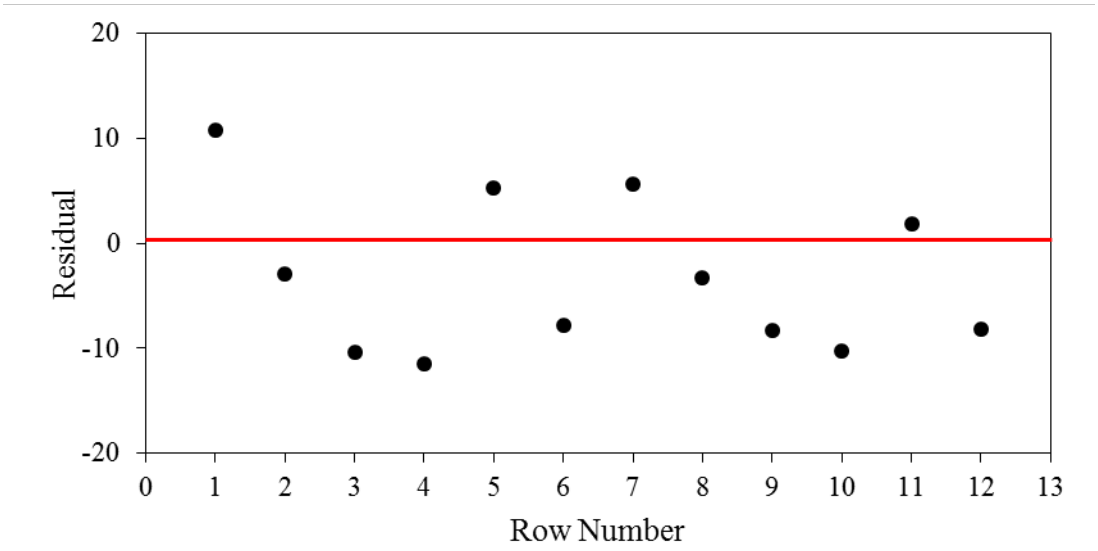

Figure 5-1 Data point order against residual of the fit for alligator cracking model

Comparing the predicted value of the alligator cracking deterioration index against the field measured for the test sections is shown in the following plot. This comparison tests the strength of the fit.

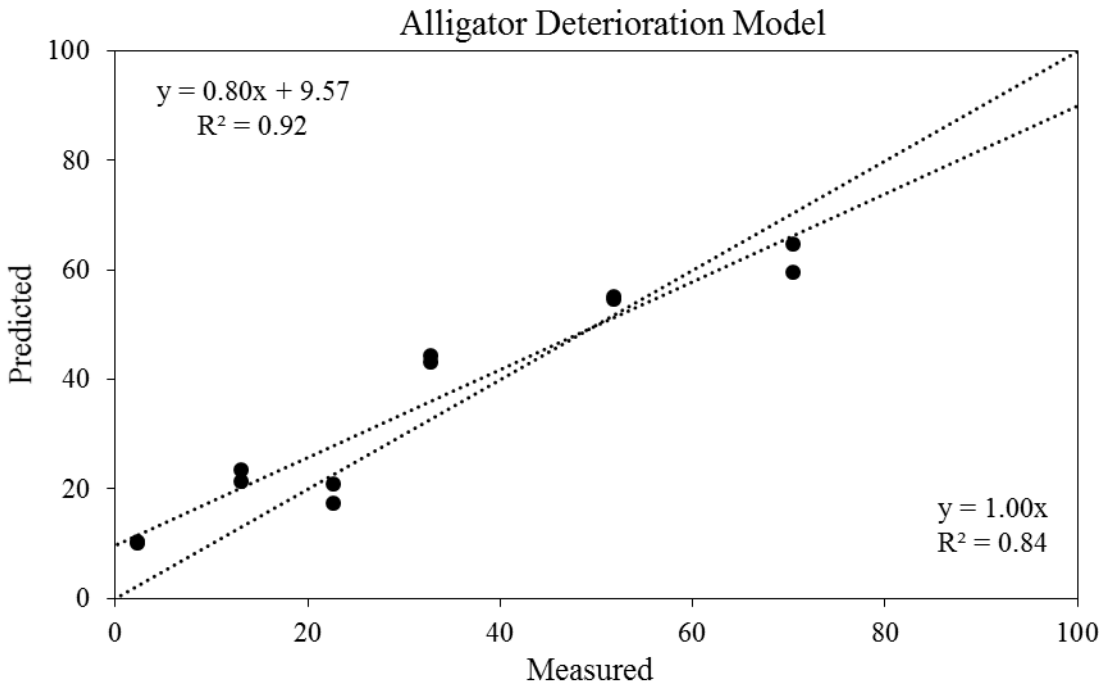

Figure 5-2 Comparison of measured alligator cracking deterioration index against predicted values

As seen in the plot, the regression model produces values that are in strong agreement with the measured values. Examining, the regression parameters, the coefficients of the independent variables follow expected trends. An increase in the intermediate true grade is associated with a higher level of alligator cracking. As the age of pavement increases, the damage level also increases. And as the cracking index from the IDEAL test increases, the mix exhibits less distress. All these trends meet the logical trends of these properties and the observed trends in chapter 4.

This model illustrates how the mix design process can be optimized for the service life of a mix. It is dependent on the binder used in the mix and the overall mixture laboratory performance test.

5.2 Rutting

The same analysis is conducted on the rutting distressed sections. The model yielded dependency on job mix formula (JMF) property, structural design, and core volumetric and mechanical properties. The coefficients for these parameters are meeting expected engineering trends at statistically significant levels. The increase of dust to binder ratio is correlated with a decreased rutting. An increase in the ratio of the surface thickness to the overall thickness is associated with increased rutting. The increase in mix density under traffic is associated with increased rutting. Finally, a higher dynamic modulus at low frequency is associated with decreased rutting.

Table 5-2 Results of the rutting regression multivariate analysis

Term	Estimate	Std Error	t Ratio	Prob>|t|
Dust/Binder Ratio	-31.516	4.062	-7.76	<.0001
Surface Lift/Overall Thickness	40.162	11.223	3.58	0.0059
Core Bulk Density	15.889	2.942	5.40	0.0004
E*@0.5Hz	-0.006	0.001	-4.19	0.0023

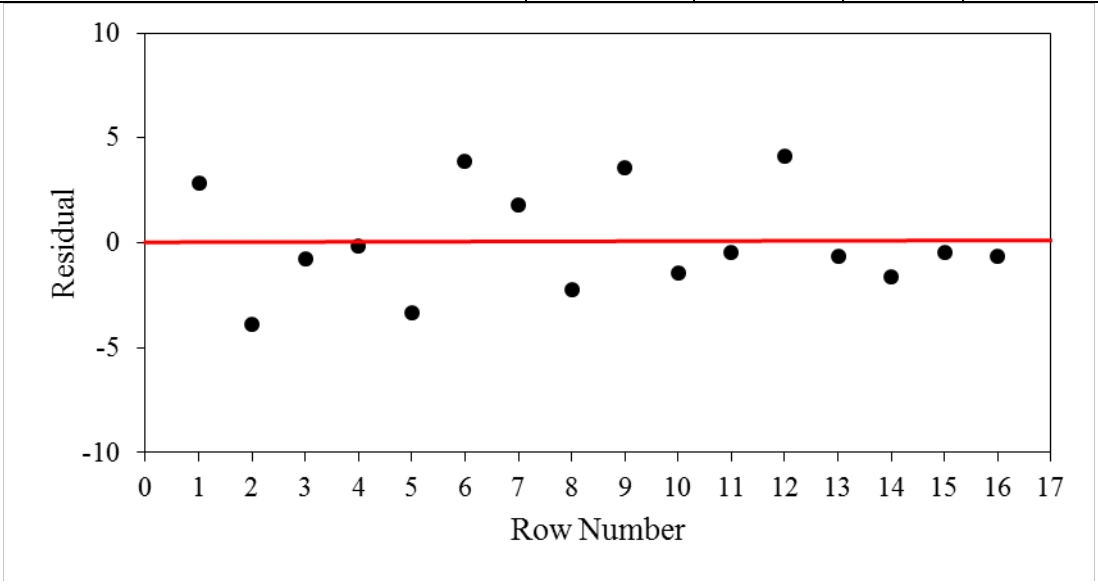

Figure 5-3 Data point order against residual of the fit for rutting model

The scatter of the residual plot confirms the unbiased nature of the model. It is important to note that the range of rutting values included in the analysis is on the low side. This is because the investigated pavements did not show significant rutting damage. Yet, as shown below, the correlation between the measured and predicted values show the ability to achieve a good level of agreement. It is important to note that the slope of the fit line is close to 1.0. Another note, the experimental plan did not include a dedicated laboratory test for rutting and it relied on the complex modulus as a means of evaluating the mechanical response of the mixes. Therefore, in adopting this analysis for performance engineered mix design, it is suggested to focus on including a rutting test that can simulate in-service performance.

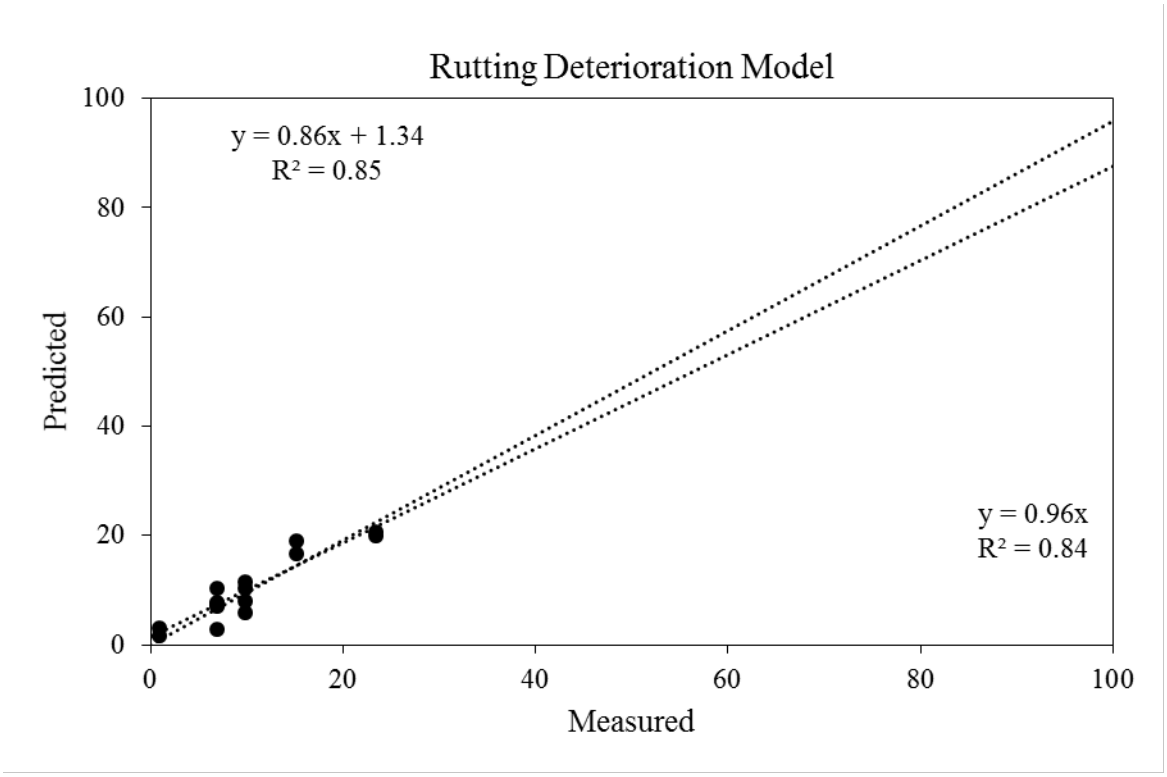

Figure 5-4 Comparison of measured rutting deterioration index against predicted values

5.3 Transverse Cracking

This distress is observed in all sections investigated. The result of the multivariate analysis shows that the extent of this distress is dependent on material and climate as shown in Table 5-3.

Table 5-3 Results of the transverse cracking regression multivariate analysis

Term	Estimate	Std Error	t Ratio	Prob>|t|
Exp(m-value)	-173.17	40.65	-4.26	0.0006
SCB Stiffness/ΔT_c	0.57	0.28	1.99	0.0636
Dust/Binder Ratio	59.91	26.73	2.24	0.0395
Log(Total Snowfall (mm))	19.57	4.19	4.67	0.0003
Surface Lift/overall thickness	151.02	62.72	2.41	0.0285

As seen in Table 5-3, the factors included in the model are highly significant given the low p-values. In addition, the dependency of the transverse cracking on these factors is logical. The model shows a balanced dependency of the transverse cracking on binder properties, mixture properties, mix design parameters, pavement structure, and climate. For the binder, the higher the m-value from the BBR (higher relaxation) the lower the transverse cracking. In fact, the m-value is the

most significant parameter in the model as shown by the lowest p-value. Another binder property that has significant influence is ΔT_c. However, the influence of this parameter is in the form of interaction with the mixture stiffness as measured by the SCB. The regression model shows that for a given mixture stiffness level, the higher the binder ΔT_c value the less prone the pavement to transverse cracking. This is critical as it provides a transfer function between laboratory mechanical testing and in-service performance. In addition, the model shows that the dust to binder ratio has a significantly detrimental effect on cracking along with the ratio between the surface lift thickness and the overall thickness of the pavement. The residual plot shown in Figure 5-5 demonstrates the unbias of the trends in the model.

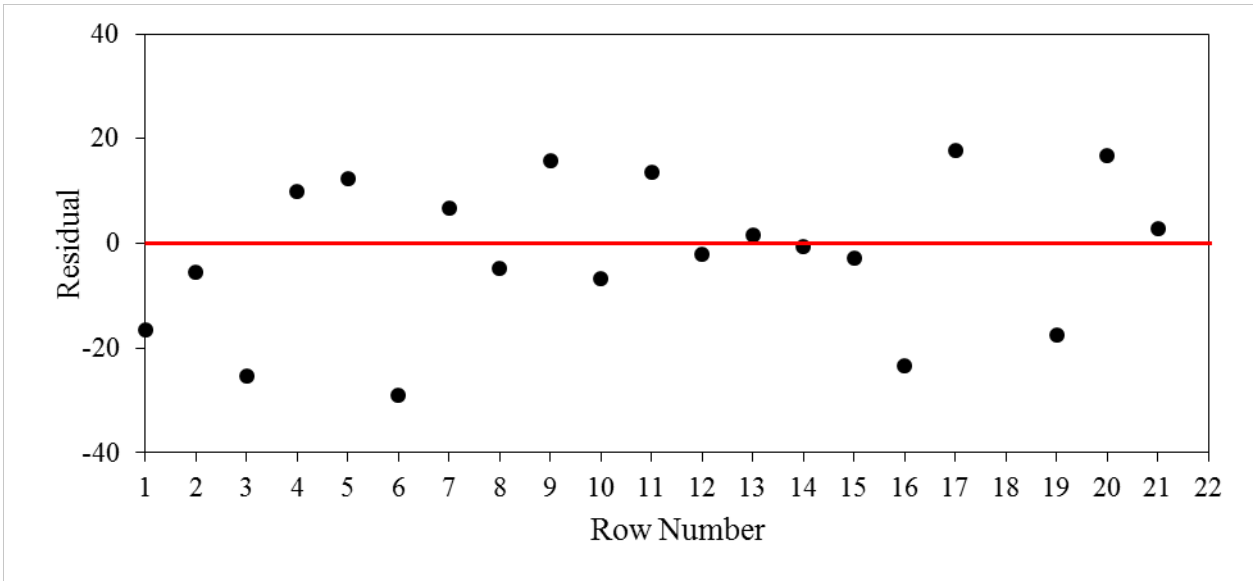

Figure 5-5 Data point order against residual of the fit for the transverse cracking model

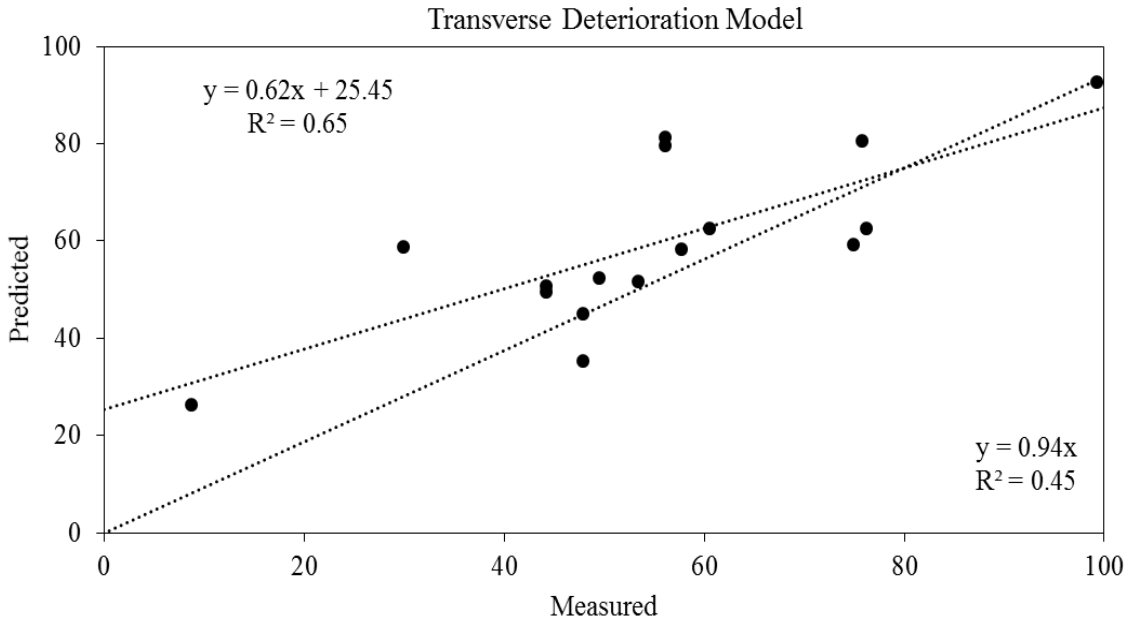

Figure 5-6 Comparison of measured transverse cracking deterioration index against predicted values

The comparison shown in Figure 5-6 illustrates the ability of the model to fit the wide range of distress deterioration index values observed in the field sections. The R^2 value for the fit is acceptable. While most of the DI values are clustered in the middle of the range, the model can capture the values on both ends of the range with relative accuracy.

5.4 Summary

The multivariate analysis summarized above is prepared to provide a link between laboratory measurable properties and in-service performance for specific distresses. These measurable properties include mix design properties, binder performance testing, and mixture performance testing. Linking the in-service performance to these parameters can provide the Wisconsin DOT the foundation for pursuing performance engineered paving (mix design, construction, and pavement management). It is highly recommended that the DOT continues to conduct similar efforts to expand the data used in the analysis.

It is important to note that the models above did not incorporate production as a variable. The intention of these models is to help relate mix design, expected traffic, and climate to targeted distresses. They serve as the basis for developing performance engineering mix designs for future roadways. However, from a deterioration prediction point of view, the limited data generated for this study is not enough to conduct a comprehensive statistical model. Therefore, the data from

this research is combined with data from previous Wisconsin Highway Research Program (WHRP) research to achieve the goal of developing performance deterioration models for the Wisconsin network. The next chapter documents this effort.

6. In-Service Performance Deterioration Modeling

For the pavement management point of view, it is important to simulate in-service deterioration over the lifetime of the pavement. Having deterioration models that can incorporate the unique properties of each pavement section such as structure design, loading, environmental condition, and most importantly quality of construction and production as the inputs of the model is important. This approach would serve to continuously improve quality programs for state transportation highway agencies and provide the essential foundation for building performance-based mix design and improve quality control programs for pavements (Bozorgzad *et al*. 2018). This approach is able to predict the behavior of the pavement at the desired stage. The objective of this chapter is to construct a framework of deterioration modeling of in-service performance effectively. This framework is constructed using georeferenced relational database architecture.

Data entries used in this chapter include those collected for this project combined with data collected in WHRP project 0092-15-05. This means that that the database is made of 42 paving projects comprising about 240 miles of Wisconsin network. The pavement sections included in this chapter's modeling include those with thickness greater than 2 inches due to the varying sensitivity of pavements thinner than 2 inches to the input parameters.

6.1 Construction of Machine Learning Models

Based on the background discussed earlier, the as-constructed and as-produced information, as well as the field data gathered for evaluation of pavement deterioration, were utilized to develop learning algorithms. Indeed, learning models were employed to forecast the total deterioration of a pavement layer, TDI, using relevant predictor variables comprised of the influencing factors on pavement performance. These algorithms were developed based on parameters such as pavement age, lot mix production air void (Va), lot mix production voids in mineral aggregates (VMA), asphalt content (AC), placement density (%Gmm), asphalt thickness, and cumulative traffic from the construction time to the date of the survey in million EASLs. All these parameters are believed to impact the in-service performance of the pavements. The descriptive statistics of the input parameters as well as the dependent target for 240 pavement sections are listed in Table 6-1.

Table 6-1 Summary of descriptive statistics of the predictor and dependent variables

Descriptive Statistics	Predictor Variables							Depended Target
	Age (year)	Production Va (%)	Production VMA (%)	Placement Density (%Gmm)	Thickness (in)	Cumulative Traffic (million EASL)	AC (%)	Total DI
Mean	5.75	4.39	14.64	93.39	4.09	9.65	5.44	32.61
Median	6.00	4.12	14.61	93.15	4.26	9.40	5.38	30.33
Standard Deviation	2.43	0.30	0.57	0.94	0.61	3.67	0.45	20.77
Range	16.00	1.60	3.15	4.74	2.75	24.07	2.37	95.99

The pavement deterioration index, DI, was defined as a function of predictor variables listed in Table 6-1. The general form of the predictive function is:

$$\boldsymbol{TDI = f(Age, Va, VMA, \%Gmm, InPlace\ Density, Thickness, Traffic)} \quad \text{(Equation 6-1)}$$

Traditional regression techniques (e.g., least-squares linear model, logistic regression, multiple regression, Bayesian approach, etc.) have been widely used in pavement-related projects as documented in Galin (1981), Moossazadeh and Witczak (1981), Hong and Prozzi (2006), Park *et al*. (2008), Kaur and Pulugurta (2008), and Wang (2019). However, the methods mentioned above are less effective in solving complex problems such as the deterioration of flexible pavements.

Data mining techniques have been gaining popularity as a powerful tool to overcome the drawbacks of traditional methods since the techniques are capable of yielding more reliable and satisfying results in complex nonlinear problems in pavement engineering (Nemati and Dave 2018; Ashtiani *et al*. 2018; Notani *et al.* 2019, Rogers *et al.* 2017). Even though the techniques are cost-intensive in terms of computational efforts, data mining can reveal the hidden relationships between the input and output variables using methods such as clustering, resampling, recursion, visualization, generalization, and randomizations (Prasad *et al*. 2006, Majidifard *et al.* 2019). In this chapter, different learning algorithms are evaluated and compared using the collected database to develop more accurate and more reliable deterioration models. The machine learning methods assessed in this study are as follows: (1) Decision Tree Regression (DTR); (2) Random Forest (RF); and Gene-expression Programming (GEP).

6.2 Decision Tree Regression (DTR)

Decision tree regressions (DTRs) are learning predictive models used for classification and regression. The preliminary form of the decision tree was constructed by Morgan and Sonquist (1963). A newer structure of the model, i.e., Classification and Regression Tree (CART), was developed in the mid-80s (Breiman *et al*. 1984 and Breiman *et al*. 1995). Popular forms of decision trees, e.g., C4.5, C5, and ID3, can be found in Quinlan (2014). Based on the goal and the nature of the data, the tree structure can be developed for either classification or regression purposes. A DTR is comprised of three sub-structures: (1) root node is the beginning part of the tree—corresponding to the best solution—which is assigned to all the training dataset. This node is divided into new intermediate nodes using an iterative process called recursion. To avoid an over-fitting prediction from the constructed decision tree after the recursion step, a pruning phase is applied that attempts to remove the highly specific sub-trees. (2) Intermediate nodes that connect the leaf and root nodes using mathematical equations; and (3) the leaf nodes (end nodes) that provide a numerical prediction. DTR is, indeed, a top-down approach which means the analysis is implemented from the root node progressing down to the end nodes (Apté and Weiss, 1997).

For this study, the structure of the DTR was constructed using a coded subroutine in Python®. The minimum number of test samples to split an internal node was optimized to be 6, while the minimum number of test samples placed at each leaf was taken to be 4. Mean Square Error (MSE) was deployed as the fitness criterion for developing the trees. MSE is determined as:

$$\boldsymbol{MSE} = \sum_{\boldsymbol{i=1}}^{\boldsymbol{n}} \frac{(\boldsymbol{x_i - y_i})^{\boldsymbol{2}}}{\boldsymbol{n}} \qquad \text{(Equation 6-2)}$$

Where x_i is the measured field deterioration index (DI), y_i is the predicted pavement deterioration index, and *n* is the number of collected samples. To predict the pavement deterioration index, a dataset including 240 fields measured test samples were used. It is worth to mention that the dataset was constructed based on not only the 12 projects in this study but also 30 more projects that were studied by the authors of this report in a previous study for WisDOT (Faheem *et al*. 2019). The data was then randomly split into training and testing subsets. 80% of the data, i.e., 190 test samples, was assigned to the training subset. Then the remained 20% of the data, i.e., 50 test samples, was kept out for testing the constructed DTR model. Figure 6-1 compares the measured field pavement deterioration index with the decision tree-predicted model for both training and

testing subsets. It is observed that the DTR is potentially successful in terms of yielding promising results as judged by the coefficient of determination, R^2, and root mean squared error, *RMSE*, for the training and testing datasets (Figures 6-1a and 6-1b).

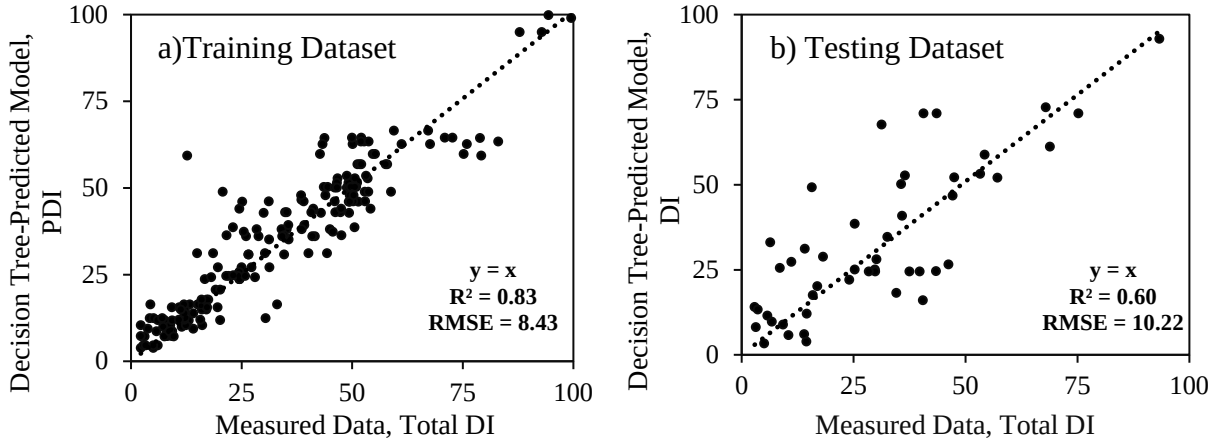

Figure 6-1 Decision tree-predicted model vs. measured field pavement deterioration: (a) training dataset and (b) testing dataset

6.3 Random Forest (RF)

Random Forest (RF) is an ensemble regression technique (Breiman, 2001). RF has been used in different studies, and in a few of them, prediction of pavement deterioration has been studied (e.g., Lee *et al*. 2015; Gopalakrishnan *et al*. 2017; Sharma *et al*. 2018, Ghasemi *et al.* 2019). RF is a specialized form of regression trees including organized constraints and boundary conditions applied sequentially in a top-down approach to the root and leaf nodes of the constructed trees. A randomly selected training subset is used for each tree during the construction of RF. The training subsets are then replaced as many times as the number of trees made in the ensemble. It should be pointed out that the bootstrap aggregation is typically used in the constructed trees. Bootstrap is a sampling process which means some of the constructed samples are replaced by the scenarios from the training subset, and some will be kept out (Svetnik *et al*. 2003).

Evaluation of the machine learning models is usually done using a large number of samples (being actual data or synthetic ones) that basically verify and test the trained algorithm. Due to the nature of field data in which its collection is cost-intensive in terms of time, energy, and money, a limited number of collected samples can be assigned for verifying the constructed RF model. Thus, different cross-validation techniques (e.g., out-of-bag, K-fold cross-validation, etc.) can be

deployed along the training process to provide better and more reliable anticipation (Svetnik *et al*. 2003). In this study, the out-of-bag (OOB) sample was selected for the purpose of cross-validation. Similar to the DTR algorithm, the constructed random forest was developed using a training subset including 80% of the collected field data. 20% of the data was left out to verify and test the model. A coded subroutine in Python® was utilized for constructing the model architecture. The RF features were optimized to yield the best prediction as follows: No. of trees in the forest = 240, minimum No. of samples required to split an internal node = 5, the minimum number of samples required to be at a leaf node = 3. Figure 6-2 shows the comparison of the random forest-predicted model and the measured DI, for both training and testing datasets. The RF model can predict pavement deterioration relatively accurate as assessed by the high coefficient of determination, R^2 = 0.68, and low root mean squared error, *RMSE* = 10.17

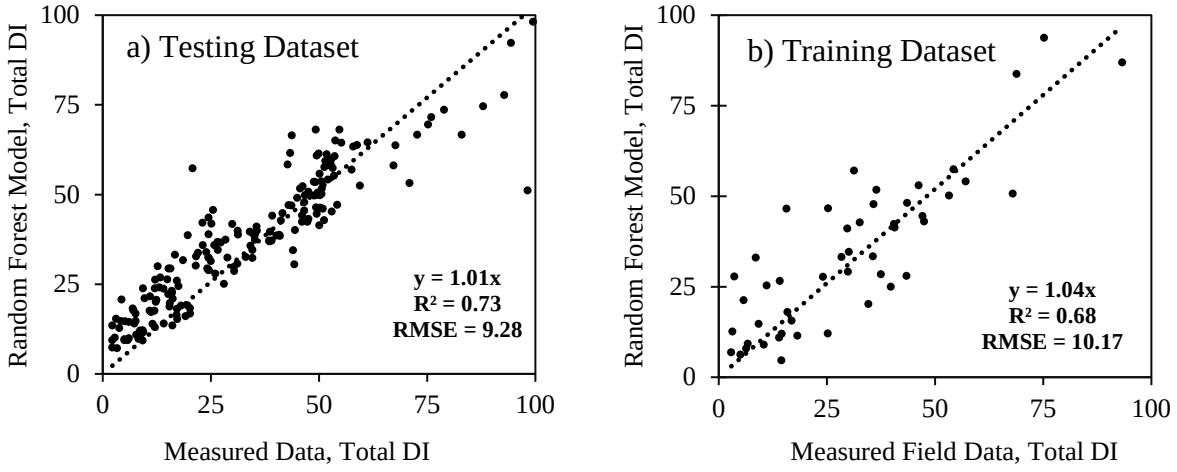

Figure 6-2 Random forest-predicted model vs. measured field pavement deterioration: (a) training dataset and (b) testing dataset

6.4 Gene-Expression Programming (GEP)

Even though, the machine learning techniques including DTR and RF are robust tools for the prediction of pavement deterioration, the product of these models may not be an easy-to-use function since the methods are incapable of developing the predictive models in the form of mathematical equations. Thus, genetic programming (GP) can be deployed to overcome the drawbacks of such methods. In this study, gene-expression programming—an evolutionary learning algorithm—is used to provide the total deterioration of pavements regarding the mathematical equation.

Genetic programming (GP) is an evolutionary computation (EC) technique that can solve complex problems in a dynamic environment using an iterative optimized process to generate the best predictive model (Poli *et al*. 2008). Gene expression programming was first adopted to produce a practical solution for prediction models by Ferreira (2001). GEP is the specialized form of genetic programming (GP) which can be referred to as a type of genetic algorithm since it is essentially composed of a population of mathematical solutions that ultimately evolves the selection of the best solution using an optimization process. In fact, the tree structures in the genetic algorithm are computer programs (Koza 1990). In GEP, the structural ordering of the tree comprises several functions and terminals. An optimization process can determine the final function of the tree. The optimization process is conducted using the fitness function with the training data. Indeed, if the fitness criterion is not satisfied, new generations of expression trees would be regenerated. The regeneration is on the basis of different processes including replication, mutation, transposition and insertion, recombination, and so on (Ferreia, 2001). In this study, the root mean squared error (*RMSE*), was used as the fitness function.

Generally, the function (f) includes the primary arithmetic operations, i.e., +, -, ×, /, etc; Boolean logic functions, i.e., AND, OR, NOT, etc; or other mathematic functions. The terminal set T contains the arguments for the functions and can consist of numerical constants, logical constants, variables, etc. The functions and terminals are initially chosen at random to construct a tree-like structure with root points with ending in a terminal node (Gandomi and Alavi 2012). An example of an expression tree is demonstrated in Figure 6-3. In this example, the terminal node symbolizes independent variables or constant values. The mathematical form of the expression tree is as:

$$e^{\left(\frac{X_1}{C_1}\cdot\sqrt[3]{X_2}\right)} \qquad \text{(Equation 6-3)}$$

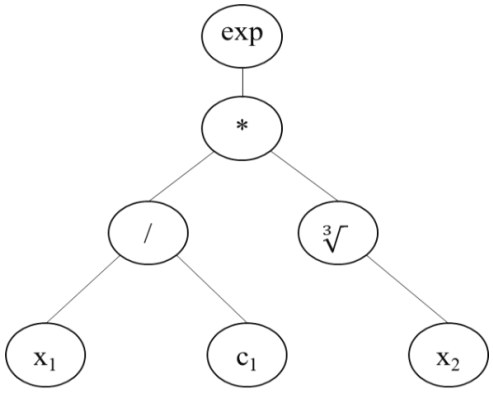

Figure 6-3 Example of an algebraic equation with an expression tree

Where x_1 and x_2 are independent variables and c_1 is the constant value. To predict DI using the GEP model, the collected database including 240 measured field samples was utilized. As the first step, the database was randomly split into the training and testing datasets. For this purpose, 80% of the database (190 cases) was assigned to the training subset and the rest (50 samples) to the testing set. The GEP structure was built using twenty-five chromosomes with three genes and the head size of ten. It is noteworthy to mention that the optimized model can be profoundly influenced by the selection of the parameters mentioned above. The size and number of GEP structure parameters were thus optimized through an iterative process.

To develop the best predictive model, the fitness function was selected as *RMSE*. The following equation was developed as the best predictive function for pavement deterioration index:

$$\mathbf{TotalDI} = \boldsymbol{C_1}\mathbf{Thickness} + \frac{1}{\boldsymbol{Thickness}} \times \Big(\boldsymbol{C_2 AC} + \boldsymbol{C_3 PlacedDensity} + \boldsymbol{C_4 Age} + \boldsymbol{C_5}\frac{\boldsymbol{VMA}}{\boldsymbol{VA}} + \boldsymbol{C_3 Cos}(\boldsymbol{C_{10} VMA}) - \boldsymbol{C_6} - \boldsymbol{C_7 VMASin}\big(\boldsymbol{C_{11}}^{\boldsymbol{Age}}\big) - \boldsymbol{C_7 VMACos}\big(\boldsymbol{C_{10} VMA}^{\boldsymbol{2sin(C_{14} PlacedDensity)}}\big) - \boldsymbol{C_3 Sin}(\boldsymbol{C_{12} PlacedDensity})\Big) + \boldsymbol{C_{13}} \times \frac{\boldsymbol{Traffic^2}}{\boldsymbol{AC \times VMA}} + \boldsymbol{C_8}\mathbf{Sin}(\boldsymbol{AC \times VMA}) + \boldsymbol{C_{13} Traffic} - \boldsymbol{C_9}\mathbf{AC} \times \boldsymbol{V}\mathbf{MA} \quad \text{(Equation 6-4)}$$

Where C_i are the constants; C_1 = 1.53, C_2 = 1.74, C_3 = 35.19, C_4 = 19.24, C_5 = 31.86, C_6 = 3417.65, C_7 =3.96, C_8 =0.18, C_9 =0.05, C_{10} =15273, C_{11} =2.99, C_{12} =297.20, C_{13}=0.02, C_{14}=-1052.06

Figure 6-4a compares the predicted DI determined by the GEP-developed Equation 6-4 with the corresponding field data. A promising estimate of the pavement deterioration can be governed by the GEP model with an R^2 of 0.63 and root mean squared error (*RMSE*) of 13.28. Figure 6-4b demonstrates the comparison of the GEP and measured field data using the testing dataset; the results show an acceptable correlation with R^2 of 0.59 and *RMSE* of 13.70. To reach the best model, about 1.8×10^6 populations of individuals were generated indicating that a computationally cost-intensive process is required to acquire the best predictive function.

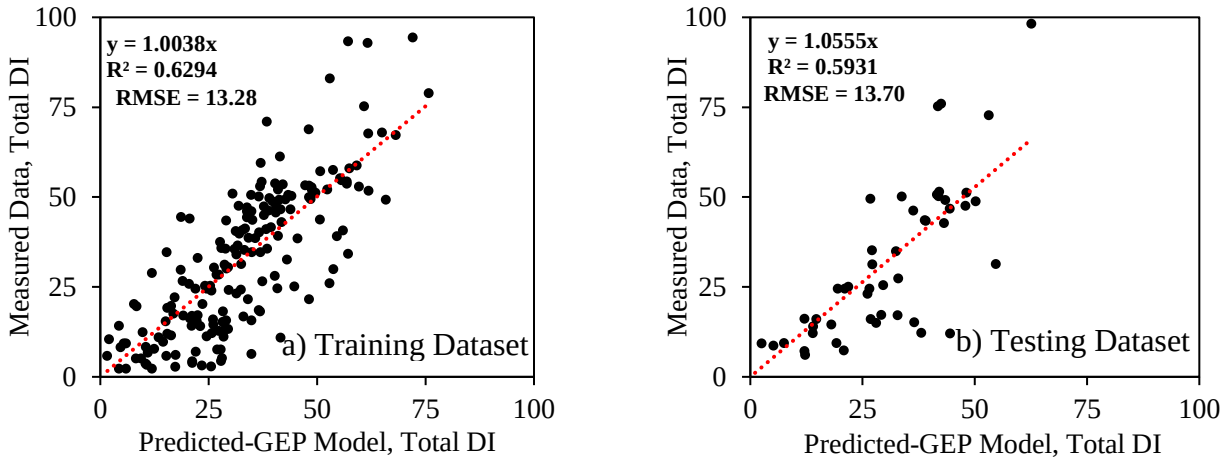

Figure 6-4 Comparison of GEP-predicted model and FE model for the pavement deterioration index (a) training dataset and (b) testing dataset

6.5 Transfer Function between PCI and DI

The performance models in this study are developed based on the total DI rather than the PCI values. This decision was made by the authors due to the fact that; a) the mechanisms, occurrence and mechanical dependency of these four distresses to the asphalt mixture properties are massively investigated and proven in the literature; b) the authors confirmed these four distresses by independent field performance surveys; c) the DI allows investigating the effects of quality of construction and production on the performance for each distress. Due to the importance of the PCI, the correlation between PCI and DI is also investigated in this study by a transfer function. The developed transfer function can bridge PCI to DI. The Function was developed based on Genetic Programming (GP). The correlation of the PCI to DI is:

$$\boldsymbol{PCI = 99 + \frac{0.079}{TDI - 4.16} - sin(0.289TDI) - sin(5.83 - 477TDI) - 0.655TDI - 8.73sin(0.098TDI)} \quad \text{(Equation 6-5)}$$

Figure 6-5 shows the predicted PCI values by using the GEP method against the actual measurements reported in the PIF. As the graph shows, the correlation is often more accurate when the PCI is in a higher range or better serviceability condition.

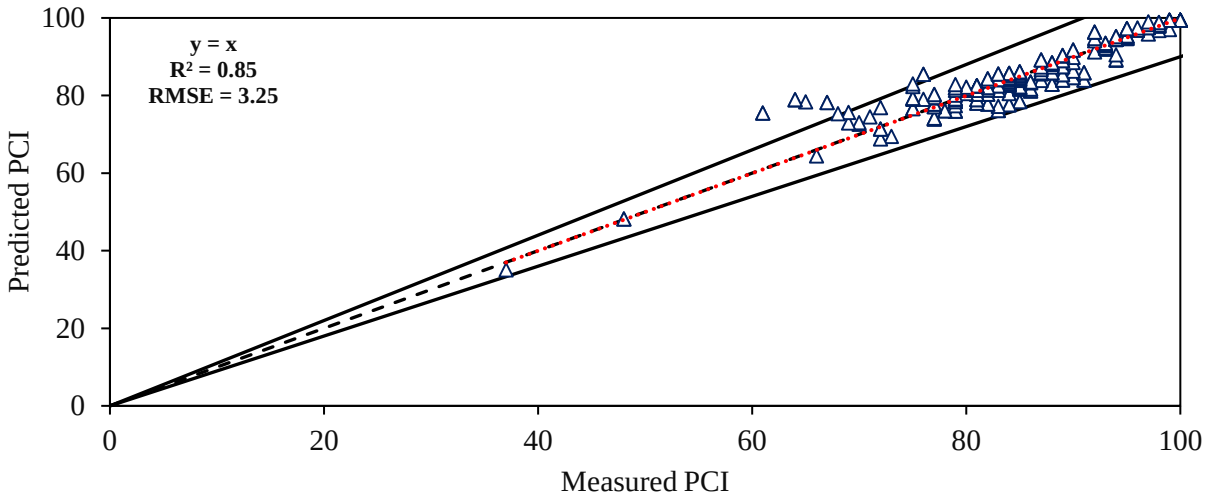

Figure 6-5 Measured PCI vs. predicted PCI

Figure 6-6 shows the validation set of data for GP predicted values against the actual field measurement. This graph provides a more detailed validation of the data points used in this study against the predicted PCI for all studied SNs. As it can be noticed, the higher accuracy achieved for, higher PCI values. The lower PCI values often represent pavements in a point that are suffering from a variety of different distresses, and not just limited to the four studied here. These pavements are potentially susceptible to other forms of deterioration such as potholes, weathering, etc., which decrease PCI to lower values, while the performance models are overlooking those distresses.

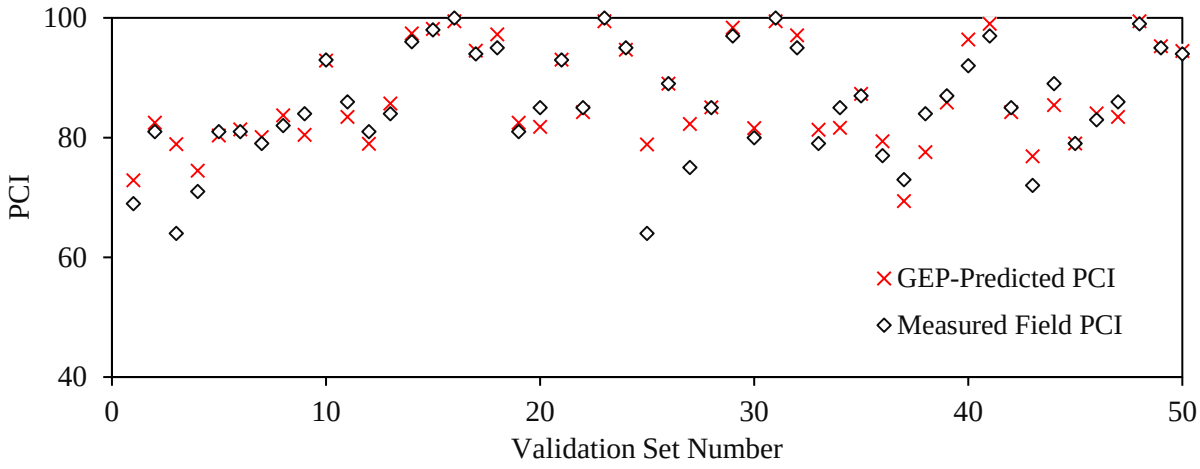

Figure 6-6 Validation of the developed transfer function

6.6 Summary

- With the help of artificial intelligence, a series of machine-learned models were developed. These models are based on the collected database in this project as well as the WHRP project 0092-15-05.
- The developed models are based on the 42 highway projects, and 240 SNs within the WisDOT highway networks. The total length of the database exceeds 240 miles.
- Input parameters used in these models are including age, production Va, production VMA, placement density, asphalt layer thickness, cumulative traffic, and AC. The models target/output parameter is the summation of DI values of the four investigated distresses of rutting, alligator, longitudinal, and transverse cracking.
- In these models, the dataset divided to 80% for training the model, and 20% for testing the accuracy of the developed models.
- The predictions made by the decision tree regression model are compared to the field data. The comparison resulted in R^2 of 0.83 for the training set, and 0.60 for the testing dataset. The RMSE values were 8.43, and 10.22 for the training and testing datasets, respectively.
- The predictions made by the random forest model is compared to the field data. The comparison resulted in R^2 of 0.73 for the training set, and 0.68 for the testing dataset. The RMSE values were 9.28, and 10.17 for the training and testing datasets, respectively.
- Gene-expression programming is used to construct the deterioration model equation. To reach the best model, about $1.8x10^6$ generations of the model were tried by using all the input parameters.
- The Gene-expression programming model predictions were compared with the actual field measurements for both training and testing datasets. The R^2 and RMSE values for the training dataset were 0.63 and 13.28, respectively. For the testing dataset, R^2 and RMSE were 0.59 and 13.70, respectively.
- Due to the fact that PCI value is widely used as an indicator of the overall performance of the pavement, a transfer function for converting the total DI value to PCI was constructed.
- The transfer function between PCI and DI was developed by using a machine learning technique of genetic programming.

- Comparing the measured PCI values with the predicted ones, the R^2 is calculated to be 0.85, and RMSE is calculated to be 3.25. The model shows more accurate predictions in the higher PCI values.

7. Summary, Conclusion, and Recommendations

7.1 Summary and Conclusions

This study was conducted to help the Wisconsin DOT relate the in-service performance to measurable variables for improved performance in the future. The data collected is used to highlight the trends and generate models to assess the influence of material properties and loading (traffic and climate) factors on specific pavement distresses. Additional data is used to create generalized performance deterioration models. The presented models employed traditional multivariate analysis as well as machine learning methods.

- This study highlighted that transverse and longitudinal cracking are the most frequent and have the highest severity level among all studied distresses. While transverse cracking is modeled in this study, longitudinal has proved to be difficult to model. This is because most of the longitudinal cracking reported in the Wisconsin database is related to joint cracking, not in-lane cracking. Thus two different mechanisms are involved in it, one is construction-related and the other is mechanical behavior. Since separating the in-lane and join cracks was not possible, it is suggested that a separate project be conducted to evaluate the influencing factors on this distress.
- The data collected and analyzed in this research shows that the Wisconsin network is performing well in terms of rutting and alligator cracking. Other types of distresses are also present but at much reduced extent.
- The discrepancy between the on-site distress survey and spider van distress survey, PIF database, is observed. The differences are in the extent of the observed distresses and severity level.
- The multivariate analysis provided a statistically significant correlation between mix performance and in-service performance. This is critical in advancing performance-based specifications.
- The deterioration model presented in this report presents pavement dependent modeling for improved pavement management practices. The input parameters are unique for each individual sequence number. Therefore, the model is implementable without major changes in the current state of practice within the state.

- Cracking (transverse and alligator) is dependent on asphalt binder properties. Rutting is less sensitive to asphalt binder properties.
- Mix design is highly critical for rutting resistance and transverse cracking.
- The asphalt content was found to be critical for transverse cracking only.
- The deterioration model is dependent on structural design, and construction quality. It can be used for effective pavement management planning, and to conduct sensitivity analysis for determining quality specification limits.

7.2 Recommendations

The recommendations based on the findings of this study are:

1- Implementing the multivariate models as the foundation for developing performance engineered mix design protocols for future pavement mixes.
2- Implementing the proposed deterioration models for a performance-based pavement management protocol.
3- Update the DOT data collection and storage technology to adopt a geo-relational pavement history system. This will create a database capable of updating the deterioration model continuously using available machine learning tools for higher accuracy. In addition, this database framework allows for developing deterioration models for different classes of pavements.
4- Update pavement performance surveying schemes with respect to technology used and segmentation of the pavement network. This is critical since the deterioration models will always be as accurate as the pavement history data.
5- Conduct a similar study on thin pavement lifts as they are a separate class. The analysis conducted for developing the deterioration models was forced to remove data pertaining to thick lifts as their performance significantly differs from thicker pavements.
6- Calibrate pavement structural designs based on the deterioration modeling proposed in this report.

7.3 Comments Regarding Implementation

This research combines laboratory testing with field evaluation and advanced data analytics. The nature of laboratory and fieldwork requires a significant level of effort and cost. The utilization of pavements history data collected at the different stages of their life cycle reduces such expenditure and increases the impact and significance of pavement research. It is understandable that historically, such data-driven research was not common. The current advances in computing, storing, and software technology have made this type of research as the new norm. Therefore, a given agency needs to go through the stages of adaptation to build the needed infrastructure for data-driven research complemented by lab or fieldwork.

In pursuing this research, the research team employed different tasks and techniques to compile the needed relational database. This section is prepared as a recommendation guide for the future implementation of such research. This section would also help the DOT in upgrading the current data management protocols for ease of implementation. The following summarizes the recommended steps to create a better environment for conducting data-driven research:

1- Divide the network into segments for monitoring performance. the current segmentation is about one mile long. This is too long of a segment, especially that only 1/10 of this segment is monitored as a sample. It is suggested that the segmentation be about ½ a mile long at most. This will significantly minimize inconsistencies in performance data and allow for self-calibration of recorded performance trends for the same pavement. For example, some of the pavements tested in this study were designated as premature failure pavements. An investigation of the PIF database as well on-site evaluation revealed that none of these pavements are out of the norm in terms of rate of deterioration. Moreover, due to the length of the current segmentation, it is observed that a given segment contains multiple construction projects. This can cause confusion in interpreting the performance measurements. A higher resolution segmentation will allow higher confidence is such designation as comparisons with segments before and after a specific position provide a starting point in the full-scale evaluation of the entire paving project. The new segmentation system should be synced with future project assignments, where the production and construction related works could be easily linked with the performance surveys.

2- Use new technology in distress surveying such as imaging techniques. This allows for conducting faster performance surveys, within a shorter time period, and at a higher area of coverage if not the full area of the segment. Such that work can significantly improve the accuracy and resolution of the deterioration models in terms of the aging effects on performance. These techniques should be able to conduct and record spot performance measurements. The new surveying techniques should be able to differentiate between the construction-related issues, such as construction-joint cracks, with the deterioration caused performance issues. This approach provides the bases for geo-tagging the distresses to investigate location-based patterns.

3- Conduct non-destructive testing on pavement sections to obtain a baseline of mechanical stability at the desired locations. With a database with a higher resolution of distress distribution, the utilization of non-destructive testing can be manipulated to validate alarming trends or verify red flags.

4- Pavement structural plans should contain locations by the stations and GPS coordinates. This is achievable at an easier level if the DOT adopts 3-D modeling in project documentation and plans. Such effort is already undertaken in Wisconsin, Iowa, Georgia, and Pennsylvania. It is also promoted by the FHWA. However, its intended utilization is for preconstruction streamlining. In-service study of transportation infrastructure offers a post-construction utilization of this new technology. This is because the 3-D models provide the basis for the geo-referencing of the data in relation to other components of the asset. This is especially critical in studying other classes of pavements and in studying bridges. The structural plans should also recognize the DOT segmentations throughout, defining the construction stations within the associated DOT segments.

5- Quality data collected during material production or during placement and compaction needs to be tagged with their GPS location. Proper labeling and storing of data needs to be a requirement as much as passing specification limits. This was a major challenge in this project. Many pavement sections were supposed to have their placement density records stored at the online portal; however, they were not. This could be due to the fact that the primary objective of this data is compliance. This needs to be changed, as it is revealed that the collected as-built information is valuable in developing more accurate prediction models and diagnostic analysis, which can consequently facilitate better-informed

decision-making. Moreover, continuous storage of the quality data would serve as a means to find the individual quality patterns for different contractors, materials, procedures, and equipment used in the state. Cloud storage is an excellent resource for storing this data and for ease of integration in larger databases.

6- Maintenance activities must be recorded by locations and time in detail. They could be connected to the 3-D model in the post-construction mode. Depending on the type of the used maintenance activity, any changes to the structural properties of the pavement should also be recorded.

7- Data for all aspects of the pavement life cycle must be accessible and connected to allow for retrieval of complete pavement history. This requires re-examining the jurisdiction and ownership of the data by the different bureaus within the DOT.

8- Once the agency's data is properly stored and geo-tagged, artificial intelligence is used to create the machine-learning deterioration models for the appropriate classes of pavement. However, these deterioration models must be updated regularly as part of the management plan. The model update needs to be synchronized with distress survey efforts, maintenance activities and other collected data.

9- In addition to the above-mentioned implementation steps, it is also suggested to;

   a. Develop a coding system for different suppliers, material types, and procedures. These codes, suggested to be barcodes, can be easily linked to the collected data during design, production, construction and performance stages. This would enable DOT to conduct a fast inquiry for this type of information at any given location, even years after the construction.

   b. Have a traffic count measurement system that can be easily synced with the DOT highway segments. It is suggested that DOT adopt a similar geo-referencing system for all traffic-related data. Traffic data can be recorded for every DOT segment within a designed time period. Such that data is crucial for a better deterioration prediction.

   c. Find the best way of representation for climate data on every DOT segment. This study developed weighting factors for every project (which includes multiple segments) to extract climate data from the nearby weather stations. This effort can be complemented at the segment level. Calibrating these factors or even developing

better means for climate data measurements at the scale of pavement segments, not for the entire project, can significantly enhance the application of the suggested framework. Having a reliable and geo-tagged climatic data for WisDOT roadway network can help to broaden the application of the developed database beyond the performance of pavements, for the soil-related problems such as landslide, expansion, collapse, freeze-thaw, and etc.

d. Adopt a universal geo-tagging system for all the highway-related tests conducted as part of research studies or other efforts that are being done on the WisDOT network. Such a system would help to store the collected data in the central database and help other researchers to extract and use them for other purposes. For example, this study discovered several datasets related to coring information, nondestructive testing results, and other field or lab tests, which were conducted as a part of state and national funded studies on the WisDOT network. This data would have been helpful to develop better prediction models. However, due to the lack of geo-referencing of such data, it was not possible to integrate them into the developed database. Using a common geo-referencing system, such as GPS location, and requiring the researchers and contractors to geo-tag the reported data, could significantly boost their application.

e. Incorporate the current and future real-time data collection systems, such as the on-site sensors in WisDOT to the pavement network database by geo-referencing their collected data. WisDOT is using sensors for collecting data on roadways regarding the weather conditions, soil properties, traffic measurements, and special structures such as bridges. Interrelating these measurements to other pavement performance-related components throughout a universal geo-referencing system can enhance their application. This can also improve the ability of DOT to faster and more accurate actions with regards to the complex problems, that cannot be reflected with the data extracted from a single parameter. For example, having a localized weak base layer may not need immediate attention, but if it combines with the received data regarding the passage of high load traffic and rapid fluctuations of water level in the base, coming from the nearby sensors, then it requires urgent actions to prevent a dangerous situation. With the current advances in the field, especially the

Internet of Things (IoT), these data collection systems can be interrelated to computing devices, mechanical and digital machines with their unique identifier which is their geo-tag. This enables them to transfer data over the network with less requirement of human-to-human or human-to-computer interactions. This is the path toward future smart cities.

Finally, the implementation of the aforementioned recommendations should be a resource for adopting data-driven performance-based specifications, either at the mix design level or the construction level. The data-driven models should serve as a verification tool for adopted limits in order to connect laboratory activities with in-service performance. The growth of the database within the network for all classes of pavements must be utilized at scheduled times as a means of self-validation of specification limits, construction practices, maintenance plans, and rehabilitation. They can serve for project scoping as a history of similar pavements with respect to location, traffic level, environmental condition, or structural design can be easily retrieved to evaluate performance and apply improvements when needed.

References:

Abkowitz, Mark, Stephen Walsh, Edwin Hauser, and Larry Minor. "Adaptation of geographic information systems to highway management." Journal of Transportation Engineering116, no. 3: 310-327. (1990).

Apté, C., & Weiss, S. Data mining with decision trees and decision rules. Future generation computer systems, 13(2-3), 197-210. (1997).

Arhin, S. A., Williams, L. N., Ribbiso, A., & Anderson, M. F.. Predicting pavement condition index using international roughness index in a dense urban area. Journal of Civil Engineering Research, 5(1), 10-17. (2015).

Ashtiani, R. S., Little, D. N., & Rashidi, M. "Neural network based model for estimation of the level of anisotropy of unbound aggregate systems." Transportation Geotechnics, 15, 4-12. (2018).

ASTM D6433-16 Standard Practice for Roads and Parking Lots Pavement Condition Index Surveys, ASTM International, West Conshohocken, PA, (2016).

Attoh-Okine, N. O., Cooger, K., & Mensah, S. Multivariate adaptive regression (MARS) and hinged hyperplanes (HHP) for doweled pavement performance modeling. Construction and Building Materials, 23(9), 3020-3023. (2009).

Bahia, Hussain, Hassan A. Tabatabaee, Tirupan Mandal, and Ahmed Faheem. Field Evaluation of Wisconsin Modified Binder Selection Guidelines-Phase II. Wisconsin Highway Research Program, (2013).

Batioja-Alvarez, D., Kazemi, S. F., Hajj, E. Y., Siddharthan, R. V., & Hand, A. J.. Statistical Distributions of Pavement Damage Associated with Overweight Vehicles: Methodology and Case Study (No. 18-05657). (2018).

Bozorgzad, A., Kazemi, S. F., & Nejad, F. M. Evaporation-induced moisture damage of asphalt mixtures: Microscale model and laboratory validation. Construction and Building Materials, 171, 697-707. (2018).

Breiman L, Friedman JH, Olshen RA, Stone CJ. "Classification and regression trees." Wadsworth & Brooks/Cole Advanced Books & Software. (1984).

Breiman, L., Friedman, J., Olshen, R., Stone, C., Steinberg, D., Colla, P. "Classification and regression trees." (1995).

Breiman, L.. Random forests. Machine learning, 45(1), 5-32. (2001).

Cooley, L.A., Prowell, B.D., Hainin, M.R., and Buchanan, M.S., Bulk Specific Gravity Round-Robin Using the Corelok Vacuum Sealing Device. NCAT Report 02-11. (2003).

Croux, C., & Dehon, C.. Influence functions of the Spearman and Kendall correlation measures. Statistical methods & applications, 19(4), 497-515. (2010).

Daniel, J. S., Corrigan, M., Jacques, C., Nemati, R., Dave, E. V., & Congalton, A.. "Comparison of asphalt mixture specimen fabrication methods and binder tests for cracking evaluation of field mixtures." Road Materials and Pavement Design, 1-17. (2018).

Faheem, A., Hosseini, A., Titi, H., Schwandt, S. “Evaluation of WisDOT Quality Management Program (QMP) Activities and Impacts on Pavement Performance.” WHRP No. 0092-15-05., (2018).

Ferreira, A., Picado-Santos, L. D., Wu, Z., & Flintsch, G.. Selection of pavement performance models for use in the Portuguese PMS. International Journal of Pavement Engineering, 12(1), 87-97. (2011)

Ferreira, C.. “Algorithm for solving gene expression programming: a new adaptive problem.” Complex Systems, 13(2), 87-129. (2001)

Flintsch, Gerardo W., Randy Dymond, and John Collura. Pavement management applications using geographic information systems. No. Project 20-5 FY 2002, (2004).

Franklin, J.. Predictive vegetation mapping: geographic modeling of biospatial patterns in relation to environmental gradients. Progress in physical geography, 19(4), 474-499. (1995).

Galin, D. Speeds on two-lane rural roads-a multiple regression analysis. Traffic Engineering & Control, 22(HS-032 645). (1981)

Gandomi, A. H., & Alavi, A. H.. A new multi-gene genetic programming approach to nonlinear system modeling. Part I: materials and structural engineering problems. Neural Computing and Applications, 21(1), 171-187. (2012)

Ghasemi, P., Aslani, M., Rollins, D. K., & Williams, R. C.. Principal Component Neural Networks for Modeling, Prediction, and Optimization of Hot Mix Asphalt Dynamics Modulus. Infrastructures, 4(3), 53. (2019)

Ghasemi, P., Aslani, M., Rollins, D. K., & Williams, R. C.. Principal component analysis-based predictive modeling and optimization of permanent deformation in asphalt pavement: elimination of correlated inputs and extrapolation in modeling. Structural and Multidisciplinary Optimization, 59(4), 1335-1353. (2019)

Gopalakrishnan, K., Khaitan, S. K., Choudhary, A., & Agrawal, A.. “Deep Convolutional Neural Networks with transfer learning for computer vision-based data-driven pavement distress detection.” Construction and Building Materials, 157, 322-330. (2017)

Harter, Gerald. "An integrated geographic information system solution for estimating transportation infrastructure needs a Florida example." Transportation Research Record: Journal of the Transportation Research Board 1617 50-55. (1998)

Hondros, G., The evaluation of Poisson’s ratio and modulus of materials of a low tensile resistance by the Brazilian (indirect tensile) test with particular reference to concrete. J. Appl Sci., 10 (3), 243–268. (1959)

Hong, F., & Prozzi, J. A., Estimation of pavement performance deterioration using Bayesian approach. Journal of infrastructure systems, 12(2), 77-86. (2006)

Huang YH. Pavement Analysis and Design. New Jersey, USA: Pearson Prentice-Hall, Upper Saddle River; (2004).

Jalali, F., Vargas-Nordcbeck, A., & Nakhaei, M.. Full-Scale Probabilistic Assessment of Asphalt Surface Treatments: The Case Study of Lee Road 159. In Airfield and Highway Pavements 2019: Design, Construction, Condition Evaluation, and Management of Pavements (pp. 208-219). Reston, VA: American Society of Civil Engineers. (2019).

Kaur, D., & Pulugurta, H.. Comparative analysis of fuzzy decision tree and logistic regression methods for pavement treatment prediction. WSEAS Transactions on Information Science and Applications, 5(6), 979-990. (2008).

Kendall, M. G., Rank correlation methods (2nd ed.). Oxford, England: Hafner Publishing Co. (1955).

Kenley, R., Managing Change in Construction Projects: A Knowledge-based Approach. Construction Management and Economics, 30 (2), 179–180. (2012)

Khademian, Z., K. Shahriar, and M. Gharouni Nik. "Developing an algorithm to estimate in situ stresses using a hybrid numerical method based on local stress measurement." International Journal of Rock Mechanics and Mining Sciences55 80-85. (2012)

Kim, H.-S.; Sun, C.-G.; Cho, H.-I. Geospatial Big Data-Based Geostatistical Zonation of Seismic Site Effects in Seoul Metropolitan Area. ISPRS Int. J. Geo-Inf. 6, 174. (2017)

Kim, Y.R., Seo, Y., King, M., and Momen, M., "Dynamic Modulus Testing of Asphalt Concrete in Indirect Tension Mode." Transportation Research Record: Journal of the Transportation Research Board, 1891 (1), 163–173. (2007)

Koza, J. R., "Genetic programming: A paradigm for genetically breeding populations of computer programs to solve problems" (Vol. 34). Stanford, CA: Stanford University, Department of Computer Science. (1990).

Lee, H.N., Jitprasithsiri, S., Lee, H., Sorcic, R.G. Development of geographic information system-based pavement management system for Salt Lake City. Transportation Research Record (1524), 16–24. (1996).

Lee, J., Nam, B., & Abdel-Aty, M.. "Effects of pavement surface conditions on traffic crash severity." Journal of Transportation Engineering, 141(10), 04015020. (2015).

Majidifard, H., Jahangiri, B., Buttlar, W. G., & Alavi, A. H. "New machine learning-based prediction models for fracture energy of asphalt mixtures." *Measurement, 135, 438-451*. (2019)

McDonald, J. H.. Handbook of biological statistics (Vol. 2, pp. 173-181). Baltimore, MD: Sparky House Publishing. (2009).

Medina, A., Flintsch, G. W., and Zaniewski, J. P. "Geographic information systems-based pavement management system." Transportation Research Record 1652, Transportation Research Board, Washington, DC, 151–157. (1999).

Moossazadeh, J., & Witczak, M. W.. "Prediction of subgrade moduli for soil that exhibits nonlinear behavior." Transportation Research Record, (810). (1981).

Morgan, J. N., & Sonquist, J. A. "Problems in the analysis of survey data, and a proposal. Journal of the American statistical association", 58(302), 415-434. (1963).

Morovatdar, A., Ashtiani, S. R., Licon, C., & Tirado, C. “Development of a Mechanistic Approach to Quantify Pavement Damage using Axle Load Spectra from South Texas Overload Corridors.” In Geo-Structural Aspects of Pavements, Railways, and Airfields Conference, GAP., (2019)

Morovatdar, A., Ashtiani, S. R., Licon, C., Tirado, C., & Mahmoud, E. “A Novel Framework for the Quantification of Pavement Damages in the Overload Corridors.” 99th TRB Annual Meeting, Transportation Research Record (TRR): Journal of the Transportation Research Board. (2019)

NCHRP Research Results Digest No 180: Implementation of Geographic Information Systems (GIS) in State DOTs. TRB, National Research Council, Washington, DC. (1991).

Nemati, R., & Dave, E. V. “Nominal property based predictive models for asphalt mixture complex modulus (dynamic modulus and phase angle).” Construction and Building Materials, 158, 308-319. (2018).

Notani, M. A., Moghadas Nejad, F., Fini, E. H., & Hajikarimi, P. Low-Temperature Performance of Toner-Modified Asphalt Binder. *Journal of Transportation Engineering, Part B: Pavements*, *145*(3), 04019022. (2019).

Osman, Omar, Hayashi, Yoshitsugu, Geographic information systems as platform for highway pavement management systems. Transportation Research Record 1 (1442), 19–30. (1994).

Park, E. S., Smith, R. E., Freeman, T. J., & Spiegelman, C. H.. A Bayesian approach for improved pavement performance prediction. Journal of Applied Statistics, 35(11), 1219-1238. (2008).

Parsons, Ogden, “Recommended Guidelines for the Collection and Use of Geospatially Referenced Data for Airfield Pavement Management.” National Academies of Sciences, Engineering, and Medicine. Washington, DC: The National Academies Press. (2010).

Peng Z.-R., A proposed framework for feature-level geospatial data sharing: a case study for transportation network data, Pages 459-481, 20 Feb (2007).

Poli, R., W. B. Langdon, and N. F. McPhee. “A field guide to genetic programming.” Published via http://lulu.com. (2008).

Prasad, A. M., Iverson, L. R., & Liaw, A. Newer classification and regression tree techniques: bagging and random forests for ecological prediction. Ecosystems, 9(2), 181-199. (2006).

Quinlan, J. R.. C4. 5: programs for machine learning. Elsevier. (2014).

Roberts, Freddy L., Prithvi S. Kandhal, E. Ray Brown, Dah-Yinn Lee, and Thomas W. Kennedy. "Hot mix asphalt materials, mixture design, and construction." (1991).

Rogers, R., Plei, M., Aguirre, N., and TaghaviGhalesari, A.. Optimizing Structural Design for Overlaying HMA Pavements with a Concrete Pavement Using Critical Stress/Strain Analysis, 11th University Transportation Center (UTC) Spotlight Conference: Rebuilding and Retrofitting the Transportation Infrastructure, Washington D.C. (2017).

Roque Reynaldo, Birgisson Bjorn, Darku Daniel, Christos A. Drakos. “Evaluation of laboratory testing systems for asphalt mixture design and evaluation, Florida Department of Transportation.” (2004).

Saha, P., Ksaibati, K., & Atadero, R. “Developing Pavement Distress Deterioration Models for Pavement Management System Using Markovian Probabilistic Process.” Advances in Civil Engineering, (2017).

Sandra, A. K., & Sarkar, A. K. Development of a model for estimating International Roughness Index from pavement distresses. International Journal of Pavement Engineering, 14(8), 715-724. (2013).

Shah, Y.U., Jain, S.S., and Parida, M., “Evaluation of prioritization methods for effective pavement maintenance of urban roads.” International Journal of Pavement Engineering. (2014).

Shahin, M.Y. “Pavement Management for Airports, Roads, and Parking Lots” ISBN: 978-0-387-23464-9, Springer, (2005).

Sharma, S., Cui, Y., He, Q., Mohammadi, R., & Li, Z. “Data-driven optimization of Railway maintenance for track geometry.” Transportation Research Part C: Emerging Technologies, 90, 34-58. (2018).

Svetnik, V., Liaw, A., Tong, C., Culberson, J. C., Sheridan, R. P., & Feuston, B. P. “Random forest: a classification and regression tool for compound classification and QSAR modeling.” Journal of chemical information and computer sciences, 43(6), 1947-1958. (2003).

TaghaviGhalesari, A. and Chang-Albitres, C., “Sustainable Design of Rigid Pavements Using a Hybrid GP and OLS method, Geo-Congress, Philadelphia, PA, (2019).

Transportation Research Board, “Pavement Management Applications Using Geographic Information Systems,” NCHRP Synthesis 335, Washington, D.C. (2004).

Wang, Y. D., Ghanbari, A., Underwood, B. S., & Kim, Y. R.. Development of a Performance-Volumetric Relationship for Asphalt Mixtures. Transportation Research Record, 0361198119845364. (2019).

Zhang S. Jianting, Muhammad Javed, and L. Gruenwald. Prototype for wrapping and visualizing geo-referenced data in a distributed environment using XML technology. In Proceedings of the eighth ACM symposium on Advances in geographic information systems. ACMGIS 2000, Washington D.C. USA, (2000).